

UCSF

UC San Francisco Electronic Theses and Dissertations

Title

The developmental control of heterochromatin formation in the Drosophila embryo

Permalink

<https://escholarship.org/uc/item/54d4n1g9>

Author

Seller, Charles

Publication Date

2018

Supplemental Material

<https://escholarship.org/uc/item/54d4n1g9#supplemental>

Peer reviewed|Thesis/dissertation

The developmental control of heterochromatin formation in the Drosophila embryo

by
Charles Seller

DISSERTATION

Submitted in partial satisfaction of the requirements for degree of
DOCTOR OF PHILOSOPHY

in

Genetics

in the

GRADUATE DIVISION

of the

UNIVERSITY OF CALIFORNIA, SAN FRANCISCO

Approved:

DocuSigned by:

Patrick O'Farrell

Patrick O'Farrell

ACD62FEECE974F7...

Chair

DocuSigned by:

David Toczyski

David Toczyski

DocuSigned by:

Todd Nystul

Todd Nystul

DocuSigned by:

Joachim Li

Joachim Li

2148B8C59FAA425...

Committee Members

ACKNOWLEDGEMENTS

To my advisor Pat O'Farrell, thank you for your patience, support, and deep insight. You challenged and broadened my notion of what the study of biology is all about. I've never encountered anyone so adept at thinking deeply across all scales of life. It's a skill that I admire deeply and hope to continue to nurture and practice in my own scientific career.

To the members of my thesis committee: Joachim Li, Todd Nystul, and David Toczyski. Thank you for your kindness and support, and for supplying refreshing guidance to both my thesis project and career.

To Dave Toczyski, if you hadn't hired me as a technician straight out of college, I don't think I would have ever ended up at UCSF for graduate school. The environment that your lab provided was so important to my maturation as a scientist. Thank you to all the members of the T-lab during my tenure, but especially to Michael Downey for teaching me much of what I know about how to conduct experiments.

To the past and present members of the O'Farrell Lab, thank you for making this place my scientific home in graduate school. Special thanks to Antony Shermoen, the practical and scientific skills that you taught me were indispensable to everything in this thesis. Thank you to Christine Wong for all the behind the scenes work that you do to keep the lab running smoothly.

To my classmates, thank you for making graduate school so much fun. Some of my best memories of UCSF are from time spent with you guys. Special thanks to the Tetrad book/wine club for inserting some high-society level sophistication into my PhD.

Thank you to my family, for your love and support, and for your patience with my perpetual studenthood. Thank you to my parents: Gary Seller, Lucy Loftin, Paula Pullenza, and Greg Vines. I couldn't have possibly gotten here without you.

Chapter 2 of this thesis is published in the journal PLoS Biology.

The text of this thesis chapter is a reprint of the material as it appears in:

Rif1 prolongs the embryonic S phase at the *Drosophila* mid-blastula transition. Seller CA and O'Farrell PH. *PLoS Biology* **16**: e2005687.

The co-author O'Farrell PH listed in this publication directed and supervised the research that forms the basis for the dissertation/thesis.

Chapter 3 of this thesis is currently in revision at the journal Genes and Development (Cold Spring Harbor Press)

The text of this thesis chapter is reproduced from the the material under the following title:

Rapid embryonic cell cycles defer the establishment of heterochromatin by Eggless/SetDB1 in *Drosophila*. Seller CA, Cho CY, and O'Farrell PH *Genes and Development in revision*

The co-author Cho CY conducted only the experiments found in Figure 3.1F and 3.1G. The co-author O'Farrell PH listed in this publication directed and supervised the research that forms the basis for the dissertation/thesis.

The developmental control of heterochromatin formation in the *Drosophila* embryo

By Charles A. Seller

ABSTRACT

In preparation for the dramatic morphogenetic events of gastrulation, rapid embryonic cell cycles slow at the mid-blastula transition (MBT). In *Drosophila* embryos the MBT involves the onset of key properties that distinguish the highly repetitive satellite sequences composing the heterochromatin from the rest of the genome. In early embryos the satellite DNA lacks the characteristic heterochromatic features of late replication and repressive chromatin modifications, like H3K9 methylation and HP1a. My thesis work has explored how the embryo controls the restoration of these conserved features to the heterochromatin. I describe and analyze the results of experiments employing a combination of fly genetics and real time microscopy on developing embryos. At the MBT, down-regulation of Cyclin:Cdk1 activity initiates cell cycle slowing by delaying replication of satellite DNA and extending S phase. I show that Cdk1 activity inhibits the chromatin association of Rif1, a repressor of origin firing. Following Cdk1 down-regulation at the MBT, Rif1 bound selectively to satellite sequences. In the next S phase, Rif1 dissociated from different satellites in a schedule that anticipated their replication. A mutant version of Rif1 lacking potential phosphorylation sites failed to dissociate and dominantly prevented completion of replication. In contrast, loss of Rif1 shortened the post-MBT S phase and rescued embryonic cell cycles disrupted by depletion of Cdc7. Following the Rif1 mediated introduction of late replication, satellite sequences begin acquiring H3K9 methylation and recruit the protein HP1a. By using a novel protein inactivation approach called JabbaTrapping, I show that the K9 methyltransferase Eggless plays a major role in the establishment of this repressive chromatin state. Additionally, live imaging of Eggless suggests that the rapid early cell cycles prevent this enzyme from introducing heterochromatic marks

before the MBT. Experimental manipulation of interphase duration showed that cell cycle speed regulates Eggless. By focusing on the initial events in the de novo formation of heterochromatin my work emphasizes how heterochromatin is integrated into the development of the embryo. Through regulation of the two proteins Rif1 and Egg, the embryonic cell cycle program times the appearance of late replication and repressive chromatin modifications, two widely conserved features of heterochromatin.

Table of Contents

Chapter 1: Introduction	1
Chapter 2: Rif1 prolongs the embryonic S phase at the <i>Drosophila</i> mid-blastula transition	10
Summary	11
Introduction.....	12
Results	16
Discussion	36
Acknowledgements	47
Figures	48
Materials and Methods	70
Chapter 3: Rapid embryonic cell cycles defer the establishment of heterochromatin by Eggless/Setdb1 in <i>Drosophila</i>.....	76
Summary	77
Introduction.....	78
Results	81
Discussion	92
Acknowledgements	99
Figures	100
Materials and Methods	116

Chapter 4: Conclusion.....119

References122

List of Figures

Chapter 2 Figures	48
Figure 2.1: Rif1 forms foci on heterochromatin as the embryonic S phase lengthens	48
Figure 2.2: Rif1 dissociates from chromatin before the underlying sequences replicate	50
Figure 2.3: Two stages of Rif1 recruitment, their contributions to specificity, and reliance on origins licensing and the replication checkpoint	52
Figure 2.4: Manipulation of Cdk1 activity alters the lifetime of Rif1 foci and the duration of S phase	54
Figure 2.5: Phospho-site mutant Rif1 does not dissociate from chromatin and blocks replication	56
Figure 2.6: <i>rif1</i> is required for the prolongation of S phase at the MBT	58
Figure 2.7: Deletion of <i>rif1</i> rescues cell cycles to Cdc7 depleted embryos	60
Figure 2.8: Sequential appearance at satellite sequences suggests that Rif1 influences late replication prior to an impact of HP1a	62
Figure 2.9: Model.....	63
Supplemental Figure 2.1: Generation and characterization of endogenously tagged Rif1::EGFP flies	64
Supplemental Figure 2.2: Further characterization of Rif1 and PCNA during S phase	65
Supplemental Figure 2.3: Analysis of potential CDK and DDK phosphorylation sites	66
Supplemental Figure 2.4: Deleting <i>rif1</i>	67

Chapter 3 Figures	100
Figure 3.1: JabbaTrap rapidly mis-localizes and blocks nuclear proteins in the embryo.....	100
Figure 3.2: Eggless is required for the embryonic establishment of heterochromatin	102
Figure 3.3: Localization and dynamics of Eggless during the establishment of heterochromatin.....	104
Figure 3.4: Windei, a cofactor of Eggless, localizes to the heterochromatin in the embryo and interacts with Eggless.....	106
Figure 3.5: Interphase duration limits the establishment of heterochromatin.....	107
Figure 3.6: Model	109
Supplemental Figure 3.1	110
Supplemental Figure 3.2	111
Supplemental Figure 3.3	112
Supplemental Figure 3.4	113

Chapter 1

Introduction

INTRODUCTION

The generation of a complex multicellular organism from a single fertilized egg is one of the most amazing processes in nature. Beginning with Aristotle, scientists have appreciated that development transforms the egg from simple and generalized to complex and differentiated. Modern biology has discovered that changes in the activity of the genome over time and across space control this transformation. Indeed, the differentiation of an initially naïve zygotic genome into specialized chromatin domains is thought to instruct much of the visible changes to the embryo. In my thesis work I have focused on the emergence of a major example of genomic differentiation – the division of the genome into euchromatin and heterochromatin – in the developing *Drosophila melanogaster* embryo.

Embryogenesis in the fruit fly exemplifies a widespread and likely ancestral mode of animal development known as the “big egg program” (O’Farrell 2004, 2015). Like most living and extinct animals on our planet, insects lay eggs that develop externally. The fertilized egg is essentially one big cell, approximately 10^5 larger than a typical somatic cell. The egg needs to be large because the embryo does not change in size, and embryonic cells proliferate without growing. During oogenesis, female flies load their eggs with enough nutrients to support embryonic development until a feeding animal hatches, now capable of supporting growth on its own. The mother also deposits gene products into the egg that compose a developmental program directing early development. The zygotic genome does not control early embryogenesis, which begins and proceeds without transcriptional input. Maternally deposited cell cycle regulators drive the mitotic divisions following fertilization at high speed. Then, during a conserved period of embryogenesis known as the mid-blastula transition (MBT) the cell cycle slows dramatically, zygotic transcription begins in full, and the embryo undergoes the morphogenetic events of gastrulation (Farrell and O’Farrell 2014; Yuan et al. 2016). At the MBT

the embryo shifts its focus from cell proliferation to differentiation, and this thesis centers around this transition period.

The pre-MBT cycles lack gap phases and so alternate between S phase and mitosis. Following the MBT, transcriptional input exerts control over the cell cycle by regulating passage from the first embryonic G2 into mitosis. Indeed cycle 14 is the first embryonic cell cycle that requires zygotic transcription for its completion (Edgar and O'Farrell 1989). The general exchange from maternal to zygotic control is often called the Maternal to Zygotic Transition (MZT), and an MZT is a general feature of embryonic development (Harrison and Eisen 2015). In *Drosophila* the MZT roughly parallels the MBT in embryonic time, but the exact time of the MZT differs for different processes (i.e. when they require zygotic transcription). Nevertheless, during cycles 13 and 14 the embryo destroys maternal mRNAs and begins transcribing thousands of genes for the first time (Renzis et al. 2007; Tadros et al. 2007; Lott et al. 2011). Zygotic genome activation is required for the key morphogenetic events that occur at the MBT. During cycle 14 the embryo cellularizes when cortical membrane invaginate and encapsulate individual nuclei. Near the end of cycle 14 cells undergo the coordinated gastrulation movements that fold and shape the embryonic tissues. Crucially zygotic transcription is controlled by maternal regulators that dictate which portions of the genome are activated and which portions are repressed. Much of this regulation centers around the packaging of DNA into distinct chromatin domains that have different genetic activity, and the organization of the genome into chromatin domains begins at the MBT. Thus, differentiation at multiple biological levels – genomic, cellular, and embryo – follow cell cycle slowing at the MBT. This precedence of the cell cycle justifies a focus on the control and the consequences of embryonic cell cycle speed.

The cell cycles before the MBT are remarkably fast, synchronous, and occur in the absence of cell membranes (syncytial). Historically, the study of cell cycle timing has focused on

the G1/S and G2/M transitions, but the early embryonic cell cycles lack gap phases and it is the duration of S phase that times cell cycle length (McClelland et al. 2009). During the first 9 nuclear cycles S phase completes in as little as 3.4 min, and nuclei begin deep within the embryo and migrate incrementally outwards towards the cortex after each division. Beginning in cycle 10 the nuclei reach the surface of the embryo forming the blastoderm. During cycles 11-13 the length of S phase gradually increases to 13 min. At cycle 14, the MBT cell cycle, interphase extends dramatically, and S phase lasts over 70 minutes and is followed by the first G2. Mitosis 14 is asynchronous, and zygotic transcription controls entry into mitosis according to a developmental pattern (Foe 1989; Edgar and O'Farrell 1990).

The control of the embryonic cell cycle centers around control of Cdk1 kinase activity, and the developmentally programmed downregulation of Cdk1 activity provides the key regulatory input into the slowing of the cell cycle at the MBT (Yuan et al. 2016). Two major points of regulation are relevant: 1) levels of activating cyclin protein and 2) the level of inhibitory phosphorylation on the Cdk1 protein (O'Farrell 2001). Cdk1 activation requires association with a mitotic cyclin partner (either cyclin A, B, or B3), which are maternally supplied. The levels of cyclins famously oscillate over the course of the cell cycle, and mitotic cyclins are destroyed in anaphase and synthesized just before entry into the next mitosis, but in the embryo evidence for even slight oscillation in cyclin levels isn't apparent until cycle 9. During the following cycles, mitotic destruction of cyclins increases, but this destruction is incomplete such that mitotic cyclins are always present during interphase (Edgar et al. 1994). Cdk1 activity is also regulated by inhibitory phosphorylation on T14 and Y15 by Wee-type kinases (Price et al. 2000; Stumpff et al. 2004). Cdc25 phosphatases (*string* and *twine*) remove these phosphorylations (Gould and Nurse 1989; Edgar and O'Farrell 1989). The DNA replication checkpoint, a signaling pathway that senses ongoing DNA replication, activates Wee-type kinases leading to the downregulation of Cdk1 by inhibitory phosphorylation. The replication checkpoint delays entry into mitosis until

the completion of S phase, and this delay becomes essential during cycle 13 to prevent a catastrophic entry into mitosis with unreplicated chromatids (Fogarty et al. 1994; Sibon et al. 1997, 1999). In a process possibly involving the zygotic transcription (Blythe and Wieschaus 2015), the activity of the replication checkpoint increases during the blastoderm cell cycles (11-13) (Crest et al. 2007; Deneke et al. 2016). Increased checkpoint activation synergizes with the downregulation of Cdc25 phosphatases to cause elevated levels of inhibitory phosphorylation on Cdk1 during the cycles approaching the MBT (Edgar et al. 1994). The embryo degrades String and Twine as it approaches the MBT, with String disappearing by cycle 13 and Twine disappearing early during interphase 14 (Edgar and Datar 1996; Di Talia et al. 2013; Farrell and O'Farrell 2013). The downregulation of Cdc25 is essential for the MBT slowing of the cell cycle and provides the key input in the control of Cdk1 activity (Edgar and O'Farrell 1990; Farrell et al. 2012).

The changes that I've outlined as the embryo approaches the MBT – increasing destruction of cyclins, increasing activation of the replication checkpoint, downregulation of Cdc25 – make cell cycle 14 special, it's the first cycle without persistent interphase Cdk1 activity. This feature is responsible for the dramatic increase in the length of cell cycle 14. S phase duration extends to over 70 minutes, and this long S phase is followed by the first embryonic G2. The prolongation of S phase at the MBT is the focus of the second chapter of this thesis and so some consideration of the process of DNA replication during S phase is warranted, but many of the details will be left for later.

Replicating a large eukaryotic genome (260 million base pairs in *Drosophila*) is a complicated business. Replication forks travel at a rate of only 3 kb/min, so to complete S phase in a timely fashion eukaryotic cells initiate replication at thousands of locations spread throughout the genome known as origins (Prioleau and MacAlpine 2016). S phase completes when all sequences in the genome have duplicated, thus the control of origin initiation is a key

component in determining the length of S phase. In principle changes in the behavior of origins could change the length of S phase in two ways. First, the density of origins could change. If origins are spaced very far apart then it would take longer to duplicate the genome. Indeed, origin spacing does increase slightly as the embryo approaches the MBT, from 7.9 kb in pre-blastoderm embryos to 10.6 kb during S phase 14 (Blumenthal et al. 1974; McKnight and Miller 1977). However, this increase in inter-origin distance cannot account for the observed change in S phase duration, from 3.4 min to 70 min. Secondly, the time when origins initiate replication during S phase can change. In a conventional S phase different portions of the genome begin replication at different times, a phenomenon known as replication timing, and the length of S phase is determined by the sequences that replicate late (Rhind and Gilbert 2013). Importantly, replication timing is not a random property, but a characteristic of certain domains of the genome. The temporal program of S phase changes dramatically as the embryo approaches the MBT. During the rapid pre-blastoderm cycles, S phase is brief because all sequence in the genome begin replication synchronously. There exists no differentiation in replication timing across the genome. Beginning in S phase 11 and continuing in succeeding cell cycles, specific portions of the genome exhibit incrementally increasing delays in their replication, and this leads to incremental increases in S phase duration. In S phase 14 these delays become extremely pronounced, and this S phase lasts over 70 min. because specific sequences wait to begin replication until very late in S phase (Shermoen et al. 2010). The onset of late replication during S phase 14 is an active event requiring both zygotic transcription and the downregulation of Cdk1 activity (Shermoen et al. 2010; Farrell et al. 2012). Thus, a major element of in the remodeling of the cell cycle at the MBT is the differentiation of the genome into distinct early and late replicating domains. In Chapter 2 I will outline evidence that demonstrates that the protein Rif1 is responsible for the onset of late replication at the MBT. Additionally, I will detail experiments that show how the regulation of Rif1 by Cdk1 integrates Rif1 mediated late replication into a developmental program controlling cell cycle slowing.

The portion of the genome destined for late replication at the MBT consists of megabase sized blocks of highly repetitive DNA known as the satellite sequences that make up about 30% of the *Drosophila* genome (Lohe et al. 1993). Tandem repeats of simple sequence (e.g. AATAC) compose the satellites, and these blocks of DNA are found adjacent to centromeres in the genomes of many eukaryotes. The satellite sequences constitute the bulk of the heterochromatin in the nucleus. Heterochromatin was originally defined cytologically by Emil Heitz in 1928 as the portion of the chromosome that does not decondense upon exit from mitosis. In contrast to the euchromatin, the DNA in heterochromatin is tightly compacted throughout the cell cycle, and throughout development (Brown 1966). Scientific progress over the last century has connected this chromatin state with a suite of biological behaviors including transcriptional repression, late replication, and decreased recombination frequency. The division of the genome into euchromatin and heterochromatin is a major instance of the regulatory possibility that chromatin structure provides to biology. Indeed, the regulation of chromatin structure has emerged as a key theme in developmental biology (Yadav et al. 2018).

First identified in *Drosophila*, the phenomenon of position effect variegation (PEV) provided early evidence that the unique chromatin structure of heterochromatin controlled the activity of the DNA found packaged within it (Elgin and Reuter 2013). Muller discovered PEV by isolating a mutant fly where the normally solid red eye was variegated in color, with patches of red and patches of white (Muller 1930). This suggested that the *white* gene was functional, but that in some cells the gene had become silenced during the development of the eye. Muller showed that in this mutant stock, X-ray bombardment had caused a translocation that relocated the *white* gene to a region of the chromosome near the border between euchromatin and heterochromatin. This discovery provided one of the first indications that the position of a gene on the chromatin fiber could alter its activity. Later, more detailed analysis demonstrated that genes exhibiting PEV were found within the heterochromatin only in the cells in which they were

silenced suggesting that the packaging of a gene into the compacted heterochromatin can prevent its expression (Zhimulev et al. 1986). Screens for modifiers of PEV have identified many of the key components of the heterochromatin machinery, and currently over 150 genetic loci have been reported to modify PEV (Elgin and Reuter 2013). Investigations primarily in *Drosophila* and the fission yeast *Schizosaccharomyces pombe* have now provided a compelling, but still incomplete, view of the molecular interactions that control heterochromatin formation.

The nucleosomes in heterochromatin are distinguished by specific histone post-translational modifications that play critical roles in enforcing the unique behaviors of heterochromatic DNA (Allshire and Madhani 2018). Histone modifications, especially those found on the amino terminal tails of histone proteins, regulate the underlying DNA by directly altering chromatin structure or by recruiting specific chromatin binding proteins. Chromatin binding proteins often contain reader domains, which are protein domains that recognize specific histone modifications. Histone modifications can serve as recruitment platforms that direct the binding of reader domain containing proteins, as well as other associated proteins that often co-occur in large multisubunit complexes. Together histone modifications and the proteins that read them generate distinct chromatin states with distinct regulatory properties.

In eukaryotes ranging from fission yeast to man, the nucleosomes in heterochromatin are hypoacetylated and di/tri-methylated at Lysine 9 on the N-terminal tail of Histone H3 (H3K9me_{2/3}). HP1 proteins recognize and bind H3K9me_{2/3} and HP1 can oligomerize and recruit additional proteins to heterochromatin (Eissenberg and Elgin 2014). The H3K9me_{2/3}-HP1 interaction forms the regulatory core, and loss of either the modification or of HP1a lead to transcriptional depression and lethality in *Drosophila* (Eissenberg et al. 1990; Penke et al. 2016, 2018). Thus, understanding the pathways leading to the deposition of H3K9me_{2/3} is key to the

study of heterochromatin, and the presence of this modification is now presented as a defining feature of heterochromatin.

The formation of heterochromatin can be conceptually divided into two phases: establishment and maintenance. Establishment involves the initial deposition of H3K9me2/3-HP1a onto naïve chromatin. Once written, the cell must maintain this modified state over the cell cycle and over development to ensure the stable regulation of heterochromatic DNA. Although the cellular heterochromatin machinery has been the focus of intense study over the last two decades, this focus has centered on biological systems that primarily probe maintenance not establishment. Studies in both unicellular organisms and differentiated metazoan systems have uncovered a suite of mutually reinforcing molecular interactions that ensure the faithful propagation of heterochromatic marks (Allshire and Madhani 2018), but in both these settings the heterochromatin has already formed, and it is unclear to what extent these mechanisms can be extended to the *de novo* generation of heterochromatin. Embryos provide a unique setting to study the natural establishment of heterochromatin because early embryos lack many of the modifications that eventually distinguish different chromatin domains, including H3K9me2/3-HP1a. In the *Drosophila* embryo these modifications appear around the time of the MBT (Kellum et al. 1995; Shermoen et al. 2010; Chen et al. 2013; Li et al. 2014; Yuan and O'Farrell 2016). Thus, embryogenesis involves the restoration of heterochromatin, and this restoration can serve as a model for how epigenetic control arises during development. The third chapter of my thesis describes a study that examines the initial steps of heterochromatin formation in the early *Drosophila* embryo. In this chapter I will outline evidence that implicates the enzyme Eggless in the earliest steps of heterochromatin formation. I will also present experiments that show how the embryonic cell cycle program integrates the action of Eggless with the development of the embryo.

Chapter 2

Rif1 prolongs the embryonic S phase at the *Drosophila* mid-blastula transition

Summary

In preparation for dramatic morphogenetic events of gastrulation, rapid embryonic cell cycles slow at the Mid-Blastula Transition (MBT). In *Drosophila melanogaster* embryos, downregulation of Cdk1 activity initiates this slowing by delaying replication of heterochromatic satellite sequences and extending S phase. We found that Cdk1 activity inhibited the chromatin association of Rif1, a candidate repressor of replication. Furthermore, Rif1 bound selectively to satellite sequences following Cdk1 downregulation at the MBT. In the next S phase, Rif1 dissociated from different satellites in an orderly schedule that anticipated their replication. Rif1 lacking potential phosphorylation sites failed to dissociate and dominantly prevented completion of replication. Loss of Rif1 in mutant embryos shortened the post-MBT S phase and rescued embryonic cell cycles disrupted by depletion of the S phase-promoting kinase, Cdc7. Our work shows that Rif1 and S phase kinases compose a replication timer controlling, first the developmental onset of late replication, and then the precise schedule of replication within S phase. In addition, we describe how onset of late replication fits into the progressive maturation of heterochromatin during development.

INTRODUCTION

Eukaryotic DNA replication begins at many locations throughout the genome known as origins. Different origins initiate at different times during S phase on a schedule governed by an elusive replication timing program. The time it takes to duplicate the genome, the length of S phase, is set by the time when the last sequence completes replication. For over 50 years, the field has appreciated that late-replicating sequences are found in the compacted portion of the genome known as heterochromatin (Lima-de-Faria 1959; Taylor 1960; Lima-de-Faria and Jaworska 1968). Late replication is presented as a general property of heterochromatin, but how this property arises is unknown (Brown 1966). Additionally, embryonic development of many animals features dramatic modifications of replication timing (Graham 1966; Snow 2008; Stepieńska and Olszańska 1983; Hiratani et al. 2008). In *Drosophila*, the length of S phase changes by over 50 fold during development (Blumenthal et al. 1974; Neufeld et al. 1998; Milán et al. 1996), and in the early *Drosophila* embryo the heterochromatin does not replicate later than the rest of the genome. Late replication is then properly viewed as a feature that must be imparted to the heterochromatin at the beginning of every new generation. How S phase is retooled to do this is unknown.

As worked out in yeast, the process of origin initiation involves a sequence of conserved biochemical steps that convert an origin into a bidirectional replication fork (Tanaka and Araki 2013; Yeeles et al. 2015). Origins are first licensed for replication through the loading onto dsDNA of two hexameric MCM2-7 helicase complexes. The resulting head-to-head double hexamer is known as a pre-Replicative Complex (pre-RC). Activation of the pre-RC requires the coordinated assembly of a multiprotein complex called a replisome. Activation, also referred to as firing, is led by the action of two conserved cell cycle kinases: a CDK (cyclin-dependent kinase) and a DDK (Dbf4-dependent kinase) (Labib 2010). CDK and DDK are recruited to pre-RCs where they phosphorylate substrates to initiate the transformation of the pre-RC into

functional replication forks (Tanaka et al. 2007; Zegerman and Diffley 2007; Sheu and Stillman 2010). Local chromatin structure is thought to influence the efficiency of this step to alter the replication-timing of different sequences (Rhind and Gilbert 2013). Multiple studies have identified a number of pathways contributing to such local inputs, such as histone modification (Vogelauer et al. 2002; Aggarwal and Calvi 2004) and chromatin binding proteins (Makunin et al. 2002; Knott et al. 2012). Additionally, global factors, such as the competition among origins for limited replication components, have been suggested to impact timing (Tanaka et al. 2011; Mantiero et al. 2011). However, we have little insight into how the varied inputs affecting the efficiency of pre-RC activation measure time to precisely schedule replication of different sequences during S phase, or how this schedule is modulated during development.

In light of these issues, the embryo provides a unique context in which to study the control of S phase duration because development profoundly changes it. Historically, the study of cell cycle timing has focused on the G1/S and G2/M transitions, but the early embryonic cell cycles lack gap phases and it is the duration of S phase that changes (McClelland et al. 2009; Shermoen et al. 2010). In the *Drosophila melanogaster* embryo, these specialized cell cycles are maternally programmed, synchronous, and occur in the absence of cell membranes. During the first 9 nuclear cycles S phase completes in as little as 3.4 min (Blumenthal et al. 1974), and nuclei remain deep within the embryo. Beginning in cycle 10 the nuclei reach the surface of the embryo forming the blastoderm. During cycles 11-13 the length of S phase gradually increases to 13 min. At the next cell cycle, the 14th, the embryo begins a conserved developmental period known as the Mid-Blastula Transition (MBT) when numerous changes occur: interphase, which extends dramatically, has an S phase 14 that lasts 70 minutes and it is followed by the first G2 (summarized in Fig 2.1A) (Farrell and O'Farrell 2014; Yuan et al. 2016). After G2 of cycle 14, cells enter mitosis in a patterned program controlled by zygotic transcription (Edgar and O'Farrell 1989). We focused on the changes that occur to the DNA replication program at the

MBT, and on how these changes are introduced. As we show here, the first introduction of late replication results from the emergence of a single regulatory input with timing function.

Prior work has shown that the prolongation of S phase at the MBT is caused by introduction of delays in the replication of satellite sequences (Shermoen et al. 2010). During the pre-blastoderm cycles all regions of the genome begin and end replication together resulting in a short S phase. Even the 30% of the genome composed of blocks of repetitive DNA known as the satellite sequences, which are considered to be constitutively heterochromatic, lack the marks of heterochromatin and replicate early. During S phases 11-13, the satellite sequences experience progressively modest delays in replication timing. Then, these satellites experience major delays in S phase 14 in which a succession of different satellites begin and complete replication on a protracted schedule. Thus, onset of late replication causes the pronounced increase in the S phase duration, but the nature of the timer coordinating this schedule was unknown. Following their late replication in cycle 14, the satellite sequences become heterochromatic and late replication will be a characteristic feature of heterochromatic satellites for the rest of development.

Uncovering how late replication develops will improve our understanding of what has been a widespread, but mysterious feature of DNA replication. We know that the onset of late replication in the embryo follows a time-course that is unrelated to appearance of other features of heterochromatin such as compaction, which is already evident in earlier cell cycles, or HP1 recruitment, which occurs after replication in cycle 14, or H3K9 methylation, which accumulates continuously and slowly over the course of interphase 14 (Shermoen et al. 2010; Yuan and O'Farrell 2016). Previous work demonstrated that activity of the Cdk1 kinase is a key determinant of the duration of S phase in the early embryo (Farrell et al. 2012). Persistent S phase Cdk1 activity during the shorter pre-MBT cycles drives heterochromatin to replicate early, and it is the programmed downregulation of Cdk1 occurring at the MBT that allows the onset of

late replication. However, it is unclear how the embryo interprets the activity of Cdk1 to produce this dramatic prolongation of S phase.

We have discovered that Rif1, a conserved protein that interacts with the protein phosphatase PP1 and impacts telomere biology, DNA damage responses and replication timing (Hayano et al. 2012; Cornacchia et al. 2012; Yamazaki et al. 2012, 2013), is an important regulator of early developmental changes in cell cycle timing. Amid reports of diverse roles for Rif1, several studies emphasize the action of Rif1 to inhibit replication, and show that Rif1 and DDK oppose each other, inhibiting or activating the pre-RC, respectively (Matarocci et al. 2014; Davé et al. 2014; Hiraga et al. 2014; Alver et al. 2017). The literature has emphasized the possibility that Rif1 recruited PP1 could counter the action of DDK by dephosphorylating this kinase's substrate, the MCM helicase complex, but genetic epistasis and molecular findings suggest that DDK also targets and inactivates Rif1 suggesting that a more complex interplay of the activating kinases and the Rif1 inhibitor contributes to pre-RC activation (Hayano et al. 2012). While it is appreciated that Rif1 and its associated PP1 can inhibit the firing of origins, the eventual firing of these inhibited origins presumably requires an input to negate or override the repressive action of Rif1. The nature of this signal, which would underlie the temporal programming for the firing of late replicating origins, is unknown. Additionally, how Rif1 contributes to developmental changes in replication timing is unknown. Our results describe how Rif1 connects the activity of Cdk1 to the onset of late replication in the embryo, thereby composing an active program that extends S phase at the *Drosophila* MBT. We provide new insights into Rif1 behavior that suggest an intimate role in a timing mechanism specifying the precise time at which different sequences replicate during S phase. In addition, our work allows us to provide a more complete description of the maturation of the heterochromatin during development.

RESULTS

Rif1 binds to compacted foci of satellite sequences as the length of the embryonic S phase increases

Due to the stereotyped nature of the embryonic cell cycles, live imaging of fluorescently tagged proteins can be especially informative. We used CRISPR-Cas9 genome editing to tag the endogenous Rif1 protein with EGFP at its C-terminus (S2.1 Fig). Rif1 is maternally provided (S2.1 Fig), and is widely distributed during the first 6 hours of embryogenesis and thereafter shows increasingly tissue-limited expression (Sreesankar et al. 2015).

Given ubiquitous presence of Rif1 protein in the early embryo, regulation of its activity ought to underlie any developmental or cell cycle modulations of Rif1 function at this stage. If Rif1 acts to delay the replication of heterochromatin, then we would expect the protein to be recruited to satellite sequences when the replication of these sequences is delayed in cycle 14. The satellite sequences form compacted regions of chromatin that can be visualized as discrete bright foci of DAPI stained DNA (Fig 2.1B). These compacted foci of chromatin first acquire heterochromatic marks during cycle 14, but, given the absence of G1 in this cycle, a program for their delayed initiation must already be in place at the beginning of interphase 14 (Shermoen et al. 2010; Yuan and O'Farrell 2016). In S phase 14, Rif1 was bound to many foci of compacted chromatin, while in the following G2 phase the heterochromatin lacked Rif1 staining (Fig 2.1). Live imaging of Rif1-EGFP embryos (S2.1 Movie) during early embryogenesis revealed the dynamics of this change. Rif1-EGFP disappeared from individual foci as S phase progressed, and only a dim nuclear background was present by G2 of cycle 14 (Cycle 14, Fig 2.1D). Tracking individual foci in high frame-rate movies showed that different Rif1 foci disappeared at different times (Fig 2.1E). Often, only a single focus remained near the end of S phase before disappearing as cells entered G2. This ordered loss of different Rif1 foci was reminiscent of the protracted schedule of late replication occurring in this cycle.

To test the correspondence of Rif1 foci and satellite sequences we marked specific satellite sequences by in situ hybridization or our recently developed TALE-lights technique (Yuan et al. 2014). In embryos fixed during early S phase 14, the single Y-chromosome linked focus of AATAC satellite detected by DNA-FISH was co-stained by Rif1 (right panels Fig 2.1C). In live embryos, a fluorescently tagged TALE-light protein engineered to bind the late-replicating satellite-repeat 1.686 showed that Rif1 also binds the four foci of this sequence (left panels in Fig 2.1C).

During cycles 11-13, S phase gradually and progressively gets longer due to incremental delays to satellite replication. In parallel with these changes, Rif1 showed weak and transient localization to foci in cycle 11 and progressively more intense and longer-lived foci in subsequent cycles (S2.1 Movie, Fig 2.1D). Disappearance of Rif1 foci within each S phase was not instantaneous: the signal decayed from the outside-in over a few frames of our records, for instance during S phase 13 high frame imaging showed that a focus of Rif1 disappeared over the course of approximately 2 minutes (S2.2 Movie, Fig 2.1F). These observations show that Rif1 binds to satellite sequences as they become late replicating during embryogenesis, and that Rif1 dissociates from satellite sequences as replication progresses.

The release of Rif1 from chromatin anticipates the initiation of late replication

The correlation between the dissociation of the Rif1 localized to satellite foci and the onset of late replication motivated a closer examination of Rif1 dynamics during S phase. We have previously validated and utilized fluorescently tagged versions of the replication protein PCNA as real time probes for the progress of S phase (McClelland et al. 2009). PCNA travels with the replicating DNA polymerase, and its recruitment to different regions of the genome marks their replication. Using a transgenic line expressing an mCherry labeled version of PCNA from its endogenous promoter (S2.2 Fig), we were able to compare active DNA replication with the localization of Rif1. During the first 10 minutes of S phase, the PCNA signal was intense,

and distributed throughout most of the nucleus. Following early replication, the generalized signal fades progressively and the PCNA signal is predominantly limited to bright apical foci, which mark the late replicating satellite sequences. Each late replicating focus appears, persists, and declines in a stereotyped schedule, with the number of active foci gradually declining during more than an hour of interphase of cycle 14 (Fig 2.2A, S2.3 Movie). Throughout this program, Rif1 did not overlap with the PCNA signal, indicating that once a region had initiated DNA replication, the Rif1 signal had already disappeared. As S phase progressed, different Rif1 foci disappeared at different times and were replaced within one minute by PCNA (S2.3 Movie). The last sequence to recruit PCNA was marked by Rif1 throughout S phase 14 until just before it recruited PCNA (Fig 2.2A). Similar analyses in cycles 12 and 13 similarly revealed separation of Rif1 staining and replication. The observed timing suggested that replication of Rif1 staining regions awaits the dissociation of Rif1. An analysis of Rif1 staining of fixed mammalian tissue culture cells similarly suggested that Rif1 protein dissociated from chromatin prior to the onset of replication (Cornacchia et al. 2012).

The S phase of cell cycle 15 provides an alternative context to observe the relationship between Rif1 and replication. By cycle 15, the embryo has completed the MBT, the cell cycle has lost synchrony and morphogenetic movements have begun. The timing of mitosis 14 and entry into cycle 15 differs with position in the embryo, but follows a stereotyped schedule that is zygotically controlled. Cycle 15 still lacks a G1, so nuclei enter S phase immediately following mitosis 14, but these cycle 15 nuclei exhibit more mature features. The satellite sequences enter cycle 15 after introduction of heterochromatic marks such as H3-K9me and localized HP1 during cycle 14. Furthermore, the distinct foci of satellite sequences seen at the beginning of cycle 14 are merged in an easily identifiable chromocenter in the apical part of the nucleus (Shermoen et al. 2010). Despite these differences, a connection between Rif1 and the replication program was still observed. At late anaphase of mitosis 14 and the onset of cycle 15,

Rif1 was recruited rapidly to separating chromosomes, and appeared especially bright over the leading edge of the advancing chromosomes, the site of pericentric satellite sequences that constitute the bulk of the heterochromatin. As the telophase nucleus formed, bright Rif1 signal was seen over the compacted chromatin of the chromocenter before the recruitment of PCNA to the nucleus (S2.4 Movie, S2.2 Fig). At the onset of S phase 15, PCNA was recruited only to euchromatic regions and it did not overlap Rif1 (Fig 2.2B). As S phase 15 progressed, PCNA was recruited to the edge of the compacted heterochromatin, where we have previously observed decompaction of HP1 staining chromatin (Shermoen et al. 2010). Although aggregated in a single mass in the nucleus (the chromocenter), individual satellite sequences remain as distinct subdomains and retain an individual replication schedule (Shermoen et al. 2010). In agreement with this, Rif1 staining was progressively limited to more restricted regions within the chromocenter, with latest Rif1 foci dispersing toward the end of S phase (Fig 2.2B). Real time records again documented a close connection between the loss of Rif1 from chromatin and the recruitment of PCNA to the underlying region.

Having followed the progress of S phase globally, we next wanted to examine the replication of a specific heterochromatic sequence, the 1.686 satellite repeat. 1.686 is a simple repeated sequence at four loci, one to the left and one to right of the centromeres of both chromosomes 2 and 3. All these foci replicate together and show characteristic delays in their replication time in cycles 13 and 14. TALE-light probes can be injected into embryos and used to track the repetitive DNA in real time (Yuan et al. 2014; Yuan and O'Farrell 2016). Purified mCherry labeled TALE-light protein recognizing the 1.686 repeat was injected into syncytial embryos and filmed. As reported previously, the TALE-light was gradually recruited to 1.686 during interphase, with the signal appearing as compact foci. During replication, the TALE-light signal became noticeably fuzzier, presumably due to the decompaction of the heterochromatic DNA during its active replication (Yuan et al. 2014). Upon completion of replication the TALE-

light signal was again compact and obviously brighter. We use this reproducible behavior to indirectly follow the replication of 1.686. During cycle 13, we observed that Rif1 was recruited to 1.686 at the beginning of S phase, and disappeared immediately before the decompaction and replication of the repeat. We observed intermediate intensities of Rif1 signal on 1.686 in the minute preceding its decompaction. Rif1 dissociation was relatively rapid, but progressive with the Rif1 signal decaying over the minute preceding 1.686 decompaction. After completing replication, 1.686 lacked Rif1 for the remainder of the cycle (Fig 2.2C, S2.5 Movie). Thus, Rif1 dissociates from this specific satellite immediately prior to the onset of its replication. We also examined fixed embryos using FISH probes to localize another heterochromatic repeat, AATAC, and showed that Rif1 was bound to this repeat AATAC during early S phase 14, but no such signal was observed in embryos aged to later in S phase after the replication of this sequence (Fig 2.2D). These observations show that Rif1 dissociates from specific satellite sequences upon their replication.

Our observations reveal that the dynamics of Rif1 interaction with chromatin parallel changes in replication timing. Rif1 association to satellite sequences began when these sequences first showed a slight delay in replication. While association was transient in the earlier cycles, Rif1 associated more persistently with satellites during the much-extended S phase of cycle 14. Most dramatically, Rif1 dissociated from individual satellite sequences at distinct times that align with the onset of PCNA recruitment to those sequences. The disappearance of the last foci of Rif1 staining marked the onset of replication of the latest replicating sequence and anticipates the end of S phase. These parallels suggest that binding of Rif1 to sequences might defer their replication until its dissociation. If so, analysis of this interaction may give us insights into the regulation of late replication and S phase prolongation.

Steps in the appearance of localized Rif1 in foci

Late replicating sequences have to be specified before the onset of replication if they are to avoid early firing. In yeast and mammalian cells in culture, this is thought to occur well before replication at a critical time during G1, known as the timing decision point (Raghuraman et al. 1997; Dimitrova and Gilbert 1999). However, in the G1-less embryonic cell cycles, the preparation for S phase is compressed and overlaps mitosis. Since cyclin:Cdk1 activity inhibits preparation of origins for replication, all of the preparations for replication happen between the down regulation of cyclin:Cdk1 at the metaphase anaphase transition and the onset of S phase upon entry into the next interphase. Real time observation of GFP tagged Orc2 protein revealed that Origin Recognition Complex (ORC) binds to the separating anaphase chromosomes prior to the midpoint of their separation (Baldinger and Gossen 2009). The MCM helicase is loaded shortly later in anaphase (Su and O'Farrell 1997). Replication begins at mitotic exit without obvious delay. This suggests that at the time of the transition from mitosis to interphase, there is already some type of feature that distinguishes the satellites so that they do not begin replication immediately (Shermoen et al. 2010). If Rif1 is to delay the replication time of specific sequences, we expect its recruitment to chromatin to occur during this period. Indeed, we observed binding of Rif1 to separating anaphase chromosomes before the recruitment of PCNA to the nucleus, which marks the start of interphase (S2.2 Fig). However, as described below in cycles prior to cycle 15, the specificity of Rif1 binding to satellite sequences emerges in concert with progression into interphase.

We examined the initial binding of Rif1 by filming mitosis 13 and early interphase 14. We observed an abrupt onset of faint and generalized binding of Rif1 to the chromosomes during late anaphase/telophase as previously observed in fixed samples (Fig 2.3A) (Xu and Blackburn 2004; Yamazaki et al. 2012; Sreesankar et al. 2015). Rif1 accumulation continued as the telophase nucleus formed. Although little was resolved in the compact and brightly staining

telophase nucleus, by 1 minute into S phase, brighter foci of staining became clear, and much of the nuclear signal quickly declined except in foci clustered at the apex of the nucleus where the foci of pericentric satellite sequences lie (S2.2 Movie, Fig 2.3A). Thus, while a low level of generalized binding is clear in mitosis, specificity in the binding became evident only in beginning of interphase, suggesting that there are two phases of binding. In contrast, in the transition to cycle 15, the initial binding of Rif1 in anaphase, while still weak, was not uniform. During late anaphase 14, Rif1 was clearly enriched at the leading region of the chromosome mass, where the pericentric heterochromatin resides (Fig 2.3B, S2.4 Movie). This localization to the heterochromatic region was visualized without interruption as Rif1 continued to accumulate with entry into interphase 15, which is accompanied by immediate onset of replication as this cycle still lacks a G1 phase. Thus, the character of the initial anaphase binding of Rif1 changes between anaphase 13 and anaphase 14. Satellite sequences acquire some of the markings of heterochromatin such as methylation and HP1 localization during interphase of cycle 14. These heterochromatic marks might then guide the initial interaction of Rif1 at anaphase 14, but they would not be available to do so in anaphase 13.

Because recruitment of Rif1 began late in anaphase, just after the time when Orc2 was recruited to chromosomes, we wondered if pre-RC formation might be involved in Rif1 binding. Indeed prior work in a *Xenopus* extract system suggests that this is true (Kumar et al. 2012). To test this, we examined Rif1 recruitment after the injection of embryos with purified geminin protein during mitosis 13. Geminin blocks the formation of the pre-RC by inhibiting Cdt1, a key helicase-loading factor and prevents subsequent replication. Injection of geminin did not block the initial generalized binding of Rif1 to the late anaphase chromosomes or its nuclear accumulation in telophase nuclei, but did block the emergence of localized Rif1 foci. Following geminin treatment Rif1 was diffusely localized throughout the nucleus during interphase 14. (Fig 2.3C). We conclude that geminin blocks the localization of Rif1 to late replicating sequences,

but emphasize that the results do not necessarily imply a direct involvement of pre-RC formation in this localization. Because geminin did not affect initial binding of Rif1, it might be the downstream consequences of a failure to assemble pre-RCs that produces the observed result.

Recruitment of Rif1 to satellite sequences prior to the MBT does not require the replication checkpoint activity

Beginning in cycle 11, the gradual lengthening of interphase depends in part on the conserved DNA replication checkpoint (Fogarty et al. 1994; Sibon et al. 1997). During cycle 13, the checkpoint is required to delay activation of Cdk1 during S phase and prevent premature entry into mitosis. Embryos mutant for the checkpoint kinase ATR (*mei41*) fail to delay mitosis 13 sufficiently and so enter a catastrophic mitosis before the completion of replication resulting in massive chromosome bridging (Sibon et al. 1999). Because Rif1 foci first became evident during these gradually slowing cycles, we wondered if the replication checkpoint might impact Rif1 recruitment. However, in *mei41* embryos, both the initial binding of Rif1 during anaphase of M12, and its subsequent recruitment to nuclear foci in interphase 13 were indistinguishable from control embryos (Fig 2.3D). We did observe that the disappearance of Rif1 foci was accelerated in *mei41* embryos, and Rif1 was lost from chromatin before entry into a catastrophic mitosis 13. We conclude that the recruitment of Rif1 to late replicating sequences is independent of the replication checkpoint, but that timing of Rif1 dispersal is accelerated in its absence.

Cdk1 activity promotes Rif1 release from chromatin during S phase

Prior work demonstrated that down regulation of Cdk1 activity at the MBT plays a key role in extending S phase (Farrell et al. 2012). Cdk1 activity during the earlier rapid cell cycles was shown to be required for satellite sequences to replicate early, and to sustain short S phases. The gradual decline in mitotic activators during cycles 11-13 contributes to the progressive lengthening of S phase. Finally, at the MBT, the abrupt drop in Cdk1 activity is

required for late replication and the resulting prolongation of S phase. These changes to Cdk1 parallel the changes we observed for Rif1 localization, so we investigated the connection between them.

Experimental reduction of Cdk1 activity by injection of RNAi against the 3 mitotic cyclins (A, B, and B3) during cycle 10 arrests embryos in interphase 13, and extends the length of S phase 13 from 13 minutes to an average of 19 minutes (Farrell et al. 2012). Cyclin knockdown also affected the dynamics of Rif1 chromatin association. In arrested embryos, foci of Rif1 binding persisted for an average of 16 minutes, compared to 8 minutes in control-injected embryos (Fig 2.4A, 2.4C). This delay in the loss of Rif1 foci paralleled, and slightly preceded, the delayed appearance of late replicating PCNA signal. In contrast, as previously reported, increasing Cdk1 activity during cycle 14, by injecting mRNA for the mitotic activator Cdc25, shortened S phase from over an hour to an average of 22 minutes and can result in an early mitosis 14, with no bridging, indicating that DNA replication was complete. Experimental Cdk1 activation also changed the Rif1 program. In Cdc25 injected embryos, foci of Rif1 association were evident for only an average of 18 minutes compared to 66 minutes in control-injected embryos (Fig 2.4B, 2.4C). Real time records documented that ectopic Cdk1 activity removed Rif1 from chromatin allowing the underlying satellite DNA to initiate replication without the characteristic delays normally observed in S phase 14 (S2.6 Movie, Fig 2.4B). We conclude that Cdk1 activity can accelerate both the release of Rif1 from chromatin and the late replication program. Both experiments demonstrate that the timing of Rif1 dissociation from chromatin and the subsequent initiation of late replication are sensitive to the activity of Cdk1 during S phase.

These results show that Cdk1 activity in early cycles normally promotes Rif1 dissociation from chromatin in pre-MBT embryos and that an artificial increase in Cdk1 in cycle 14 can do the same. The parallel effects of the experimental manipulations on Rif1 association and the progress of S phase further support suggestions that Rif1 association suppresses replication

and that activation of origins in satellite sequences occurs in conjunction with Rif1 dissociation. The influence of Cdk1 on Rif1 suggests that the developmental program of Cdk1 down regulation guides the observed changes in Rif1 dynamics and thereby, S phase duration. In light of these findings we can interpret the accelerated loss of Rif1 in *mei41* embryos (Fig 2.3D) as a consequence of the faster activation of S phase Cdk1 in the absence of the replication checkpoint (Deneke et al. 2016). The observations suggest that activity of the Cdk1 kinase directly or indirectly regulates Rif1 interaction with chromatin.

A phospho-site mutant Rif1 does not release from heterochromatin and prevents completion of DNA replication

Work from both *S. cerevisiae* and *S. pombe* indicates that the kinases CDK and DDK act on conserved phosphorylation sites to inhibit Rif1 and limit its ability to inhibit replication (Davé et al. 2014; Hiraga et al. 2014). In these yeasts, phosphorylation of Rif1 is thought to block Rif1's ability to recruit PP1, hence preventing Rif1 inhibition of replication initiation. Like yeast Rif1, the dipteran Rif1 homologs have a cluster of conserved CDK and DDK sites near the phosphatase interaction motif in the C-terminal part of the protein (Fig 2.5A, S2.3 Fig). This region of Rif1 is also proposed to contain a DNA binding domain (Sreesankar et al. 2012). These potential phosphorylation sites cluster in a region of the protein having high intrinsic disorder (Sukackaite et al. 2017) (S2.3 Fig) a feature associated with phosphorylation events that regulate interactions (Holt et al. 2009). Of particular interest are a number of conserved SS/TP motifs. DDK is known to phosphorylate the first serine in SSP motifs only after a priming phosphorylation by CDK on the second serine. Full phosphorylation of such sites is likely to require the dual input of both CDK and DDK. We further examined the role of the more C-terminal potential phosphorylation sites in regulating the late replication activity of Rif1.

To determine if Rif1 is phosphorylated *in vivo*, we examined Rif1 from 1-hour old embryos, a time when the abundant maternally provided Rif1 protein would be held inactive by

Cdk1. Protein extracts from pooled staged embryos were run on a phos-tag SDS-PAGE gel before or after treatment with lambda phosphatase and subjected to western blotting. All detectable Rif1 exhibited a phosphatase-reversed shift, indicating that most Rif1 is phosphorylated in the pre-MBT embryo (Fig 2.5B). Comparison of protein samples from pre-MBT and MBT age embryos revealed that the extent of the shift is somewhat reduced at the MBT stage, consistent with developmentally regulated reduction in the degree of phosphorylation (Fig 2.5B).

Two studies in yeast suggested that phosphorylation of Rif1 inhibits its function by blocking interaction with PP1a (Davé et al. 2014; Hiraga et al. 2014), although direct evidence for this idea is lacking, and the prior literature did not define a mechanism by which the repressive action of Rif1 is overcome. *Drosophila* Rif1 has previously been shown to bind to PP1a (Sreesankar et al. 2015), so we looked for a change to this interaction in conjunction with the developmental down regulation of Cdk1. As shown above, high Cdk1 activity in early pre-MBT embryos suppresses Rif1 association with chromatin and promotes a short S phase, whereas down regulation of Cdk1 at the MBT is required for Rif1 mediated extension of S phase. Rif1 was immunoprecipitated out of lysates derived from 20-minute collections of embryos aged for either 30 minutes (pre-MBT) or for 2 hours and 15 minutes (post-MBT). While we expected minimal association of PP1 to Rif1 in pre-MBT extract when Rif1 is robustly phosphorylated, western blotting showed a robust PP1 signal (Fig 2.5E). Additionally, Rif1 immunoprecipitated from the post-MBT extract was accompanied by a similar amount of PP1. Hence, the interaction between Rif1 and PP1a, at least at bulk levels, is not regulated in a way that explains the onset of late replication, and Rif1 appears to interact effectively with PP1 at early stages when it is phosphorylated and held inactive by Cdk1 kinase.

To further explore possible regulation of Rif1 by phosphorylation, we mutated candidate phospho-sites. We selected 15 S/T residues within CDK or DDK consensus motifs located in

the C-terminus of Rif1 and mutated them to alanine (Fig 2.5A) to prevent their phosphorylation. We reasoned that this phospho-site mutant Rif1, hereafter referred to as Rif1.15a, might not be inhibited by S phase kinases and so act as a dominant gain-of-function allele. Ectopic expression of Rif1.15a during the blastoderm divisions by injection of in vitro transcribed mRNA causes extensive anaphase bridging as typically seen when DNA replication is incomplete (Fig 2.5C). We never observed this effect after injection of mRNA encoding wild-type Rif1 arguing that this is not a simple overproduction phenotype. To test if the gain-of-function Rif1 mutant still operated through its associated phosphatase, we mutated the conserved PP1 interaction motif RVSF in the Rif1.15a construct. Ectopic expression of the resulting Rif1.15a-RaSa mutant did not disrupt cell cycle progression (Fig 2.5C). In addition, we generated transgenes expressing either wild-type Rif1 or Rif1.15a under UAS control. Overexpression of Rif1 in the eye imaginal disc (and more weakly throughout much of the head capsule) using the *eyeless*-Gal4 driver did not disturb eye formation whereas expression of Rif1.15a caused complete lethality with pupae developing into headless nearly adult flies (Fig 2.5D). The severity of this phenotype suggests that expression of Rif1.15a disrupted the early proliferative period of the eye-antennal disc. These assays suggest that Rif1.15a has a damaging gain-of-function action, as might be expected if it were immune to regulation of its ability to inhibit DNA replication.

Because our data indicated that the chromatin binding of Rif1 was regulated during S phase by Cdk1 activity, we examined the influence of mutation of the phospho-sites on Rif1 localization. Using mRNA injection, we expressed a GFP tagged version of Rif1.15a and followed its localization and the consequence of its expression in live records. Embryos were injected with Rif1.15a-GFP mRNA during cycle 12. The timing of this injection allowed sufficient fluorescent protein to accumulate that its behavior could be followed throughout cell cycle 14, while still minimizing the damage due to induced catastrophic mitoses in the earlier cycles. Rif1.15a was recruited to specific chromatin foci normally at the start of S phase, indicating that

the mutated residues are not required for the binding specificity of Rif1. Imaging Rif1.15a-GFP throughout cycle 14 yielded several interesting results that were never observed when imaging endogenous Rif1-GFP or ectopic wildtype Rif1-GFP expressed by mRNA injection. Unlike the dynamics of the wild-type protein, Rif1.15a continued to accumulate on heterochromatin throughout most of S phase 14. It then showed a slow decline but remained bound in the following G2 and into mitosis 14 (Fig 2.5E). The Rif1.15a foci on newly condensed mitotic chromosomes were localized to pericentric regions, where the satellites reside. On progression into anaphase, bridges were seen connecting the separating chromosomes and Rif1.15a-GFP specifically labeled these chromatin bridges (Fig 2.5E inset). As bridged nuclei exited mitosis, an unbound pool of Rif1.15a was recruited to the chromocenter, presumably after new pre-RCs were loaded. This abrupt recruitment of Rif1.15a shows that mutation of the selected sites did not fully eliminate cell cycle regulated behavior of Rif1. Nonetheless, the dramatic consequence of the phospho-site mutations shows that these sites contribute importantly to Rif1 dissociation from chromatin and that in the absence of dissociation Rif1.15a is capable of blocking replication to give anaphase bridging when chromosomes are driven into mitosis. In contrast to previous suggested mechanisms, we conclude that the repressive action of Rif1 on DNA replication is regulated by kinase driven dissociation from chromatin.

Rif1 is dispensable for survival and fertility

A recent study reported that Rif1 was an essential gene in *Drosophila* based on partial lethality of a ubiquitously expressed RNAi against Rif1 (Sreesankar et al. 2015). We created a precise deletion of the Rif1 ORF using Crispr-Cas9 (S2.4 Fig). While homozygotes for this allele have reduced survival, reproductively competent adult flies are produced, and *rif1* null flies can be propagated as a stock. Zygotic loss-of-function *rif1* mutants develop to adulthood with a reduced survival and a male to female ratio of 0.4 (n = 189 flies). Additionally, embryos laid by

rif1 homozygous mothers (hereafter called *rif1* embryos) have a reduced hatch rate (55% of control, n = 500 embryos). We conclude that Rif1 is dispensable in *Drosophila* at least in our genetic background, and we suspect that the previously reported lethality/sterility included enhancement of the loss-of-function phenotype by off-target effects of the RNAi. Though surprised by the viability of the Rif1 delete, it provided an opportunity to examine the phenotype of complete absence of function.

Rif1 is required for the onset of late replication and the prolongation of S phase at the MBT

Next we utilized the *rif1* null mutation to assess the role of Rif1 in the onset of late replication during cycle 14. As discussed previously, real time records of fluorescent PCNA allow us to follow the progress of S phase and estimate its overall length. In a wild-type S phase 14, PCNA is widely distributed throughout most of the nucleus during the first 10 minutes, but resolves into bright puncta that are obvious for over an hour into interphase, after which only a dim nuclear background is visible. During the final 30 minutes of S phase, a small number of bright PCNA foci appear and then disappear sequentially as a result of a protracted schedule of late replication (Fig 2.6A). By using the disappearance of the last PCNA focus as an indication of the completion of replication, we determined that the average S phase 14 lasts for 73 minutes (Fig 2.6A). In contrast, S phase 14 in *rif1* embryos from *rif1* mothers was significantly shorter, lasting an average of 27 minutes. Additionally, there were clear differences in the appearance of the PCNA signal as S phase progressed. The initial period of widespread early replication resolved into PCNA foci, but appearance of these foci was more simultaneous than sequential, and there was no protracted sequence of late foci (Fig 2.6A). Thus, this S phase 14 resembled the earlier S phases, in showing a marginal extension with slightly delayed replication of some foci. However, the normally dramatic extension of S phase 14 is dependent on *rif1*. Failure to extend S phase 14 was observed in all embryos derived from homozygous mothers even

though heterozygous fathers were included in the cross. We conclude that maternal Rif1 is required for the normal extension of S phase 14.

Because we had observed that the satellite 1.686 recruited Rif1 during S14, we wondered if its replication time would be altered in *rif1* embryos. To measure the replication time of this repeat, we injected the GFP-1.686 TALE probe into wild-type and *rif1* embryos expressing mcherry-PCNA and recorded S phase 14. We used the transient recruitment of mcherry-PCNA, and the obvious decompaction of the marked 1.686 sequences as indicators of active replication of 1.686. In control embryos, the 1.686 repeat began replication 18 minutes into S14 and completed by 30 minutes (Fig 2.6B). In contrast, in *rif1* embryos, 1.686 began replication by 4 minutes into S14 and completed by 13 minutes (Fig 2.6B). We conclude that the 1.686 satellite sequence replicates with a minimal delay in S phase 14 in the absence of Rif1, and that the normally substantial delay requires Rif1.

During the MBT, the embryo degrades both the mRNA and protein of the mitotic activator Cdc25. This allows the introduction of the first embryonic G2 after the completion of the prolonged S phase 14. Mitosis 13 is then the last synchronous division during development, and mitosis 14 relies on the developmentally patterned zygotic expression of new Cdc25. Perturbations that interfere with the downregulation of Cdk1 can lead to an additional synchronous mitosis. Additionally, since down regulation of Cdk1 occurs during S phase 14, the embryo can also progress to an additional synchronous mitosis if S phase is eliminated or dramatically shortened, as seen following injection of geminin or alpha-amanitin, respectively (McClelland et al. 2009; Shermoen et al. 2010). We noticed that a small number of *rif1* embryos (7%) executed an early mitosis 14 at approximately 30 minutes into interphase. The observed mitoses were complete, with no bridged chromosomes, but there was substantial nuclear fall in (Fig 2.6C, S2.7 Movie). We interpret the incomplete penetrance of the extra-division phenotype to be an indication that the duration of S phase in *rif1* null embryos is close to a threshold, so

that in most embryos the cyclin:Cdk1 activity declines enough to introduce a G2, but in some embryos the residual maternal cyclin:Cdk1 function remains high enough to trigger mitosis upon the completion of the shorten S phase. The result shows that Rif1 is important for reliable coordination of the MBT.

Previous work has shown that before the MBT, Cdk1 is required for driving a short S phase. Our finding that Cdk1 activity suppresses Rif1 function in cycle 14 (Fig 2.4) suggests an explanation for the early role of Cdk1 in promoting short S phases; interphase activity of Cdk1 prevents Rif1 from prematurely introducing late replication. This model predicts that reducing Cdk1 activity would not be able to prolong a pre-MBT S phase in the absence of *rif1*. To test this idea we examined S phase 13 in wild-type or *rif1* embryos after knockdown of mitotic cyclins, essential activators of Cdk1, by RNAi. Wild-type control injected embryos exhibit transient but obvious foci of PCNA staining during late S phase 13 and replicate their satellite sequences with a slight delay in this S phase. While *rif1* embryos still exhibit PCNA foci, these foci are even shorter lived (Fig 2.6D). Following injection of mitotic-cyclin RNAi, wild-type embryos increased the duration of S phase 13 from 14 minutes to 20 minutes. In contrast, *rif1* embryos did not extend S phase after cyclin knock down (Fig 2.6D). This demonstrates that the requirement for Cdk1 in the timely completion of S phase 13 can be bypassed by loss of *rif1*. However, S phase 13 in the *rif1* mutant embryos is still longer than very early embryonic S phases, which can be as short as 3.4 min. Thus, Cdk1 down regulation of Rif1 contributes to S phase prolongation in cycle 13, but there must be additional factors influencing the progressive prolongation of early cycles.

Cdc7* is essential during the early embryonic S phases and the requirement can be substantially bypassed by removal of *rif1

The Cdc7-Dbf4 kinase complex (or DDK – Dbf4 dependent kinase) is required for origin initiation in many systems. In *S. cerevisiae*, the essential function of DDK is thought to be the

phosphorylation of the MCM helicase complex during pre-RC activation (Sheu and Stillman 2010). In both *S. pombe* and *S. cerevisiae*, the deletion of *rif1* partially rescues S phase and viability in *cdc7* mutants. Two functional interactions have been proposed to contribute to this finding. DDK appears to phosphorylate and inactivate Rif1, thereby activating replication by a derepression input. Indeed, the presence of conserved DDK phosphorylation motifs in Rif1 suggests that DDK may synergize with CDK in the inactivation of Rif1. This input would be dispensable in a *rif1* mutant. Additionally, Rif1 is thought to inhibit replication by recruiting PP1 to the origin and dephosphorylating the MCM helicase, an action that opposes DDK. The loss of this opposing activity in a *rif1* mutant might reduce, but would eliminate the DDK activity required for MCM phosphorylation. We wanted to assess the possible parallels in *Drosophila* to clarify the involvement of Rif1 in replication control.

Despite strong conservation, *cdc7* has not been well studied in *Drosophila*. In *Drosophila*, *cdc7* is an essential gene, and recent work has demonstrated that in complex with the *dbf4* ortholog *chiffon*, *Drosophila* Cdc7 can phosphorylate Mcm2 *in vitro*, and that *cdc7* is required for endocycle S phases in follicle cells (Stephenson et al. 2015). However, the function of DDK during mitotic S phase has not been described.

To address this issue, we first tagged endogenous *cdc7* with GFP using CRISPR-Cas9. The resulting *cdc7-GFP* stock was healthy and fertile indicating that the tag did not disrupt the essential function of Cdc7. Time-lapse imaging of Cdc7-GFP embryos during syncytial development revealed that Cdc7 localization was cell cycle regulated. Cdc7 was nuclear during interphase, dispersed into the cytosol during mitosis, and was rapidly recruited to late anaphase chromosomes and concentrated in the telophase nucleus (Fig 2.7A). Initial Cdc7 recruitment featured two transient bright foci followed by fine puncta suggesting that it is recruited to chromatin at the time at which pre-RCs are undergoing activation during the syncytial cell cycles. Comparison of nuclear Cdc7 at equivalent times in subsequent cell cycles (early S

phase) leading up to the MBT revealed a decline in the per-nucleus protein signal. Since nuclear size decreases with each division, if the amount of Cdc7-GFP in each nucleus were constant throughout these cycles, then the local intensity (concentration) of nuclear fluorescence would increase with each division. Instead brightness decreases. This observation is consistent with subdivision of limited and/or declining pool of Cdc7 among an increasing number of nuclei. If level were limiting, this would result in diminishing availability of Cdc7 to fire origins in later cycles (Fig 2.7B, S2.8 Movie).

To determine if *cdc7* is required for DNA replication during the early cell cycles, we depleted DDK from the embryo using maternal-tubulin Gal4 to drive RNAi against *cdc7* during oogenesis. This setup did not interfere with egg production, although we found that expression of RNAi against *cdc7* using the earlier acting MTD-Gal4 did cause severe defects in egg morphology, indicating that *cdc7* does play a role in the female germline. Embryos depleted of Cdc7 using maternal-tubulin Gal4 failed to hatch. Cytological examination of Cdc7 depleted embryos revealed penetrant defects during the early pre-blastoderm divisions. We observed multiple highly fragmented DNA masses that were unevenly distributed in the embryo interior, along with scattered abnormal mitotic structures (Fig 2.7C). In all cases nuclei failed to form a blastoderm, although in many cases centrosomes appeared to continue to duplicate in the absence of any associated DNA (Fig 2.7C). Such a dissociation of the embryonic nuclear and centrosome cycles has been described before in embryos injected with the DNA polymerase inhibitor aphidocolin during the pre-blastoderm cycles (Raff and Glover 1988). We conclude that Cdc7 is essential for effective nuclear cycles in the early embryo consistent with a requirement in DNA replication.

Next, we tested for a genetic interaction by depleting Cdc7 from *rif1* mutant embryos using maternally expressed RNAi at 29°C. In the absence of *rif1*, 2% (n=242) of Cdc7-depleted embryos hatched. While Cdc7-depleted embryos from mothers heterozygous for *rif1* (*rif1*⁺)

never hatched (Fig 2.7E). Cytological examination demonstrated that removal of *rif1* restored cell cycle progression to Cdc7-depleted embryos. *rif1* mutants completed substantially more cell cycles than heterozygous control embryos, with most progressing to the blastoderm stage. Many of the blastoderm rescued embryos showed abnormalities such as substantial nuclear fall in, disorganized nuclear spacing, and non-uniform nuclear density. Nonetheless, some of the observed embryos attempted cellularization and gastrulation (Fig 2.7D) with the rare cases of hatching indicating occasional success. Reducing the temperature to 25°C, thereby reducing the activity of the Gal4 protein driving the RNAi, improved the hatch rate of *rif1* mutant embryos to 21% (n=281) while still causing 100% lethality in embryos from *rif1* heterozygous mothers (Fig 2.7E). We conclude that deletion of *rif1* can restore embryonic cell cycle progression and early development to Cdc7-depleted embryos. However, this rescue is incomplete, likely because of altered regulation of the restored S phase in such doubly defective embryos.

The Rif1-regulated onset of late-replication precedes the establishment of heterochromatic marks

Early embryonic chromatin lacks specializations that come to distinguish different regions of the genome at later stages. Thus, the order of appearance of different specializations can give us insight into the hierarchy of regulation. Since late replication is considered a feature of heterochromatin, we expected its emergence to follow the embryonic appearance of the hallmarks of heterochromatin. Our recent work described the onset of localized H3K9me2/3 and HP1a (Yuan and O'Farrell 2016). While a very low level of modification and chromatin bound HP1a was detected before the MBT, a period of abrupt accumulation of HP1a and more extensive H3K9me2/3 modification only occurred later, during S phase 14. Here we explore the relationship between this HP1a-centered program and the action of Rif1 in the control of late replication.

During cycle 14, Rif1-GFP and HP1a-RFP bound to localized foci in the same position, but never at the same time. Rif1 foci disappear sequentially during cycle 14, while HP1a is diffusely localized in early cycle 14 and is subsequently recruited to apical foci that multiply and intensify. Importantly, in live imaging of Rif1-GFP and HP1-RFP, we don't observe any overlap between the two signals in S14 (Fig 2.8A). This finding is in accord with our finding that PCNA foci and Rif1 do not overlap (above), and our previous demonstration that PCNA and HP1 foci do not overlap in cycle 14 (Shermoen et al. 2010). Together with the timing of recruitment of these proteins to specific satellites, these observations show a sequence in which satellites lose associated Rif1 before they initiate replication as marked by PCNA, and then complete replication before binding HP1. We conclude that the introduction of late replication by Rif1 precedes the binding of HP1a in cycle 14. In contrast, at the start of cycle 15 both Rif1 and HP1a are rapidly recruited to the chromocenter, with Rif1 binding slightly earlier (Fig 2.2B, 2.3B), and we have previously detected an influence of HP1 on replication timing in this cycle (Yuan and O'Farrell 2016).

Given the earlier binding of Rif1 to satellite sequences in cycle 14, Rif1 might direct subsequent heterochromatin formation. In fission yeast, Rif1 is required for the maintenance of silencing at some heterochromatic sites in the genome (Zofall et al. 2016). We examined whether Rif1 influences the emergence of HP1a-bound heterochromatin. GFP-HP1a was injected into either wild-type or *rif1* null embryos and imaged during cycle 14. We observed no difference between HP1a recruitment between the two genotypes, indicating that HP1a binds independently of Rif1 in the fly embryo (Fig 2.8B).

We had previously found that the recruitment of HP1a to the 359 bp-repeat satellite-sequence during cycle 14 occurred only after its replication and was unimportant to the replication timing of this satellite in S phase 14. However, this recruitment of HP1a was required for a shift of 359 replication to a much later time in S phase of cycle 15 (Yuan and

O'Farrell 2016). Because our results demonstrate that the recruitment of HP1a to the heterochromatin during S phase 14 is independent of Rif1, we wondered if the replication time of 359 was altered in *rif1* embryos in cycle 15. Live imaging of mCherry-PCNA expressing *rif1* embryos injected with GFP-359 TALE probes indicated that 359 still replicates late during S15 (Fig 2.8C). We conclude that an HP1a dependent program can delay replication of 359 sequences in cycle 15 without Rif1 input. It seems likely that this HP1a dependent program operates to influence the replication of many heterochromatic sequences after cell cycle 14.

DISCUSSION

We studied the onset of late replication in its natural setting during early embryogenesis. We evaded complexities that are added later, by this focus on the first delays in replication of particular sequences. We achieved three things of importance. We show how S phase is dramatically extended at the embryonic MBT by Rif1 mediated temporal programming of replication. We show that this temporal program does not rely on other features of heterochromatin, such as HP1 binding, that are only introduced later in development. We detail precise coordination of Rif1 dissociation from chromatin foci with the onset of their replication. Together, our findings suggest that an interplay of Rif1 and S phase kinases governs developmental prolongation of S phase at the MBT and underlies a timer of the replication program in this first extended S phase.

One of our central findings is that Rif1 function is responsible for the onset of the late replication program in cell cycle 14. Since Rif1 is provided maternally and present at high levels during the earlier rapid cycles, something must be limiting its action prior to the MBT. Previous work showed that timely completion of the pre-MBT S phases requires persistent Cdk1 activity. We found that Cdk1 activity promotes dissociation of Rif1 from chromatin and inhibits its function as a replication inhibitor, and that the requirement for high Cdk1 for a rapid early S

phase was eliminated in Rif1 mutant. Thus, Cdk1 activity suppresses pre-MBT function of Rif1 to promote early rapid S phases. But Cdk1 does not appear to act by itself in suppressing early Rif1 function. While early embryonic cycles were arrested by depletion of Cdc7, loss of Rif1 suppressed this defect, suggesting that a major role of Cdc7 is to suppress the maternal pool of Rif1. Thus, while Cdc7 may also act to directly stimulate the replicative helicase, it appears to act as suppressor of the replication inhibitor Rif1, an action that is bypassed if Rif1 is absent. Consequently, we suggest that both CDK and DDK kinases are critical to prevent pre-loaded Rif1 from interfering with rapid S phase completion in early cycles. Indeed, SS/TP motifs, whose full phosphorylation is expected to require priming by CDK followed by DDK action, are conserved among distantly related insects (Fig S2.3). We suggest that collaboration between CDK and DDK is essential for the full regulation of Rif1. After the MBT downregulation of Cdk1, DDK may function with Cdk2, but together they are less proficient at driving Rif1 dissociation from late origins.

Importantly, the ability of Cdk1 to limit Rif1 function provides a key link in the developmental control of the MBT. A developmental decline in Cdk1 triggers the extension of the cell cycle at the MBT (Farrell and O'Farrell 2014; Yuan et al. 2016). However, it was not previously apparent how a decline in Cdk1, a mitotic kinase, would trigger the abrupt extension of S phase that marks the onset of cell cycle slowing at the MBT. We show that decline of Cdk1 activity is necessary and sufficient to release constraints on the pool of Rif1, which then acts to extend the S phase 14 (Summarized in Fig 2.9). Unlike other cell cycle transitions, which are associated with marked regulatory changes, the end of S phase is defined simply by the completion of replication. Due to a progressive reduction in the amount of DNA undergoing replication as S phase progresses, assessments of the very end of replication are expected to vary depending on sensitivity as well as methods of replication detection and timing. The real-time observation method that we have used here defines the end of S phase as the time of

dissipation of the last PCNA focus. It was previously validated as a measure of S phase length in studies comparing incorporation of injected fluorescent deoxy-triphosphates to the progressive dispersal of fluorescent PCNA foci in the *Drosophila* embryo (Shermoen et al. 2010). We show that Rif1 binds the last-detected focus of replication until it begins its much-delayed replication during S phase 14. This long S phase is then followed by the first embryonic G2, and a mitosis that is triggered by patterned zygotic transcription of Cdc25.

Embryos provide a unique situation in which to study the role of time in biology, because development progresses through a stereotyped sequence of events. Our work takes advantage of this in two ways. First, because events that occur early cannot be caused by events that happen only later, our description of the sequential emergence of the different features and behaviors that characterize heterochromatin tests the interdependence of these features. During the rapid pre-MBT cell cycles the satellite DNA is already compacted prior to appearance of other heterochromatic features (Shermoen et al. 2010). Upon Cdk1 down regulation at the MBT, we now show that Rif1 binds to the satellite sequences and delays their replication, marking onset of late replication in cycle 14. Satellite-repeat sequences only begin to accumulate obvious HP1a after their replication in cycle 14, on time to contribute to delayed replication in later cycles but not during S phase 14 (Shermoen et al. 2010; Yuan and O'Farrell 2016). Second, embryos provide us with precision. By following a natural late replication program in a specific cell cycle using live imaging, we achieve high temporal resolution. During the first post-MBT S-phase different satellite sequences replicate according to a stereotyped schedule (Shermoen et al. 2010); we now detail precise coordination of Rif1 dissociation from chromatin foci with the onset of their replication. We further show that Rif1 is required for this temporal program and that a mutant of Rif1 that resists dissociation blocks replication. Finally, the impact of CDK/DDK on Rif1 suggests that interplay of Rif1 and S phase kinases underlies a timer for a late replication program.

Isolating a function of Rif1 as a developmental regulator of the replication timing program

Rif1 is widely conserved and it has been implicated in several functions, notably, the control of telomere growth, replication timing, and DNA damage response (Mattarocci et al. 2016). Despite this complexity, the association of Rif1 with replication timing in our studies appears to be uncomplicated by other actions of Rif1. Two factors are likely to contribute to this. First, it is not clear that Rif1 serves the same spectrum of functions in all of the organisms in which it is found. For example, the distinctive telomeres of *Drosophila* do not appear to be regulated by Rif1 (Sreesankar et al. 2012). Additionally, previous tests of the function of *Drosophila* Rif1 in cultured cells and when ectopically expressed in other species suggested that *Drosophila* Rif1 protein might lack some functions attributed to the Rif1 of other species (Sreesankar et al. 2012). Second, even if the *Drosophila* Rif1 protein has additional functions at other stages in the life of the fly, the first time Rif1 functions in embryogenesis, its role appears to be to impose a replication-timing program on S phase. Thus, this developmental context can isolate the replication-timing role of Rif1 from other potential functions.

Programmed interaction of Rif1 with satellite sequences guides their timing of replication

Developmentally programmed association of Rif1 with satellite sequences marks the onset of late replication: We have previously characterized the program of replication of satellite sequences. Prior to cell cycle 11, when satellite sequences are early replicating, we did not detect significant recruitment of Rif1 to chromatin. In subsequent pre-MBT cycles, when slight and incrementally increasing delays in satellite sequence replication occur, we see brief association of Rif1 to individual blocks of satellite sequence, and an advance in their replication in *rif1* mutant embryos. In pace with the gradual increase in the delay of satellite replication, this Rif1 association persists longer in successive cycles (Fig 2.1D). In time with the MBT and a

dramatic extension of cell cycle 14, we detect more persistent association of Rif1 to satellite sequences.

Within each cell cycle, Rif1 dissociation from individual satellite sequences marks the onset of their replication: Individual satellites, each a distinct array of repeats, initiate replication as a unit at a particular time within S phase 14 (Shermoen et al. 2010). The disappearance of different Rif1 foci during S phase parallels the schedule of late replication for the different satellite repeats. Indeed, high-resolution imaging demonstrated that the dissociation of Rif1 is followed closely by the recruitment of PCNA and replication. In addition, TALE-light probes against the satellite 1.686 allowed us to visualize the association of Rif1 with this repeat during S phase. Rif1 staining overlapped that of the satellite early in S phase and Rif1 dissociated in mid S phase just before the decompaction and replication of the underlying DNA (Fig 2.2). Finally, expression of the Rif1.15a gain-of-function mutant blocked dissociation of Rif1, and prevented complete replication (Fig 2.5). Thus, the dissociation of Rif1 coincides with and is needed for onset of replication.

Phosphorylation controls the association of Rif1 with late replicating chromatin: The control of pre-RC activation by the kinases CDK and DDK appears to be widely conserved among eukarya (Siddiqui et al. 2013). The two kinase-types act by parallel mechanisms phosphorylating their respective target sites in the N-terminal regions of MCM2 and MCM4 to promote activation of the pre-RC. Activation usually requires collaboration of the two kinases. These kinases are active from the outset of S phase, suggesting that the timing program of replication within S phase involves local regulation of their action. Rif1 has emerged as a key regulator of this same step and it appears to have two types of interactions with the activating kinases. Rif1 inhibits and delays replication initiation by recruiting PP1 to the genome where its ability to dephosphorylate kinase targets counters the action of DDK and likely CDK. Additionally, DDK and CDK inhibit Rif1, resulting in de-repression that further promotes pre-RC

activation in a feed-forward action (Fig 2.5 and 2.7) (Davé et al. 2014; Hiraga et al. 2014). We document the opposing action of Rif1 and DDK in the early fly embryo by showing that the Rif1 mutation dramatically suppresses the phenotype of a knockdown of Cdc7, a genetic interaction analogous to those shown in yeasts.

When Cdk1 activity is especially high at metaphase, Rif1 is absent from chromosomes. After metaphase/anaphase inactivation of Cdk1, Rif1 associates with the separating anaphase chromosomes (Fig 2.3) (Xu and Blackburn 2004). Manipulations and mutations that promote Cdk1 activity accelerate dissipation of Rif1 from chromatin (Fig 2.3D, Fig 2.4). Reciprocally, inhibition of Cdk1 during pre-MBT S-phases increases the amount of time Rif1 spends in foci. Additionally, Rif1 has conserved clusters of Cdk1 target sites, and we observed increased phosphorylation of Rif1 during the early cycles when Cdk1 activity is high and when Rif1 shows minimal association with chromatin. Finally, mutation of 15 CDK and DDK consensus sites in the C-terminus of Rif1 largely prevented dissociation of Rif1 from chromatin and blocked completion of DNA replication. Additionally, DDK also appears to contribute to suppression of Rif1 activity in early embryos. This follows from our finding that Rif1 mutation restored cell cycle progression to embryos blocked by knockdown of DDK (Cdc7). Apparently, Rif1 is active (destructively) in the early embryo without DDK suppression. Thus, both types of S-phase-activating kinase suppress Rif1 activity, a coherent feed-forward input that supports direct action of these kinases to activate the Pre-RC (Fig 2.9).

In budding and fission yeast, it was suggested that DDK inhibits Rif1 by promoting release of PP1 [37][38]. *Drosophila* Rif1 also interacts with PP1a, but we have not detected a change in this interaction when comparing two stages, one in which high Cdk1 prevents Rif1 function and a stage when Cdk1 is inactive (Fig 2.5). Instead, we see regulation in the association of Rif1 to chromatin. The addition of ectopic Cdk1 activity during S phase 14 drove rapid dissociation of Rif1 from chromatin and completion of late replication without delay (Figure

2.4B, S2.6 Movie). Although we can't exclude regulation of phosphatase binding, our results demonstrate a key role for phosphorylation-regulated chromatin binding of the *Drosophila* Rif1. Perhaps both mechanisms operate. Since the regulatory architecture is the same, different organisms might emphasize different means of Rif1 inhibition.

The observed program of Rif1 dissociation suggests that the process could play a role in a mysterious feature of replication timing. At least in higher organisms, large domains of the genome replicate as temporal units at a specific time during S phase, a phenomenon that requires coordinate firing of many linked origins (Jackson and Pombo 1998). Concerted dissociation of Rif1 from each satellite sequences is followed by the recruitment of PCNA to the entire domain, suggesting that behavior of Rif1 might coordinate the firing of the numerous origins within each large block of repeating sequence. How might region-specific dissociation of Rif1 itself be coordinated? Our data suggests that dissociation is promoted by phosphorylation of Rif1 (Fig 2.9). Since Rif1 is known to recruit PP1, the localized phosphatase could counter the action of the kinases, protecting Rif1 from dissociation. This antagonism between kinase activity and localized PP1 could create a bistable circuit. Domains enriched in Rif1 would also be enriched in PP1, which could locally protect Rif1 from the kinases. However, even a slow rate of Rif1 release would eventually give the kinases the upper hand within the domain. At the tipping point dissociation of Rif1 would accelerate. Since our findings show coordinate release of Rif1 from large domains of the genome and show that Rif1 release is coupled to onset of replication, we suggest that the circuit regulating Rif1 release functions both as timer and as a means of coordinating the firing of origins in local domains.

S phase extension at the MBT involves interplay of Rif1 and kinases

Our identification of the role of Rif1 in extending S phase and identification of kinase inputs influencing Rif1 activity have implications regarding the control of early embryonic development and mechanisms governing the slowing of the cell cycle at the MBT. In

Drosophila, the early increases in cell cycle duration are coupled to increases in the time required for S phase (McClelland et al. 2009; Shermoen et al. 2010; Edgar et al. 1994; Sibon et al. 1997). This increase in S phase duration is due to the onset of delays in the replication of satellite sequences in S phase (Shermoen et al. 2010). Prior work showed that the activity of Cdk1 influences the delays in satellite replication and the extension of S phase (Farrell et al. 2012). The speed of the early cycles required high Cdk1, and the abrupt extension of S phase at cycle 14 depended on an MBT associated sharp reduction in interphase Cdk1 activity. The findings reported here show Rif1 associates with satellite sequences and delays their replication upon the downregulation of Cdk1. Thus, the regulatory connection between Cdk1 and Rif1 couples S phase prolongation, and hence cell cycle prolongation with Cdk1 downregulation.

We found that maternally supplied Rif1 is present ubiquitously throughout the pre-MBT cell cycles, and so we suggest that CDK and DDK kinases are critical to prevent maternally supplied Rif1 from interfering with rapid S phase completion in early cycles. There is progressive reduction of Cdk1 activity in successive interphases prior to the MBT [48] that allows limited Rif1 association to satellites during cycles 11-13, and this association persists longer in each cycle. Cdk1 activity is normally required during these S phases for their timely completion, and we show that this requirement can be bypassed by mutation of *rif1* (Fig 2.6). However, while the abrupt cycle-14 extension of S phase required *rif1*, only a portion of the incremental and progressive extension of S phase required *rif1* and gradual prolongation of S phase still occurred in *rif1* mutant embryos, suggesting that there are other inputs.

Rif1 independent contributions to S phase duration

In *rif1* embryos, the early 3.4 min S phase is extended to 27 min by cycle 14. Although much shorter than the 72 minute S phase 14 in wild-type embryos, this *rif1*-independent extension of S phase resembled progression normally seen in the earlier blastoderm cycles (11-13). A long-standing suggestion for embryonic slowing of the cell cycle is that the increasing

number of nuclei titrate factors required for the speedy early S phases. Several factors might limit pre-RC activation. For example, Cdc7 has an input as demonstrated by its genetic interaction with Rif1. Given that we saw diminishing concentration of nuclear Cdc7 as it was distributed to an increasing large number of nuclei over successive divisions, it is possible that developmental declines in this activating input could contribute to slowing of S phase, although at present we do not have evidence demonstrating that this decline is of regulatory importance. Notably, the concentrations of several proteins that are recruited to the pre-RC during its maturation influence the speed and efficiency of pre-RC activation in yeast and in *Xenopus* (Mantiero et al. 2011; Collart et al. 2013).

Investigations of S phase extension occurring at the *Xenopus* MBT have emphasized multiple inputs influencing activation of the pre-RC (Collart et al. 2013; Walter and Newport 1997). A recent analysis suggested that Drf1, the activating subunit for the Cdc7 kinase in the *Xenopus* embryo, is subject to active destruction at the MBT (Collart et al. 2017). Failure to down regulate DDK sensitized embryos to the further stress of overproduction of three replication factors that promote pre-RC maturation. Indeed, the authors suggest that titration of the maternal supply of these three replication proteins cooperate with active destruction of Drf1 to slow S phase at the MBT. Thus, evolution appears to have brought the same regulatory step under developmental control in very different organisms, but many factors complicate a comparison between systems, and here we emphasize that the detail of the dissection of the process in *Drosophila* has led us to a specific conclusion regarding Rif1 control of cell cycle slowing at the MBT in this organism.

In contrast to the early progressive slowing of the cell cycle in *Drosophila* embryos, the abrupt extension of cell cycle 14 shows features of a distinct regulatory transition. It has switch-like features (Lu et al. 2009). The triggering of this sudden extension of S phase is not simply due to a limitation of a factor, because, unlike the earlier progressive extension of S phase,

inhibition of transcription prevents the abrupt extension (Shermoen et al. 2010). This shows that existing materials are adequate to support another relatively fast cycle and that the extension of cycle 14 involves an active process. And importantly, we have previously shown that the key event in triggering the extension is the downregulation of cyclin:Cdk1 (Farrell et al. 2012; Farrell and O'Farrell 2013). Here, we show that it also depends on the positive action of Rif1 as a repressor of replication and that this activity of Rif1 depends on the downregulation of Cdk1. In summary we suggest that there are two distinct phases of S phase prolongation operating in the *Drosophila* embryo, one progressive and earlier and one abrupt and occurring at the onset of cycle 14. The *rif1* mutant is defective in the abrupt event that marks the MBT.

Implications of the dispensability of Rif1

We found it surprising that *rif1* mutants have a highly penetrant phenotype with a specific failure to prolong S phase 14, but yet produce viable progeny. This means that the prolongation of S phase 14 is not essential and that subsequent contributions of *rif1* to development and survival are also dispensable. We would like to put this in context.

Our *rif1* deletion allele is not without major consequences. Both hatching of maternally deficient embryos and survival of zygotically deficient flies are compromised. So Rif1 appears to be important, but a detailed characterization will be required to understand its contributions to survival. Nonetheless, it is clear that mutant embryos with a 27 min S phase 14 instead of the normal S phase duration of more than an hour can hatch. *rif1* mutant embryos still undergo an MBT and the majority of the embryos slow their cell cycle because they arrest in a G2 after their abnormally fast S phase 14. A minority of the embryos undergoes a complete or partial extra syncytial cycle suggesting that S phase timing contributes to regulation that normally introduces a G2 into the cell cycle at the MBT with great reliability.

The late replication program in cell cycle 14 precedes obvious appearance of heterochromatic marks on satellite sequences (Yuan and O'Farrell 2016). These marks do appear later in cell cycle 14 and their appearance was not compromised in the absence of Rif1. Thus, neither the selective localization of Rif1 to satellite sequences nor the specific time of replication of the satellites in cycle 14 are required to trigger or guide the appearance of the heterochromatic marks. Importantly, we showed previously that recruitment of HP1a and associated acquisition of other heterochromatin marks delays replication of the X chromosomal 359-satellite repeat in cycle 15 (Yuan and O'Farrell 2016). Here we show that in the absence of Rif1, the 359 repeat still exhibits late replication in cycle 15, suggesting that heterochromatin can act by a Rif1 independent pathway to cause replication delay. While *rif1* mutant embryos may show subtle alterations in the program of late replication in later cycles, presently the unique dependency of replication timing on Rif1 function appears limited to a narrow window of developmental time. Thus, survival of *rif1* mutants does not assess the importance of late replication per se, only the impact of the delay in cycle 14.

Concluding remarks

Embryonic development presents early cell cycles with an unusual challenge – regulating cell division in the absence of transcription. Perhaps because of this early constraint, the biology of early embryos is streamlined and lacks many regulatory processes that appear later in development. When development introduces complications, it does so incrementally, highlighting individual regulatory circuits. By focusing on early development, we have been able to isolate and study the contributions of Rif1 to late replication and to S phase length. Our work uncovers a special developmental function for Rif1 in controlling the timely prolongation of S phase at the Mid Blastula Transition, and provides new insight into the control of late replication.

ACKNOWLEDGEMENTS

We thank past members of the O'Farrell laboratory, especially Kai Yuan, Antony Shermoen and Mark McClelland, for guidance and reagents. We also thank Danielle O'Farrell for early work on this project. The Bloomington stock center and *Drosophila* community provided important reagents throughout this work.

FIGURE 2.1

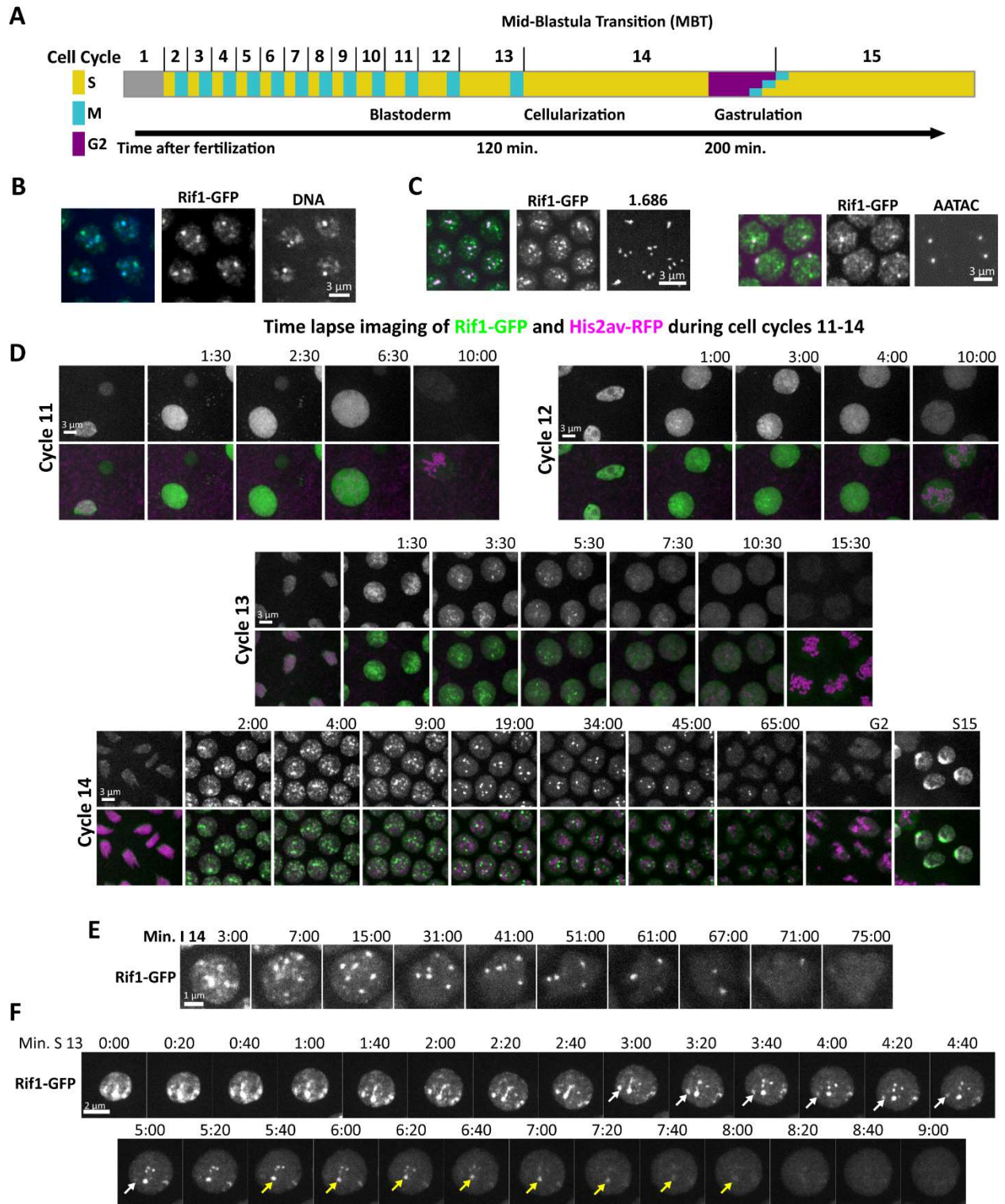


Fig 2.1. Rif1 forms foci on heterochromatin as the embryonic S phase lengthens. (A)

Diagram highlighting the key changes to the cell cycle and to embryonic morphology during early development. The initial prolongation of the cell cycle is due to the increase in the length of S phase. This occurs gradually during cycles 11-13, and then the onset of a late replication program in S phase 14 extends interphase considerably. The first G2 is introduced in cycle 14, after which cells enter mitosis 14 asynchronously, according to a developmental pattern. **(B)** Nuclei from an S phase 14 Rif1-GFP embryo stained for GFP (green in the merge) and DNA (DAPI: blue in the merge). Rif1 co-localizes with regions of the interphase nucleus that stain intensely with DAPI. **(C)** Specific satellites (magenta in the merge), either 1.686 detected live by TALE-light or AATAC detected by DNA FISH co-localized with Rif1-GFP (green in merge) during early cycle 14. **(D)** Frames from live imaging (accompanied by S1 Movie) showing Rif1-GFP and H2aV-RFP in developing embryos during cell cycles 11-14. Note the initial presence and increasing persistence of nuclear Rif1 foci as interphase lengthens. **(E)** Magnified images from time-lapse records of Rif1-GFP during S phase 14. Individual nuclear foci of Rif1 disappeared at different times across S phase. **(F)** Frames from time lapse showing Rif1-GFP in a single nucleus at 20 sec intervals during S phase 13 (accompanied by S2 Movie). Arrows indicate two specific foci at the time that their fluorescence declined.

FIGURE 2.2

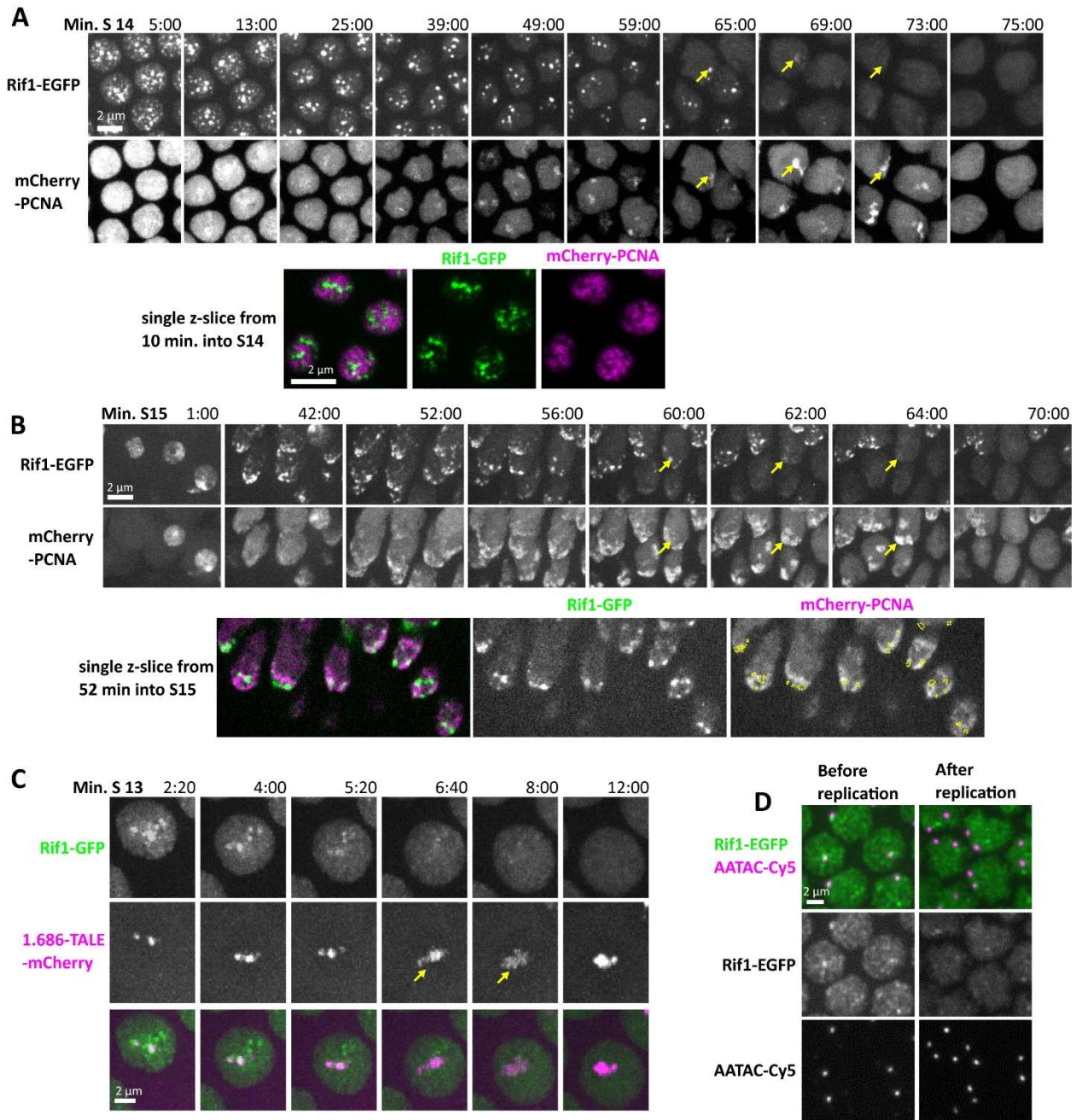


Fig 2.2. Rif1 dissociates from chromatin before the underlying sequences replicate. (A) Stills from time-lapse microscopy of Rif1-GFP and mCherry-PCNA during S phase 14 (S3 Movie). Though both form foci on satellite sequences, the signals do not overlap. Rif1 marks numerous satellites early and the number of foci progressively declines. After early widespread staining, PCNA, a marker of active replication, transiently marks a progression of different satellites. At different positions, the period of PCNA staining seems to follow loss of Rif1. Yellow arrows track the replication of a Rif1 marked sequence. Below, a single z plane from 10 min into S phase 14 that more clearly shows that the signal from Rif1 does not overlap with that from PCNA. **(B)** Stills from time-lapse microscopy of Rif1-GFP and mCherry-PCNA during S phase 15 (S4 Movie). During this S phase the late replicating heterochromatin is clustered into an obvious chromocenter. As in S phase 14, Rif1 marks late replicating chromatin, and Rif1 dissociates from these sequences before the acquisition of PCNA. Yellow arrows track the replication of a single Rif1 marked sequence. Below, a single z plane from 52 min. into S phase 15 shows that Rif1 does not colocalize with PCNA. **(C)** Live imaging of Rif1 and the satellite 1.686 using an mCherry tagged TALE protein (S5 Movie). Yellow arrow indicates the decompaction and replication of 1.686. After its replication, the 1.686 repeat re-compacts and appears brighter. Rif1 dissociates from this sequence prior to its replication. **(D)** Nuclei in S phase 14 stained for Rif1 and for the Y-chromosomal satellite repeat AATAC. Rif1 is bound to AATAC during early S14 before the AATAC repeat replicates. During late S14 the duplicated AATAC sequence lacks Rif1 stain.

FIGURE 2.3

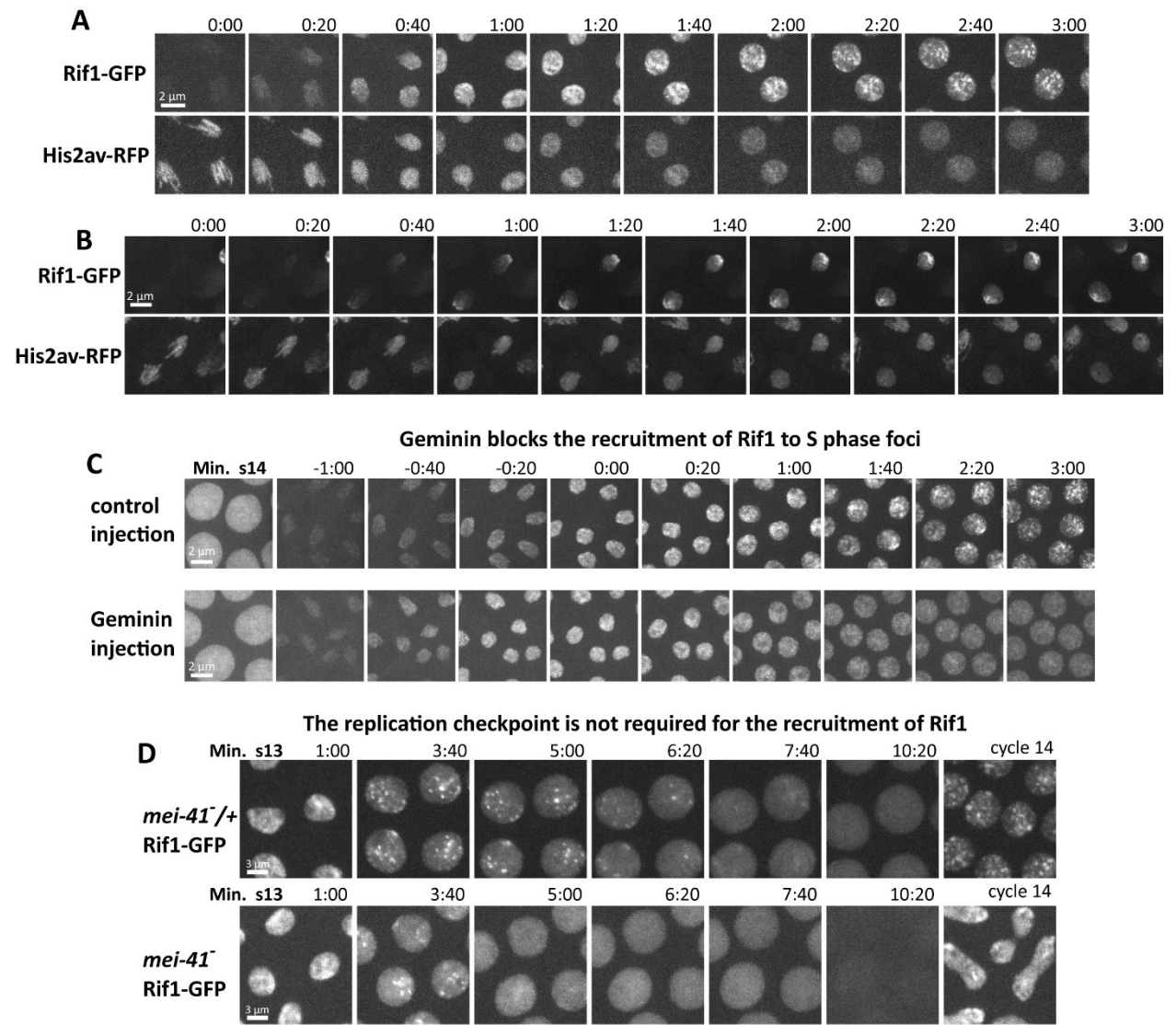


Fig 2.3. Two stages of Rif1 recruitment, their contributions to specificity, and reliance on origin licensing and the replication checkpoint. Time-lapse confocal microscopy on Rif1-GFP, His2av-RFP embryos showing the initial binding of Rif1 during transit from one cell cycle to the next. (A) During late anaphase 13, on the approach to cycle 14, chromosomes first exhibit faint and ubiquitous Rif1 staining that accumulates for about 1 min. During the following min as S phase begins, accumulation continues but is now localized to foci that become clearer as the nuclei swell. See also S2 Movie. (B) During late anaphase 14, on the approach to cycle 15, the early stage of Rif1 staining shows some specificity for the pericentric regions of the chromosomes and forming chromocenter. This specificity is amplified as the interphase-15 nucleus forms and S phase begins. (C) Time-lapse imaging of Rif1-GFP during the normal transition from cycle 13 to 14 and in an embryo injected with purified geminin protein in interphase of 13. Times are indicated with reference to the start of S phase 14. The geminin block to pre-RC formation prevented the recruitment of Rif1 to foci, but did not block the initial generalized binding during mitotic exit. (D) Imaging of Rif1-GFP during cell cycle 13 in control (*mei41/+*) and *mei41* null embryos. The Me141-dependent replication checkpoint is essential during cycle 13 to prevent premature entry into mitosis (10:20 frame). Rif1 foci still form in the absence of a replication checkpoint, but the Rif1 foci are lost earlier and the premature mitosis leads to bridging and defective cycle 14 nuclei.

FIGURE 2.4

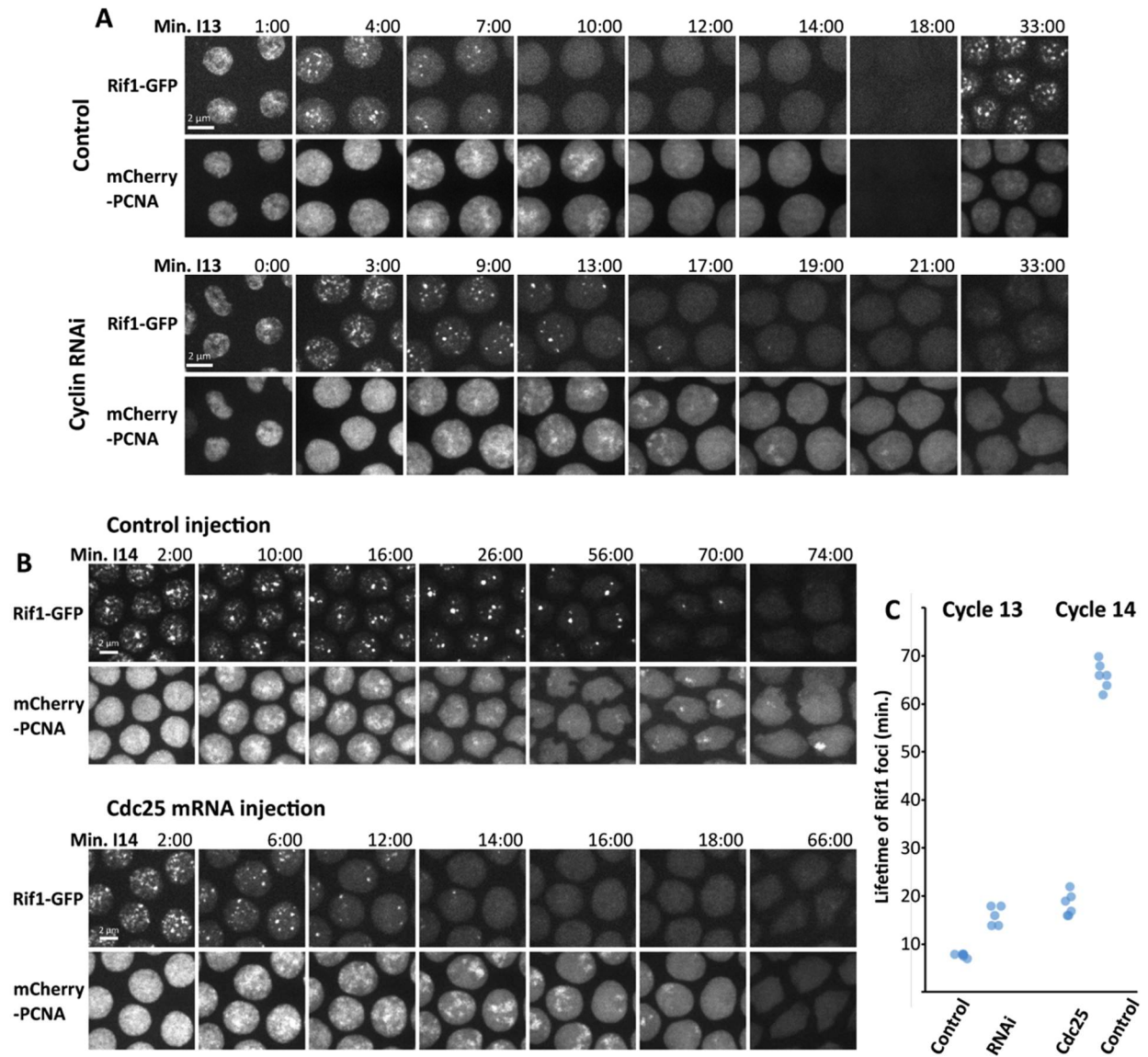


Fig 2.4. Manipulation of Cdk1 activity alters the lifetime of Rif1 foci and the duration of S phase. (A) Stills from time-lapse imaging of Rif1-GFP and mCherry-PCNA during cycle 13 after injection of either buffer (control) or dsRNA against the three mitotic cyclins (A, B, and B3) in cycle 10. The knockdown of the cyclins increases the persistence of Rif1 foci, extends S phase (PCNA staining) and blocks progression to cycle 14. The time of the last frame showing a Rif1 focus is indicated as the lifetime of Rif1 foci in (C). **(B)** Stills from time-lapse imaging of Rif1-GFP and mCherry-PCNA during cycle 14 after injection of either buffer (control) or mRNA encoding the Cdk1 activator Cdc25 (twine) in cycle 13. Artificial activation of Cdk1 during S phase 14 accelerates both the dissociation of Rif1 and late replication. In the control embryo, Rif1 foci were detected 70 min into S phase 14, and prominent foci of PCNA were documented at 74 min. Expression of Cdc25 resulted in the loss of Rif1 foci by 16:00 and the final late replicating PCNA signal documented was at 18:00 (S6 Movie). **(C)** Plot of lifetime of Rif1 foci in minutes during either S phase 13 or S phase 14 following the indicated injection.

FIGURE 2.5

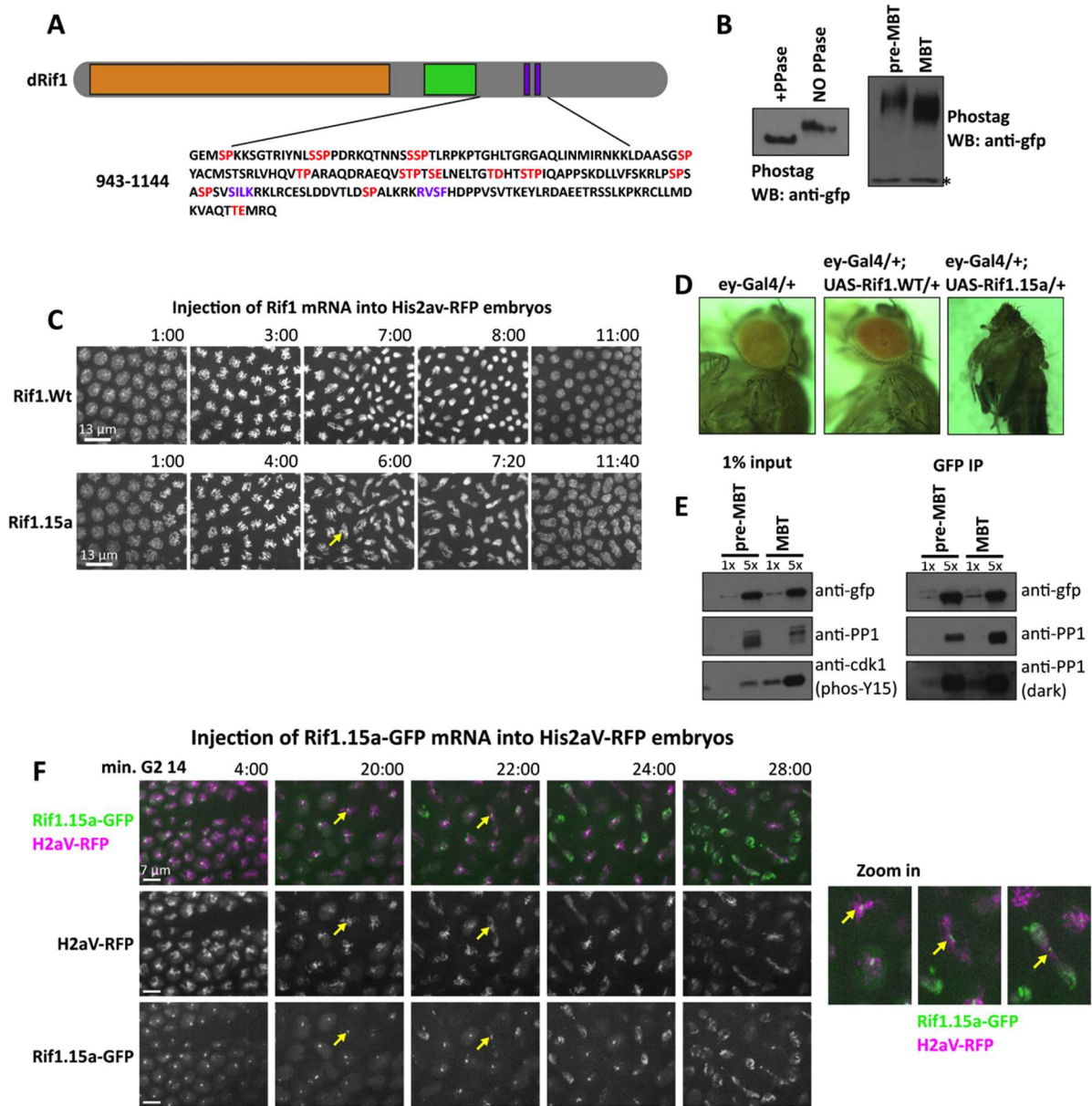


Fig 2.5. Phospho-site mutant Rif1 does not dissociate from chromatin and blocks replication. **(A)** Schematic (above) of Rif1 protein with N-terminal HEAT repeats (orange), putative DNA binding domain (green), and PP1 interaction motifs (purple boxes). The amino acid sequence (below) of the indicated portion of the Rif1 protein shows candidate CDK and DDK phosphorylation sites (red). These 15 S/T residues were mutated to alanine to create the Rif1.15a phospho-mutant allele. **(B)** Left panel shows anti-gfp Western blots used to detect Rif1-GFP from 1-hour old embryos. Protein extracts were treated with lambda phosphatase or buffer only for 1 hour and then were run on SDS-PAGE gels cast with phostag to decrease the migration of phosphorylated proteins. Right panel shows phostag western blots used to detect Rif1-GFP from embryos aged to one hour (pre-MBT) or to 2.5 hours (MBT). Asterisk denotes background band. **(C)** Ectopic expression of the indicated versions of Rif1 by injection of mRNA during cycle 11. After injection, embryos were filmed during mitosis 13. The yellow arrow points to an example of an anaphase bridge. **(D)** Images of flies (left) and a pharate pupa (right) show the consequence of expression of either Rif1 (middle) or Rif1.15a (right) in the developing fly eye/head capsule using Eyeless-Gal4. **(E)** Anti-GFP immunoprecipitation followed by Western blotting with the indicated antibodies. Protein extracts were prepared from embryos harvested before the MBT (1 hour old) or after aging to the MBT (2.5 hours old). Phos-Y15 (left-bottom) indicates the inactive phosphorylated form of Cdk1. **(F)** Frames from live imaging of nuclei starting in G2 of 14 and progressing into a defective mitosis following expression of Rif1.15a-GFP from injected mRNA. Yellow arrows indicate extensive anaphase bridging with a residue of Rif1.15a-GFP. Magnified images (right) show progression of one nucleus.

FIGURE 2.6

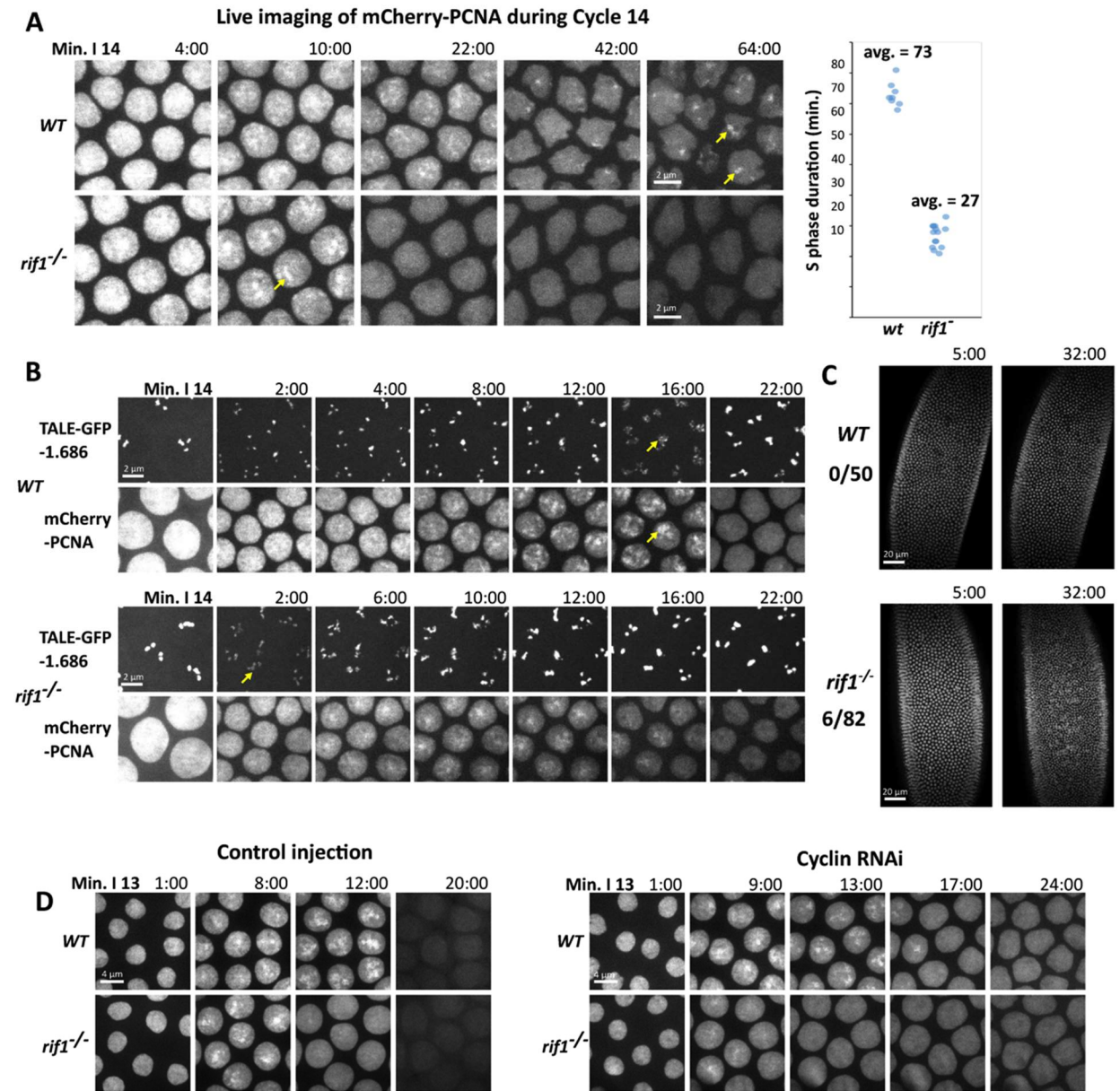
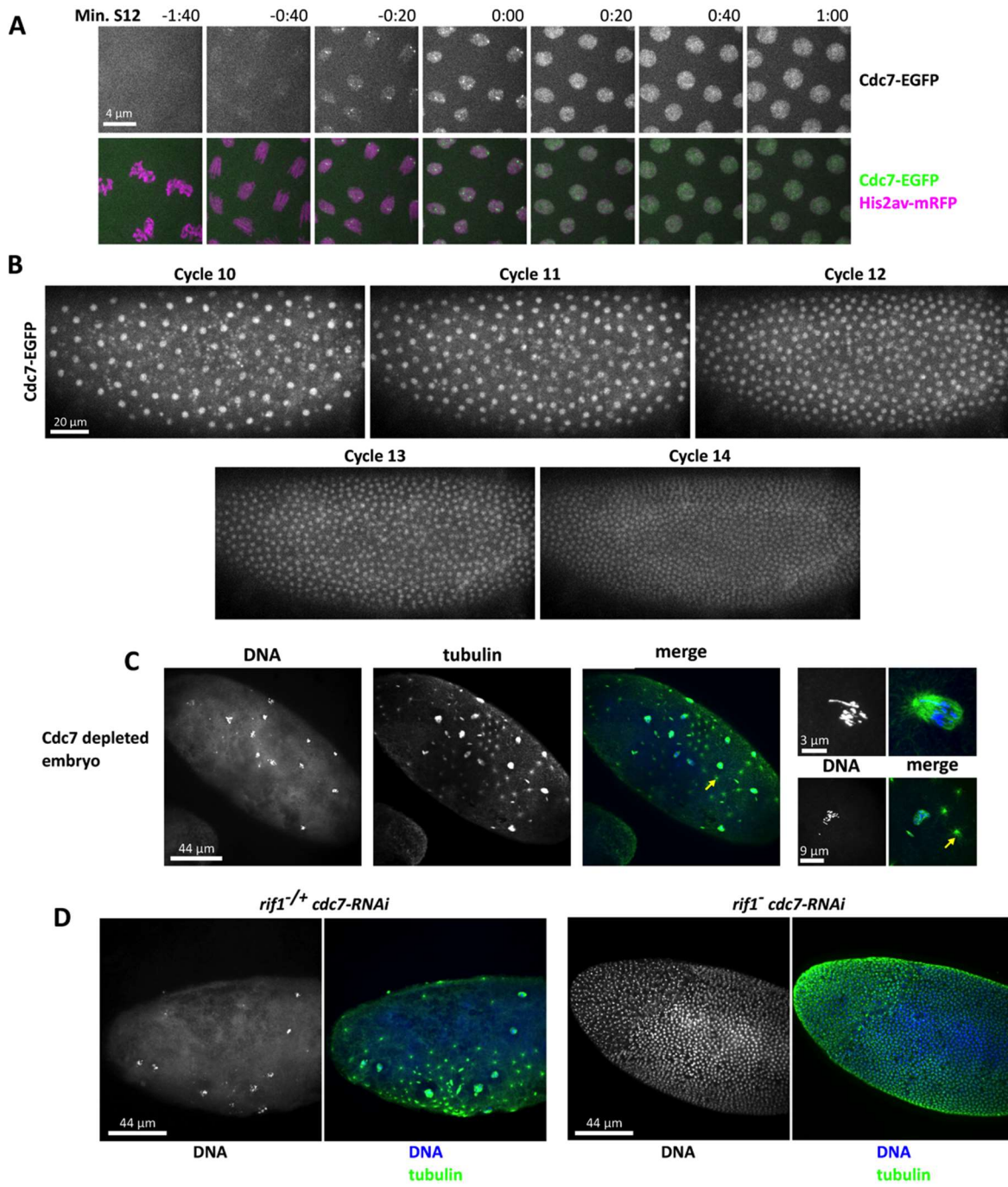


Fig 2.6. *rif1* is required for the prolongation of S phase at the MBT. (A) Stills from time-lapse imaging of mCherry-PCNA during S phase 14 in wild-type (top) or *rif1* mutant (bottom) embryos. Yellow arrows indicate late replication foci. The plot on the right displays the total duration of S phase 14 in wild-type and *rif1* embryos. Each data point represents a distinct embryo. The duration of S phase was scored from real time records of PCNA dynamics. **(B)** Stills from time-lapse imaging following the TAIL-light probe for the 1.686 satellite (upper) and mcherry-PCNA to follow replication during S phase 14 in wild-type and *rif1* embryos. Yellow arrows indicate the decompacted signal from the 1.686 TALE-light during the replication of the 1.686 repeat. **(C)** Wild-type (top) or *rif1* (bottom) embryos were injected with GFP-HP1a to visualize nuclei and filmed during cycle 14. 6/82 *rif1* embryos underwent an early mitosis 14 (S7 Movie). **(D)** Still frames from movies following mCherry-PCNA during S phase 13 in wild-type and *rif1* embryos after either control or triple cyclin RNAi injection. Mitotic-cyclin knockdown arrests the cell cycle, but extends S phase in wild-type but not *rif1* embryos.

FIGURE 2.7



E

Maternal <i>Gal4</i> > <i>UAS-shRNA:cdc7</i>	Maternal Genotype	Percent hatching (25 °C)	Percent hatching (29 °C)
	<i>rif1^{+/+}</i>	0 (n = 273)	0 (n = 268)
	<i>rif1^{-/-}</i>	21 (n = 281)	2 (n = 242)

Fig 2.7. Deletion of *rif1* rescues cell cycles to Cdc7 depleted embryos. (A) Cell cycle regulated recruitment of Cdc7 to the nucleus during early interphase shown by time-lapse microscopy of Cdc7-GFP, His2av-RFP during nuclear cycle 12 using a 100x objective. (B) Live imaging of Cdc7-GFP embryos during cycles 10-14 reveals dilution of nuclear Cdc7 over the pre-MBT divisions. (C) Fixed *cdc7* depleted embryos stained for DNA and tubulin. Yellow arrow indicates a centrosome not associated with a DNA mass. Adjacent enlarged images display magnified views of abnormal mitotic structures. (D) Fixed *rif1* mutant embryo after maternal RNAi against *cdc7* stained for DNA and tubulin. Deletion of *rif1* restores cell cycles and early development to *cdc7* depleted embryos. (E) Hatch rate of embryos laid from mothers either heterozygous or homozygous for a deletion of *rif1* and expressing maternal RNAi against *cdc7*. The total number of embryos counted is indicated in parentheses. The temperature at which both the flies were reared, and the hatch rate performed is indicated.

FIGURE 2.8

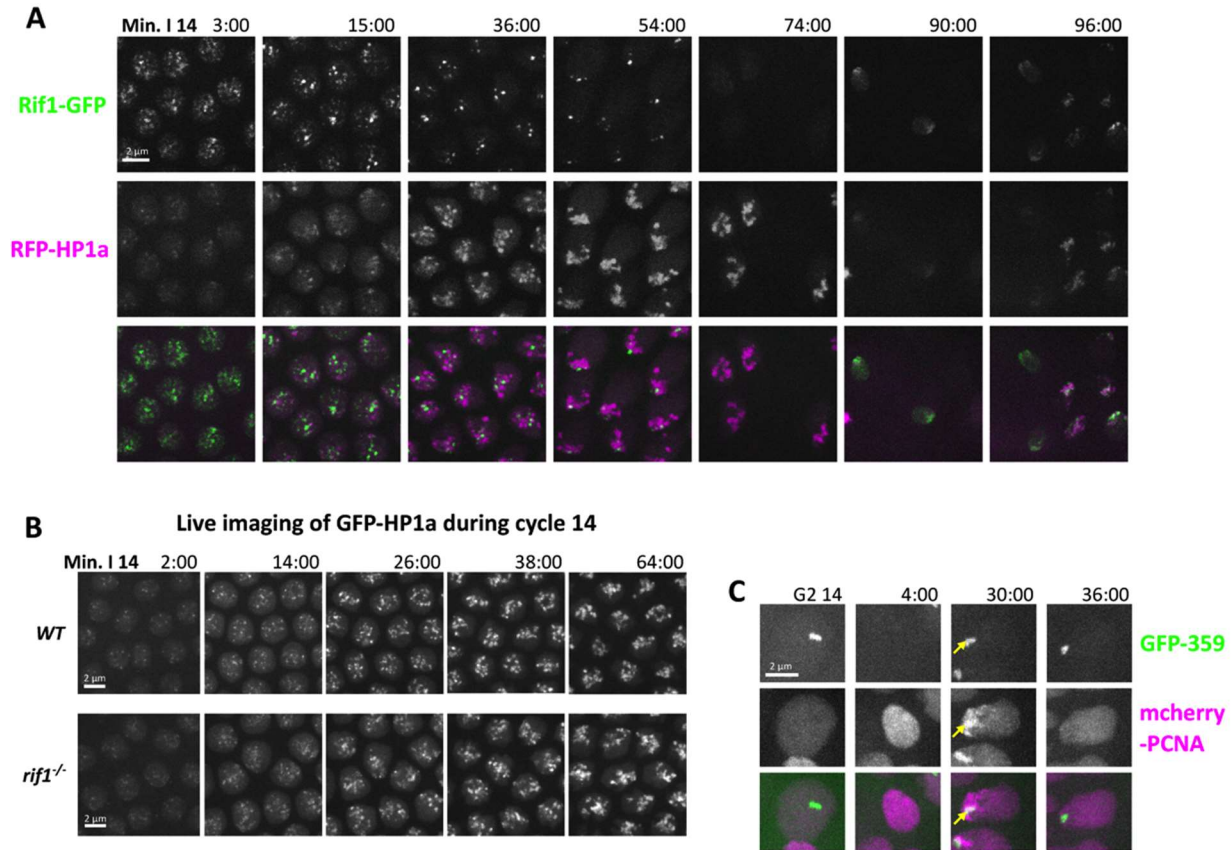


Fig 2.8. Sequential appearance at satellite sequences suggests that Rif1 influences late replication prior to an impact of HP1a. (A) Still images from time-lapse imaging of Rif1-GFP and RFP-HP1a during cycle 14 (early S phase through mitosis). During S phase the number of Rif1 foci decline as the number of HP1a foci increase. G2 nuclei lack Rif1 foci, but retain strong HP1a foci (74 min). During the asynchronous mitosis 14 (74/90/96 min), both proteins are lost, but are rapidly recruited to late anaphase chromosomes (90/96 min). (B) Still images from time-lapse imaging of GFP-HP1a protein injected into wild-type embryos (above) and *rif1* embryos (below) during S phase 14. HP1a recruitment to the heterochromatin proceeded similarly in control and mutant embryos. (C) Still images from time-lapse imaging of the replication of the 359-satellite progressing from G2 of cycle 14, until completion of its replication in cycle 15. Note that the TAIL-light signal is not immediately visible following mitosis (4:00 min frame). We previously described how HP1a binds to the 359 bp repeat following its replication during S phase 14 and subsequently delays its replication in S phase 15. In *rif1* embryos, the 359-repeat also replicated late in S phase 15 (In frame 30:00, yellow arrow indicates where the 359 TALE signal overlapped with PCNA).

FIGURE 2.9

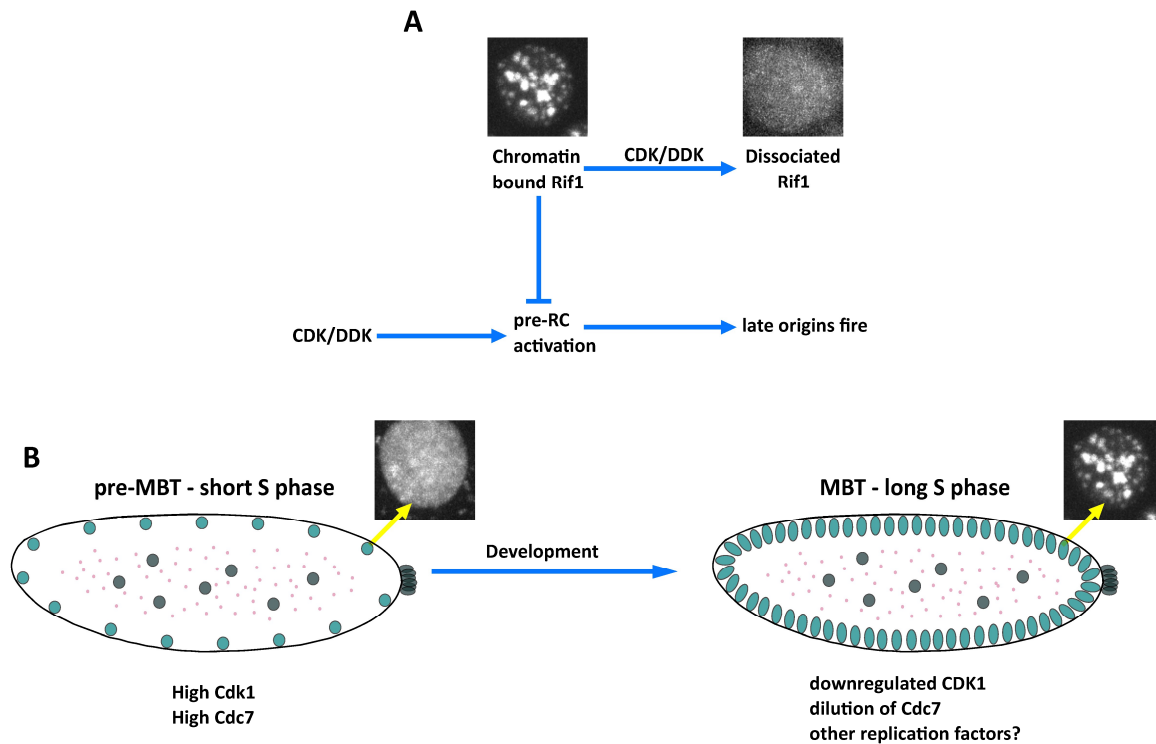
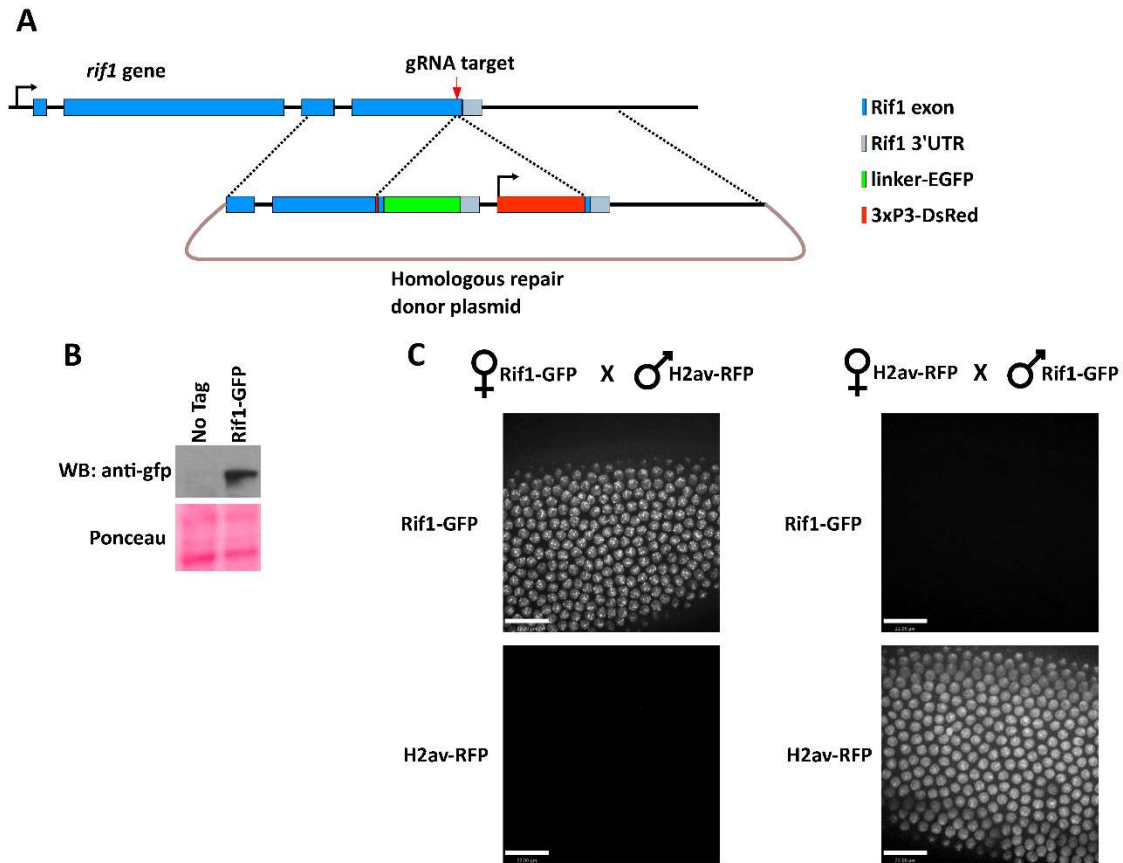


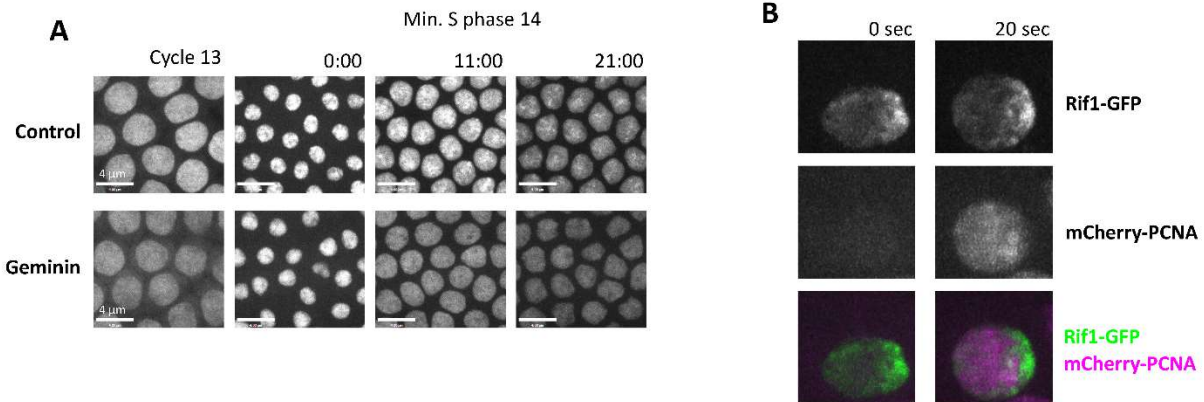
Fig 2.9 Model. (A) Interactions of the S phase kinases and the Rif1 inhibitor create a late replication program. In a nucleus in early S phase (left) foci of compacted late replicating satellites have bound Rif1 that creates a phosphatase rich domain through its interaction with PP1a. This protects the pre-RC from the activating influence of S phase kinases, CDK and DDK. With time (to the right) the S phase kinases act on Rif1, first gradually, to promote its dissociation, and then abruptly as the kinases overwhelm the weakened domain of phosphatase dominance. At this time, the S phase kinases can successfully directly target and activate the pre-RC. **(B)** During the early pre-MBT cycles, high CDK and DDK activities rapidly drive Rif1 dissociation so that delays in replication are initially negligible. A progressive lengthening of the embryonic S phase is associated with incrementally increasing delays in satellite replication. Part of this delay is due to declining CDK and increasing, but still transient, Rif1 association. However, Rif1 independent factors, likely the titration of several replication proteins, such as Cdc7, also contribute to this slowing. Then, at the MBT, developmentally programmed downregulation of Cdk1 allows persistent binding of Rif1 to satellite DNA and the introduction of a late replication program, thereby extending the duration of S phase.

SUPPLEMENTAL FIGURE 2.1



S2.1 Fig. Generation and characterization of endogenously tagged Rif1::EGFP flies. (A) Schematic showing the gene structure of *drif1* and the CRISPR-Cas9 tagging strategy. Briefly, a single guide RNA was chosen to direct Cas9 cleavage in the extreme C-terminus of the rif1 ORF. A donor plasmid containing approximately 1.5 kb of homology to either side of the break point was used to insert a GlyGlySer (linker)-EGFP tag in addition to a DsRed selectable maker under the control of the eye specific 3xP3 enhancer. **(B)** Anti-GFP western blot on embryonic protein extract to confirm successful tagging. **(C)** Still frames from time-lapse confocal imaging of embryos produced from the indicated crosses. Selected images are from individual embryos at 10 minutes into interphase of cycle 14. The Rif1 protein present at the MBT is maternally provided.

SUPPLEMENTAL FIGURE 2.2



S2.2 Fig. Further characterization of Rif1 and PCNA in S phase (A) Injection of geminin eliminates S phase 14 foci of mCherry-PCNA. In control embryos, mCherry-PCNA marks nuclear locations of active DNA replication resulting in bright PCNA foci later in S phase. When pre-RC formation is blocked by the injection of purified geminin protein during interphase 13 the nuclear PCNA signal is overall less intense, and never resolves into replication foci. We conclude that transgenic mCherry-PCNA faithfully marks replicating sequences. **(B)** Stills from time-lapse imaging of Rif1-EGFP and mCherry-PCNA during the start of S phase 15. Note that the recruitment of Rif1 precedes the recruitment of PCNA to chromatin. Once S phase begins PCNA is spread throughout the early replicating euchromatic portion of the nucleus, but the PCNA signal does not overlap with the Rif1 bound late replicating heterochromatin which by cycle 15 is concentrated to one edge of the nucleus.

SUPPLEMENTAL FIGURE 2.3

A

```

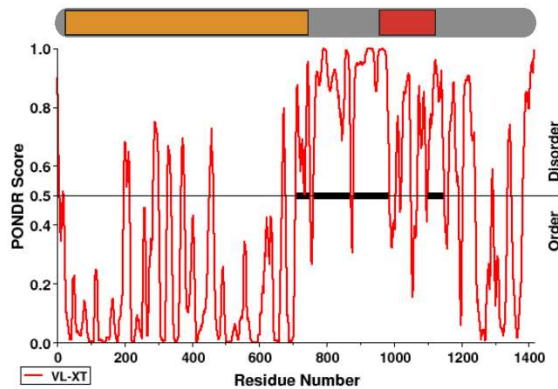
Aedes      SPASGSGEKRTSSRIMEREKGPVSPITRRTRNSFPVLPAAVANLRNRTPQSTPRSPKTG
Drosophila SP-----KKSGETRIYN-----L-----SSPPD-----RKQIN--NSSPTLRPKP
Musca      SP-----KKTNPARETP-----L-----SSPPD-----RKLIN--NSSPTLRPKP
          **      * , ; * :      :      , ***      :      *      , ; *      .

Aedes      MIELRCRGAQLINLIRSQQNEMSPKPAALPPPQSSSTPKPVSNNPSSDRSMLRKLATAAT
Drosophila TGHLTGRGAQLINMIRNKKLDAASGSPYAC-----MSTSR-LVHQVTFARAQ
Musca      SSHLTGRGAQLINMIRNKKVDISASAATST-----ASS-----FFTSSV
          . * ***** : * : : :      :      :      :

Aedes      ATNATTAPAVQSPFLSKP-LPFVEKEKEKNDYLVFSKVLPSQASPAASILKRNQD
Drosophila DRAEQVSTPTSELNELTGDHTSTPIQAPPSKDLVFSKRLPSFASPSVSIKRLRCE
Musca      STPSQQRNPAELMELTGTDTSTFVQ---HKDFLVFSKRLPSFTASPSASILKRLRND
          * :      ** :      . :      : * ***** ** * : ***** . :

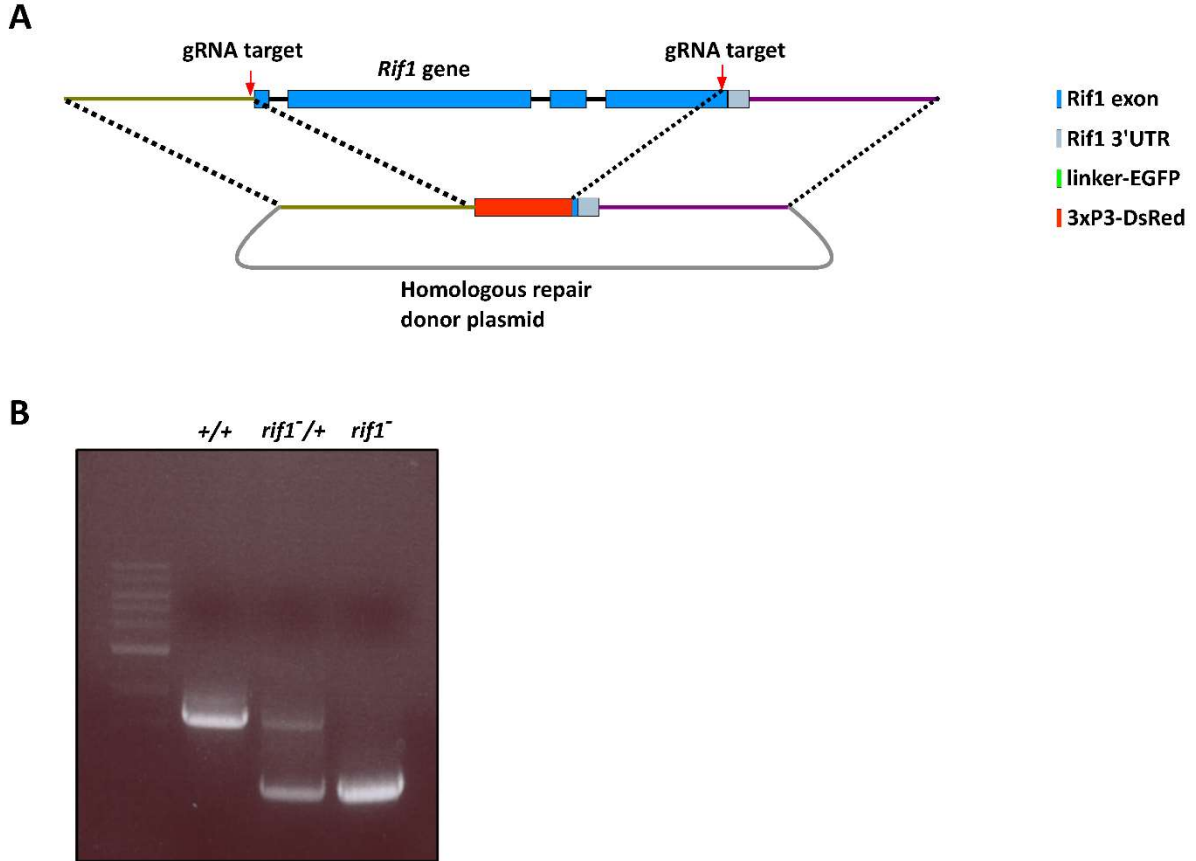
Aedes      DSG-DDLESPANKRKRVSF
Drosophila SLDDVTLDSPALKRKRVSF
Musca      SIEDLSFDSPAFKRRKVSF
          . : ** * *****
  
```

B



S2.3 Fig. Analysis of potential Rif1 CDK and DDK phosphorylation sites. (A) Multiple sequence alignment of the indicated portions of the Rif1 protein sequences from *Aedes aegypti* (1345-1541), *Drosophila melanogaster* (946-1103), and *Musca domestica* (1041-1189) using Clustal Omega. Potential DDK and CDK phosphorylation sites are highlighted in red. Both CDK and DDK are serine/threonine kinases where specificity is encoded by the residue in the +1 position. CDK phosphorylates S/T residues followed by a proline. DDK targets S/T residues followed by an acidic group which can be provided by an acidic amino acid (D or E) or by a previous phosphorylation (e.g. SSP). PP1 interaction motifs are highlighted in purple. **(B)** Analysis of the *D. melanogaster* Rif1 protein sequence using the Predictor of Natural Disordered Regions (PONDNR) tool to score for regions of intrinsic disorder. PONDNR scores above 0.5 suggest regions of intrinsic disorder. Above the graph is a schematic of the relevant regions of the Rif1 protein. The N-terminal heat repeats are represented by the yellow box, and the portion Rif1 containing the potential CDK and DDK phosphorylation sites analyzed in **(A)** is represented by the red box.

SUPPLEMENTAL FIGURE 2.4



S2.4 Fig. Deleting *rif1* (A) Schematic showing the gene structure of *rif1* and the CRISPR-Cas9 editing strategy used to generate the *rif1* null allele. Briefly, two CRISPR target sites were selected, one site directly upstream of the start codon, and one site directly upstream of the stop codon. Approximately 1.5 kb of DNA homologous to the genomic sequence on either upstream or downstream of the break points was used to direct the replacement of the *rif1* ORF with the visible 3xP3-DsRed marker. (B) Confirmation of correct replacement of the *rif1* ORF by PCR.

Supplemental Movie legends.

S2.1 Movie Rif1 forms dynamic nuclear foci as the embryonic cell cycle lengthens. This video accompanies Figure 1D. Live imaging of a Rif1-GFP (green) and H2aV-RFP (magenta) in an embryo completing the blastoderm cell cycles and the MBT. Video begins at mitosis 10 and ends in S phase 15 (post-MBT). In each cycle, green Rif1 foci appear upon exit from mitosis, disappear progressively as interphase progresses, and reform in the next cycle. With each cycle Rif1 foci become more numerous and more persistent in parallel with the slowing of the cell cycle. Imaging is at the ventral midline, and, at the onset of gastrulation (late during cycle 14), dramatic movements are associated with invagination of the ventral furrow. Towards the end of the movie, cells that flanked the invaginated furrow (domain 14 cells) divide and are evident as a row of paired cells running laterally along the ventral midline and featuring Rif1 foci. These cells are now in S phase 15 and are bordered on either side by cells still in G2 of the previous cycle. Z stacks were acquired every 1.5 minutes on a 100x oil objective.

S2.2 Movie Imaging the appearance and disappearance of Rif1 S phase foci. This video accompanies Figure 1E and Figure 3. Live imaging of Rif1-GFP (green) and His2aV-RFP (magenta) at high frame rate (every 20 seconds) using a 100x oil objective during cycles 12, 13, and 14. Because of the obvious photobleaching using this imaging protocol, each cell cycle is a separate imaging experiment done on a different embryo. Low level binding of Rif1 is evident on the chromosomes during anaphase, but obvious foci become apparent only after the beginning of interphase. When Rif1 dissociates from the chromatin the focus of Rif1-GFP erodes from the outside over the course of 2 minutes as the signal fades. Note that for the cycle 14 sample the movie ends in the middle of S phase 14.

S2.3 Movie Coordination of Rif1 dissociation and DNA replication. This video showing Rif1-GFP (green) and mCherry-PCNA (purple) during S phase 14 accompanies Figure 2A. Movie starts at the end of S phase 13 and follows nuclei through S phase 14. Rif1 dissociates from chromatin before the underlying sequences acquire PCNA signal indicating onset of late replication. Absence of coincidence of the two signals is evident throughout the sequence. While complicated by nuclear movements, recruitment of PCNA to previously Rif1 staining regions is apparent near the close of S phase. Z stacks were acquired every 2 minutes on a 100x oil objective.

S2.4 Movie Rif1 is recruited to the late replicating heterochromatin during Mitosis 14 before the beginning of S phase 15. This video accompanies Figure 2B. Live imaging of Rif1-GFP (green) and mCherry-PCNA (magenta) during mitosis 14 and the start of S phase 15. Rif1 binds to the chromatin during mitotic exit, and is enriched at the leading edge of the chromosome mass where the late replicating pericentric heterochromatin resides. Rif1 binding is evident before the appearance of PCNA signal on the chromatin, which marks the start of S phase. Once S phase begins, the Rif1 stained heterochromatin does not overlap with the PCNA stained early replicating euchromatin. Z stacks were acquired every 20 seconds on a 100x oil objective.

S2.5 Movie Imaging Rif1 and the replication of the 1.686 satellite repeat. This video accompanies Figure 2C. Live imaging of Rif1-GFP (green) and the late replicating satellite

1.686 using an mCherry labeled TALE-light protein (magenta) during S phase 13. Before 1.686 replicates, it is marked by Rif1 (coincident signal appears white). Rif1 then dissociates (at 00:04:20) before this repeat decondenses (at 00:04:40) and replicates. After replication, the TALE-light signal appears brighter and re-compacted (00:09:00), but lacks a Rif1 signal. Finally, the 1.686 loci separate, align, and then lose fluorescence upon progression to mitosis. Z stacks were acquired every 20 seconds on a 100x oil objective.

S2.6 Movie Ectopic activation of Cdk1 during S phase 14 drives Rif1 dissociation and accelerates late replication. This video accompanies Figure 4B. Live imaging of Rif1-GFP (green) and mCherry-PCNA (magenta) during S phase 14 following injection of Cdc25 mRNA during cycle 13. Introduction of this Cdk1 activator accelerates the loss of Rif1 foci and drives the underlying sequences to replicate earlier in S phase (S3 Movie). Z stacks were acquired every 2 minutes on a 100x oil objective.

S2.7 Movie *rif1* embryos undergo an early mitosis 14. This video accompanies Figure 6C. Live imaging of GFP-HP1a injected into in a wild-type embryo (left) and a *rif1* embryo (right). Movies begin in cycle 12 and follow embryos through cycle 14. Note that the *rif1* embryo undergoes an extra synchronous mitosis approximately 23 minutes into interphase 14. Z stacks were acquired at minute and twenty second intervals on a 20x air objective.

S2.8 Movie Level of nuclear Cdc7 decline over the blastoderm cycles leading up to the MBT. This video accompanies Figure 7B. Live imaging of Cdc7-GFP (green) and His2av-RFP (magenta) during cell cycles 11 through 14. Z stacks were acquired every minute on a 20x air objective.

METHODS

Fly stocks

All *Drosophila melanogaster* stocks were cultured on standard cornmeal-yeast medium. The following fly strains were used in this study: w¹¹¹⁸ Canton-S (wild type), his2av-mRFP (Bloomington stock number 23650 or 23651), mRFP-HP1a (30562), eyeless-gal4 (5535), maternal tubulin-gal4 (7063), UAS-shRNA^{cdc7} (TRiP GL00585), mei41^{D3} (gift from Tin Tin Su, University of Colorado Boulder), mCherry-pcna (this study), rif1-EGFP (this study), cdc7-EGFP (this study), rif1⁻ (this study), UASp>Rif1-3xFlag (this study), UASp>Rif1-15a-3xFlag (this study).

Generation of transgenic lines described in this study

All transgenesis injections were performed by Rainbow Transgenic Flies, Camarillo, CA.

The stocks rif1-EGFP and cdc7-EGFP were generated using CRISPR-Cas9 editing to modify the endogenous rif1 and cdc7 genes (diagrammed in S1 Fig) as described in Gratz et al 2014. Briefly, a single CRISPR target site was selected as close to the stop codon as possible. To direct homologous repair, approximately 1.5 kb of DNA on either side of the cut site was amplified from gDNA isolated from the vasa-Cas9 stock (51324). Both homology arms, a 6xGlyGlySer-EGFP tag, and the endogenous 3'UTR were cloned into the pHD-DsRed vector using Gibson Assembly. To generate guide RNA plasmids, annealed DNA oligos were cloned into the pU6-BbsI-chiRNA vector. The donor plasmid and the gRNA plasmid were co-injected into vasa-cas9 embryos by Rainbow Transgenic Flies. After screening for DsRed⁺ progeny, successful modification was confirmed by PCR genotyping and anti-GFP immunoblotting. A single male containing a successful modification was backcrossed to our lab's w¹¹¹⁸ Canton-S stock for five generations to establish a stock.

CRISPR-Cas9 editing was used to generate the *rif1* null allele (S4 Fig) by replacing the *rif1* ORF with a visible 3xP3-DsRed marker. Two CRISPR target sites were selected, one site directly upstream of the start codon and one site 14 bp upstream of the stop codon. Gibson assembly was used to construct a homologous repair donor plasmid containing approximately 1.5 kb of DNA homologous to the genomic sequence directly upstream of the first cut site, the DsRed marker, and approximately 1.5 kb of DNA homologous to the genomic sequence directly downstream of the second cut site. Both gRNA plasmids and the donor plasmid were co-injected into *vasa-cas9* (51324) embryos by Rainbow Transgenic Flies. After screening for DsRed⁺ progeny, successful replacement of the *rif1* ORF was confirmed by PCR genotyping (S4 Fig) and by Sanger sequencing across the recombinant breakpoints. A single male carrying the *rif1* null allele was backcrossed to our lab's wild-type strain for five generations to establish the *rif1*⁻ stock.

To generate the mCherry-*pcna* transgenic stock approximately 1 kb of sequence upstream of the *pcna* start codon, the mCherry-5xGlyGlySer tag, and the *pcna* gene were cloned into the pw+attB vector using Gibson Assembly. The resulting transgenesis plasmid and phiC31 mRNA were co-injected into attP-9a embryos (9744) to perform phiC31 mediated integration.

To generate the UAS-Rif1.WT-3xFlag and UAS-Rif1.15a-3xFlag transgenic lines either the *rif1* ORF was amplified from embryo cDNA and into the pENTR-D vector by TOPO cloning. In order to generate the phosphomutant Rif1.15a, a DNA fragment containing the mutated sequence was synthesized (Integrated DNA Technologies, Redwood City, CA) and used to replace the corresponding wild-type sequence in the ENTRY plasmid by Gibson Assembly. The ENTRY vectors were then recombined with the pPWF-attB construct using the LR Clonase II kit (Invitrogen, Carlsbad, CA). The resulting transgenesis plasmids and phiC31 mRNA were co-injected into attP-9a embryos (9744) to perform phiC31 mediated integration.

Plasmids and DNA sequences are available upon request.

Embryo staining

Embryos were collected on grape agar plates, washed into mesh baskets and dechorinated in 50% bleach for 2 minutes. Embryos were then devitellinized and fixed in a 1:1 mixture of methanol-heptane, before storing in methanol at -20°C. Embryos were gradually rehydrated in a series of increasing PTx:Methanol mixtures (1:3, 1:1, 3:1) before washing for 5 minutes in PTx (PBS with 0.1% Triton). Embryos were then blocked in PBTA (PTx supplemented with 1% BSA and 0.2% Azide) for 1 hour at room temperature. Blocked embryos were then incubated with the primary antibody overnight at 4°C. The following primary antibodies were used: rabbit anti-GFP at 1:500 (Invitrogen A11122), and mouse anti-tubulin at 1:100 (DSHB 12G10, AA12.1-s, and AA4.3-s). Embryos were then washed with PTx for three times 15 minutes each, and then incubated with the appropriate fluorescently labeled secondary antibody (Molecular Probes) at 1:300 for 1 hour in the dark at room temperature. Embryos were then washed again with PTx for three times 15 minutes each. In order to detect total DNA, DAPI was added to the second wash. Finally, stained embryos were mounted on glass slides in Fluoromount.

To detect both Rif1-EGFP and the AATAC satellite repeat, formaldehyde fixed embryos were blocked in PBTA for 1 hour, incubated with rabbit anti-GFP at 1:500 (Invitrogen A11122) for 1 hour at room temperature, washed three times for 15 minutes each in PTX, incubated with fluorescently labeled secondary antibody at 1:300 for 1 hour at room temperature in the dark, and then washed three times for 15 minutes in PTX. Embryos were then post-fixed in 4% formaldehyde for 20 minutes. FISH was then performed as described in Shermoen et al., 2010 using a Cy5 labeled AATAC 30-mer oligo probe (IDT).

Protein extract preparation and immunoprecipitation

Protein extracts were prepared by homogenizing embryos in embryo lysis buffer (50 mM Tris-HCl pH 8.0, 100 mM NaCl, 1% Triton X-100, 1 mM EDTA) supplemented with 1X protease

inhibitor cocktail (Pierce), PMSF, 100 mM Sodium Fluoride, 100 mM β -glycerophosphate, and 10 mM sodium pyrophosphate. After lysis, 2X Sample Buffer was added to the extract, and samples were boiled for 5-10 minutes. For dephosphorylation reactions protein extracts were prepared as above except for the omission of phosphatase inhibitors. Extracts were then supplemented with 1 mM $MnCl_2$ and incubated with λ phosphatase for 30 minutes at 30°C. The reaction was terminated by adding 2X Sample Buffer and boiling for 5-10 minutes.

For immunoprecipitation of GFP tagged Rif1 dechorinated embryos were lysed using a dounce homogenizer in 500 μ l of ice cold RIPA buffer (50 mM Tris-HCl pH 8.0, 150 mM NaCl, 1% Triton X-100, 0.5% Sodium deoxycholate, 0.1% SDS, 1 mM DTT) supplemented with 1X protease inhibitor cocktail (Pierce, Waltham, MA), PMSF, 100 mM Sodium Fluoride, 100 mM β -glycerophosphate, and 10 mM sodium pyrophosphate. The resulting extract was cleared by spinning twice at 12,000 rpm for 10 minutes each at 4°C, after which the supernatant was incubated with 20 μ l of GFP-TRAP Magnetic beads (Chromotek, Martinsried, Germany) for 1 hour at 4°C on a nutator. The beads were then washed for three times with lysis buffer using a magnetic rack, and proteins were eluted by boiling in 30 μ l of 2x Sample Buffer.

Western Blotting

For standard western blotting, protein extracts were separated by electrophoresis in precast 4-15% polyacrylamide gels (Biorad, Hercules, CA). To separate phosphorylated forms of Rif1, protein extracts were run on a 0.5% agarose strengthened 3% polyacrylamide gel containing 20 μ M Mn^{2+} -Phostag (AAL-107, Wako Chemicals, Japan). Proteins were then transferred to a PVDF membrane using a wet transfer system. The membrane was blocked in TBST (TBS with 0.1% Tween-20) supplemented with 2.5% BSA and then incubated in the appropriate primary antibody at a dilution of 1:1000 overnight at 4°C. The blot was then washed three times for 10 minutes each in TBST, and then incubated in the appropriate secondary antibody at a dilution of 1:10,000 for 1 hour at room temperature. The blot was then washed three times for 10 minutes

each in TBST, and then treated with Pierce SuperSignal West Pico ECL, and used to expose autoradiography film. The following antibodies were used: rabbit anti-GFP (ab290, Abcam, Cambridge, United Kingdom), rabbit anti-PP1a (2582, Cell Signaling, Danver, MA), Goat anti-Rabbit HRP conjugated (Biorad).

Microinjection

Embryo microinjections were performed as described in Farrell et al., 2012. In vitro transcribed mRNA was prepared using the CellScript T7 mRNA production system (CellScript, Madison, WI) as described in Farrell., et al 2012 and injected at a concentration of 600 ng/μl. The purified proteins used in this study were described in Yuan and O'Farrell, 2016.

Microscopy

For live imaging embryos were collected on grape agar plates, and aged at 25°C when appropriate. After dechorination in 50% bleach, embryos were aligned and glued to glass coverslips, and then covered in halocarbon oil before imaging. Embryos were imaged using a spinning disk confocal microscope, and the data were analyzed using Volocity 6 (Perkin Elmer, San Jose, CA). For most experiments, approximately 30 embryos were watched under the microscope, and only the embryos at the appropriate developmental stage were filmed. When comparing different conditions, all images acquired in a single experiment were acquired at the same time and with identical microscope settings. Choice of objective and z-stack size were determined by experimental need. Unless otherwise noted all images shown are projections of a z-stack series. When imaging embryos following microinjection, the objective was centered in the portion of the embryo nearest the site of injection to record the area of maximum effect.

Reproducibility

The development of embryos is highly stereotyped, and the quality of the data is founded in the resolution of the imaging. Still images and movies presented in this paper are representative of

multiple embryos filmed during a single experiment (technical replicates) and of identical experiments performed on embryos collected from independently sorted flies (biological replicates). Choice of embryos for imaging was dictated by developmental stage and by embryo health (unfertilized and clearly damaged embryos were excluded). Western blots reported in this paper were performed in two biological replicates (separate protein extracts from independent embryo collections).

Chapter 3

Rapid embryonic cell cycles defer the establishment of heterochromatin by Eggless/SetDB1 in *Drosophila*

SUMMARY

Acquisition of chromatin modifications during embryogenesis distinguishes different regions of an initially naïve genome. In many organisms, repetitive DNA is packaged into constitutive heterochromatin that is marked by di/tri methylation of histone H3K9 and the associated protein HP1a. These modifications enforce the unique epigenetic properties of heterochromatin. However, in the early *Drosophila melanogaster* embryo the heterochromatin lacks these modifications which only appear later when rapid embryonic cell cycles slow down at the Mid-Blastula Transition or MBT. Here we focus on the initial steps restoring heterochromatic modifications in the embryo. We describe the JabbaTrap, a technique for inactivating maternally provided proteins in embryos. Using the JabbaTrap we reveal a major requirement for the methyltransferase Eggless/SetDB1 in the establishment of heterochromatin. In contrast, other methyltransferases contribute minimally. Live-imaging reveals that endogenous Eggless gradually accumulates on chromatin in interphase, but then dissociates in mitosis and its accumulation must restart in the next cell cycle. Cell cycle slowing as the embryo approaches the MBT permits increasing accumulation and action of Eggless at its targets. Experimental manipulation of interphase duration shows that cell cycle speed regulates Eggless. We propose that developmental slowing of the cell cycle times embryonic heterochromatin formation.

INTRODUCTION

The transformation of the egg into a multicellular organism remains one of the wonders of the natural world. By the 18th century, scientists viewed this process as an example of epigenesis, where the simple and formless fertilized egg progressively differentiates into a complex organized creature. We now know that the transformation of the egg from simple to differentiated is preceded and caused by a similar transformation of the naïve zygotic genome. The division of the genome into distinct euchromatin and heterochromatin is the most obvious example of genomic differentiation. Eukaryotes constitutively package significant portions of their genomes into heterochromatin (Brown 1966), and such packaging is critical for the stability of the genome (Janssen et al. 2018). Constitutive heterochromatin displays conserved genetic and molecular properties that are stably transmitted throughout development and across generations (Allshire and Madhani 2018). However, embryogenesis interrupts this stability, and the early embryos of many animals lack true heterochromatin. Thus, embryogenesis involves the restoration of heterochromatin, and this restoration can serve as a paradigm for how epigenetic control of the genome arises during development.

In general, constitutive heterochromatin is transcriptionally silent, late replicating, and low in recombination. The chromosomes of many species contain large megabase sized arrays of simple repeated sequences, known as satellite DNA, surrounding their centromeres, and it is this pericentric repetitive DNA that composes the bulk of the constitutive heterochromatin. Although heterochromatin was originally defined cytologically – it remains condensed throughout the cell cycle – modern studies often emphasize the set of conserved modifications to its chromatin. Heterochromatic nucleosomes are hypoacetylated and di/tri-methylated at lysine 9 on the N-terminal tail of Histone H3 (hereafter H3K9me_{2/3}). The deposition of H3K9me_{2/3} creates a binding site for HP1 proteins (Eissenberg and Elgin 2014) and HP1 can

oligomerize and recruit additional heterochromatin factors which could then generate a distinct compartment in the nucleus.

Studies in *Drosophila* have historically made major contributions to our understanding of heterochromatin (Elgin and Reuter 2013). Many key regulators of heterochromatin were discovered in genetic screens for modifiers of Position Effect Variegation (PEV), a phenomenon where a reporter gene close to the border between euchromatin and heterochromatin is differentially silenced among different cells in an all or none fashion. Currently over 150 distinct genetic loci are reported to impact PEV, highlighting the complexity of heterochromatin control. Critically, the pathway depositing H3K9me_{2/3}-HP1a forms the regulatory core and null mutations in *Su(var)2-5* (HP1a), and replacement of H3K9 with arginine (H3K9R) to block its modification are both lethal (Eissenberg et al. 1990; Penke et al. 2016, 2018). The *Drosophila* genome encodes three K9 methyltransferases: *Su(var)3-9*, *eggless/SetDB1*, and *G9a*, and all three have been reported to modify PEV (Mis et al. 2006; Brower-Toland et al. 2009). To our knowledge, no study has systematically assessed the contributions of these enzymes to the establishment of heterochromatin in the embryo.

Although a dispensable gene (Tschiersch et al. 1994), *Su(var)3-9* is the best studied and most strongly associated with the constitutive heterochromatin in the literature (Elgin and Reuter 2013; Allshire and Madhani 2018). Loss of *Su(var)3-9* leads to strong suppression of PEV. Additionally, analysis of salivary gland polytene chromosomes revealed that *Su(var)3-9* is required for the localization of H3K9me_{2/3} and HP1a to the chromocenter, the region where the pericentric heterochromatin clusters in the nucleus (Schotta et al. 2002). *G9a* is dispensable in *Drosophila* and thought to function primarily at euchromatic sites (Seum et al. 2007b). *Eggless* is the only essential K9 methyltransferase. Studies in larval and adult stages have emphasized that *egg* plays a specialized role in depositing H3K9me_{2/3} at Chromosome 4 (Seum et al. 2007a; Tzeng et al. 2007) which forms a distinct chromatin structure (Riddle et al. 2012).

H3K9me2/3-HP1a is missing from chromosome 4 in the polytene chromosomes of *egg* mutants, but unaffected at the chromocenter. These findings suggested that *egg* does not regulate the pericentric heterochromatin. Further analysis demonstrated that *egg* is also required in both the soma and germline for the completion of oogenesis (Clough et al. 2007, 2014; Wang et al. 2011). *Egg* plays a major role in the piRNA pathway that silences transposons in the germline (Rangan et al. 2011; Sienski et al. 2015; Yu et al. 2015). Although they have yielded much information, these studies focused on the maintenance of heterochromatin, but not on its embryonic emergence.

Like most animals, the *Drosophila* embryo begins development with a stereotyped series of rapid cell cycles following fertilization that are driven by high levels of cyclin-CDK1 activity (Farrell and O'Farrell 2014; Yuan et al. 2016). These divisions occur in a syncytium, are synchronous, lack gap phases, and run entirely by maternal gene products. The first 8 divisions are remarkably fast (each with an interphase of less than 4 min) and occur deep within the embryo. Starting at cycle 9, nuclei migrate to the surface of the embryo to form a syncytial blastoderm. Interphase duration extends progressively and incrementally from cycle 10 through 13 (from 7 min to 14 min). Beginning at cycle 14 the embryo enters the Mid-Blastula Transition, or MBT, a conserved embryonic transformation. At the MBT, the cell cycle slows down dramatically due to the programmed downregulation of CDK1, and the embryo switches its focus from cell proliferation to morphogenesis and patterning. Concomitantly, the zygotic genome activates in full and stable patterns of histone modification emerge (Chen et al. 2013; Li et al. 2014). Zygotic transcription then drives morphogenetic events like cellularization and gastrulation. The slowing of the cell cycle is critical for the developmental events that follow it because short cell cycles inhibit productive transcription (Shermoen and O'Farrell 1991; Strong et al. 2017). Additionally, rapid cell cycles could impair the installation of chromatin modifications

that regulate gene expression, but to our knowledge no direct examination of the enzymes installing these modifications at the MBT exists.

Prior work from our lab has outlined a series of changes made to the heterochromatin as the embryo reaches the MBT. Surprisingly, the conserved features of heterochromatin appear at different times during embryogenesis, indicating that diverse mechanisms contribute to the introduction of its otherwise well correlated properties. The compaction of satellite DNA is evident as early as cycle 8, before the onset of late replication and the association of H3K9me2/3-HP1a (Shermoe et al. 2010). Upon Cdk1 downregulation at the MBT select satellite repeats then recruit the protein Rif1 which acts to delay their replication (Seller and O'Farrell 2018). During the prolonged interphase 14 some satellites become stably associated with H3K9me2/3-HP1a (Yuan and O'Farrell 2016), and by the cycle 15 the satellites coalesce into a clear chromocenter. The emergence of the key features of heterochromatin follows a stereotyped schedule centered around the MBT, and we suggest that this period represents the establishment of mature heterochromatin in the embryo. Following the MBT the satellites faithfully exhibit these characteristics for the rest of development. We want to understand the developmental control of establishment, but first need to discover the key molecules in this process. Here we identify the methyltransferase Egg as a key initiator and propose that heterochromatin formation is timed by the limitations imposed on Egg by rapid embryonic cell cycles.

RESULTS

The JabbaTrap inactivates maternally deposited proteins by rapid mislocalization

The power of fly genetics is nearly incontestable, but the early embryo does present a significant challenge to it. Over 80% of genes are supplied to the embryo as maternally deposited mRNA and protein, and consequently development of the embryo up to the MBT

does not require zygotic gene products. Removing maternal contributions is of course possible when the mother fly is mutant for the gene under study, but many interesting genes have essential zygotic functions. Germline clone techniques can serve as a workaround for the study of essential genes, but only if the mutation under study does not interfere with oogenesis. Here the genetics of *egg* serves as a clear example of the dilemma. Zygotic null mutants for *egg* have poor viability, and *egg* is required at multiple points in both the soma and germline during oogenesis. Therefore, no study has examined a potential role for *egg* during the establishment of the heterochromatin in the early embryo.

Alternative strategies for removing maternally supplied function are needed. Although some methods do exist, they depend on the stability of their targets and can be slow and incomplete. Here we developed an approach in the spirit of the Anchors Away technique (Haruki et al. 2008) for inactivating GFP tagged proteins in the early embryo by selective mislocalization. As schematized in Fig 3.1A, target proteins are mislocalized by the expression of an anti-GFP nanobody (Rothbauer et al. 2008) fused to the lipid droplet binding protein Jabba (Li et al. 2012), which we call the JabbaTrap. Lipid droplets act as storage organelles during early embryogenesis and are distributed throughout the cytoplasm (Welte 2015), and we reasoned that trapping nuclear proteins on lipid droplets would block their function.

As an initial test, we targeted the protein Orc2, an essential component of the Origin Recognition Complex (ORC). Orc2 has a highly reproducible pattern of localization during the cell cycle and is required for S phase completion in mitotic cycles (Baldinger and Gossen 2009). Orc2-GFP embryos were injected with either water (control) or synthesized JabbaTrap mRNA and then immediately filmed by confocal microscopy. In control injected embryos Orc2-GFP resided in the nucleus in interphase, diffused into the cytoplasm upon mitotic entry, and then rapidly bound along the anaphase chromosomes in preparation for the next S phase (Fig. 3.1B, first row). In contrast, in embryos expressing the JabbaTrap, Orc2-GFP displayed aberrant

localization. During the first mitosis following injection, Orc2 was present on numerous cytoplasmic puncta as well as on membranous structures surrounding the mitotic spindle (Fig. 3.1B, second row, 3:00, Supplemental Movie 1). Upon mitotic exit Orc2 coalesced around the reforming nuclear envelope but did not bind to the chromosomes and remained in the cytoplasm during the subsequent S phase. As expected, without chromatin bound Orc2 nuclei entered mitosis after a delay but then underwent catastrophic anaphase bridging (Fig. 3.1B, second row, 19:00). Importantly, expression of the JabbaTrap in embryos with untagged Orc2 did not disrupt cell cycle progression (Fig. 3.1B, third row).

As a second test we used the same approach to mislocalize the protein Zelda, a pioneering transcription factor required for proper zygotic genome activation (Liang et al. 2008). We injected *sfGFP-zelda; His2Av-RFP* embryos with JabbaTrap mRNA during nuclear cycle 10, and then followed them by time lapse microscopy. Zelda is a nuclear protein that forms foci on interphase chromatin. Expression of the JabbaTrap blocked the nuclear localization of Zelda near the injection site (Fig. 3.1D). Embryos with JabbaTrapped Zelda failed dramatically at cellularization and gastrulation, events known to require zygotic transcription. Nuclei near the injection site did not undergo the shape changes characteristic of cellularization, but rather appeared swollen and ultimately fell out of the cortical layer (Fig. 3.1C).

Next, we established transgenic lines for the JabbaTrap. Lipid droplets form during oogenesis and we reasoned that by driving the expression of the JabbaTrap with a Maternal-tubulin Gal4, which activates transcription after egg chamber budding, embryos would already have the JabbaTrap deployed when they begin developing. To test this idea, we injected purified mCherry-HP1a and GFP-HP1a proteins into embryos collected from mothers expressing the JabbaTrap. Following protein injection, we immediately filmed embryos by confocal microscopy. As expected mCherry-HP1a quickly localized to the nucleus after its delivery (Fig. 3.1E, in magenta). In contrast, injected GFP-HP1a localized to numerous

cytoplasmic puncta and was excluded from the nucleus throughout the cell cycle (Fig. 3.1E, in green).

As a further test we used our transgenic JabbaTrap to block the Polycomb group protein Su(z)12, an essential component of PRC2 with well characterized mutant phenotypes at different stages of development. Polycomb group proteins are required for the repression of the homeotic genes and determine their anterior boundary of expression in the developing embryo. However, zygotic null mutants for *Su(z)12* die during L1 or L2 stages without any obvious polycomb phenotypes, likely due to the confounding impact of maternal supply (Birve et al. 2001). Germline clone analysis using null alleles revealed that *Su(z)12* is also essential for oogenesis. To test an embryonic function for *Su(z)12*, Birve et al. crossed females with germline clones of the weak *Su(z)12²* allele with males heterozygous for a deficiency spanning the gene region. The resulting embryos misexpressed the homeotic gene *Ubx*, a classic polycomb phenotype. To determine if our JabbaTrap approach could produce a similar loss of function situation we tagged Su(z)12 with sfGFP at its endogenous locus using CRISPR-Cas9 (Supplemental Fig. 3.1) and expressed our JabbaTrap maternally in this background. This resulted in high embryonic lethality (2.7% hatch rate, n = 150) and clear misexpression of *Ubx* (Fig. 3.1F). In control embryos Su(z)12 formed nuclear foci in gastrulating embryos – a stage when polycomb bodies first become evident. In contrast, expression of the JabbaTrap prevented nuclear localization of Su(z)12 (Fig. 3.1G)

Eggless is required for the establishment of the heterochromatin at the MBT

Our prior study characterized the appearance of H3K9me_{2/3} during early embryogenesis using antibody staining and observed little evidence of this modification before cycle 13 (Yuan and O'Farrell 2016). To understand the dynamics of H3K9me₂ deposition we took advantage of the Fab-based live endogenous modification (FabLEM) technique (Hayashi-Takanaka et al. 2011). We injected GFP-HP1a expressing embryos with Cy5 labeled Fab

fragments recognizing H3K9me2 to follow both modifications in real time over cycles 12-14 (Fig. 3.2A, Supplemental Movie 3.2). In doing so we made several interesting observations. Within a cell cycle, the K9me2 Fab accumulated progressively in chromatin foci as interphase proceeded, but the signal dissipated upon entry into mitosis. At telophase the K9me2 Fab was again recruited to chromatin, and in each successive cycle the intensity of this telophase signal increased. We interpret this as an indication of the amount of H3K9me2 carried over from the previous cell cycle, and by cycle 14 this telophase signal is significant (Fig. 3.2A, Cycle 14 0:00). Additionally, as interphase duration increased in successive cycles the chromatin bound Fab signal accumulated to greater extent. This was particularly dramatic during interphase 14 when the K9me2 Fab signal became quite bright and eventually covered the chromocenter (Fig. 3.2A, Cycle 14 64:00). The recruitment of HP1a to chromatin foci closely paralleled the appearance of K9me2 Fab signal. We conclude that H3K9me2 increases progressively during cycles 12-14 as interphase duration extends, and that modifications deposited in earlier cycles can carry over to later cycles.

Because the association of HP1a during interphase 14 tracked closely the accumulation of H3K9me2 we used its recruitment to assess the contributions of the different *Drosophila* K9 methyltransferases to the establishment of heterochromatin. As mentioned above, *G9a* and *Su(var)3-9* are dispensable genes, allowing us to analyze embryos from null backgrounds. Embryos of either *WT*, *G9a^{RG5}*, or *Su(var)3-9^{06/17}* background were injected with mCherry-HP1a and the recruitment of this protein to heterochromatin was recorded during cycle 14 by confocal microscopy. The timing and extent of HP1a recruitment to heterochromatic foci appeared similar between *WT* and *G9a^{RG5}* embryos, and by the end of cycle 14 these foci had fused into a chromocenter (Fig. 3.2B, 2nd row). Surprisingly, although HP1a recruitment in *Su(var)3-9* embryos was altered, with both delayed and reduced appearance of foci, these embryos still formed significant amounts of heterochromatin (Fig. 3.2B, 3rd row). TALE-light probes allow us

to follow specific satellite repeats in live embryos (Yuan et al. 2014). Using this technique, we previously documented that the 359 bp repeat, a 20 Mb sized satellite on the X chromosome, acquires H3K9me2/3-HP1a during cycle 14. By co-injecting mCherry-HP1a and 359-TALE-GFP proteins we observed that neither *G9a* or *Su(var)3-9* was required for the recruitment of HP1a at 359 (Fig. 3.2C). We conclude that *G9a* is not required for the establishment of heterochromatic modifications, and that *Su(var)3-9*, while contributing, is not required for initiating HP1a recruitment.

Our development of the JabbaTrapping technique allowed us to assess the contributions of *eggless* to establishment. First, we used CRISPR-Cas9 to tag endogenous Egg with GFP at its N-terminus (Supplemental Fig. 3.1), the resulting line was healthy and fertile indicating that our tag is functional. In JabbaTrap expressing embryos GFP-Egg was mislocalized to small cytoplasmic puncta and blocked from entering the nucleus throughout the cell cycle (Supplemental Fig. 3.2). Like the behavior of lipid droplets, these puncta were prominent and surrounded the nuclei during the syncytial cycles but appeared to drop out of the cortical layer by cycle 14. Additionally, embryos with JabbaTrapped Egg had poor viability (15% hatch rate, n = 283).

To assess the effect that mislocalization of Egg had on the establishment of the heterochromatin JabbaTrap control and JabbaTrapped GFP-Egg embryos were injected with mCherry-HP1a and imaged by confocal microscopy during cycle 14. In control embryos HP1a formed foci that grew in number and intensity over time, and then ultimately fused into a large chromocenter. Once established during cycle 14, HP1a association at the chromocenter is inherited in subsequent cell cycles, and nuclei begin interphase 15 with HP1a enriched at the chromocenter (Fig. 3.2D, Supplemental Movie 3.3). In contrast, the mislocalization of Egg substantially reduced and delayed the recruitment of HP1a to heterochromatic foci (Fig. 3.2D, Supplemental Movie 3.4). Even by the end of cycle 14 the amount of HP1a marked

heterochromatin was clearly less than control, indicating that some of the sequences that normally acquire HP1a fail to do so in the absence of Egg. Indeed, following JabbaTrapping of Egg, HP1a did not localize to the 359 bp repeat (Fig. 3.2G). In control embryos, HP1a was recruited to the 359 bp repeat during the middle of interphase 14, but JabbaTrapping of Egg blocked this accumulation (Fig. 3.2F and Supplemental Fig. 3.3). Additionally, the deficit in HP1a localization to the chromocenter was inherited into cycle 15 (Fig. 3.2D).

Next, we directly examined K9 methylation using the K9me2-Fab. JabbaTrapping Egg completely prevented the appearance of H3K9me2 at 359 during cycle 14, and significantly reduced its accumulation throughout the chromocenter (Fig. 3.2E). However, we note that the mislocalization of Egg did not completely abolish the formation of either HP1a or H3K9me2-Fab foci, these could represent sequences that rely on methylation by G9a or Su(var)3-9, or that recruit HP1a by a methylation independent pathway. To confirm these results, we stained fixed gastrulation stage embryos for HP1a and H3K9me3. Control embryos had a clear chromocenter that stained positively for both modifications. In contrast, in JabbaTrapped Egg embryos K9me3 was undetectable, and although a few HP1a foci were present, they were faint and disperse (Supplemental Fig. 3.3C).

We conclude that Egg plays a major role in the restoration of repressive chromatin modifications on the satellite DNA during the MBT and is required for the establishment of H3K9me2/3-HP1a at the 359 bp repeat. In addition, Egg is unique in this respect among the three K9 methyltransferases in *Drosophila*.

Live imaging of Egg reveals the dynamics of heterochromatin establishment

Although prior studies had documented enrichment of Egg at Chromosome 4 and not to the chromocenter, our JabbaTrap experiments revealed a major role for Egg in the formation of the constitutive heterochromatin. We thus decided to examine the localization dynamics of Egg

by live confocal microscopy in the early embryo. However, endogenous levels of Egg were relatively low in the embryo making long term and high-resolution imaging of GFP-Egg difficult. To solve this issue, we took advantage of the HaloTag system in combination with the JF549 fluorescent dye which has improved brightness and photostability compared to EGFP (Grimm et al. 2015). We used CRISPR-Cas9 to insert the HaloTag at the N-terminus of the endogenous *egg* gene. The resulting flies were viable and fertile. After permeabilization with Citrasolv, the HaloTag ligand JF549 could directly enter the embryo allowing easy *in vivo* labeling. Examination of embryos with both Halo549-Egg and GFP-Egg revealed that the two proteins had equivalent localization during late cycle 14 (Supplemental Fig. 3.4D). Additionally, the JF549 labeling was specific to embryos containing the Halotag (Supplemental Fig. 3.4E).

In late cycle 14 embryos Halo-Egg colocalized with GFP-HP1a and the H3K9me2-Fab at the satellite sequences (Fig. 3A). Interestingly, the Egg signal was contained within a broader nuclear region labeled with HP1a and K9me2 indicating that at this stage, when the heterochromatin has matured, Egg does not fill the entire heterochromatin domain. By altering the parental origin of tagged *egg/less* we determined that the Egg present during cycle 14 is primarily maternally supplied (Supplemental Fig. 3.4C). Not all satellite sequences acquire H3K9me2/3 during the MBT, the 1.686 repeat remains free of this modification until much later in development (Yuan and O'Farrell 2016). In accordance with this fact, by using different TALE-light probes we see that Egg binds to 359, but not to 1.686 (Fig. 3.3B). *Eggless* contains a tandem tudor domain (Supplemental Fig. 3.4A), a structure known to mediate chromatin targeting in other proteins. Therefore, we generated a transgene to express a version of GFP-Egg lacking the tandem tudor sequence and expressed this mutant protein in the early embryo. We observed that the tandem tudor domain was required for the nuclear localization of Egg (Supplemental Fig. 3.4B). For comparison we also examined the localization of the G9a methyltransferase because our previous experiments demonstrated that it was not required for

heterochromatin establishment. Unlike Egg, G9a did not co-localize with HP1a during cycle 14, but rather was diffusely present in the nucleus (Fig. 3.3C).

As early as cycle 10, we documented multiple bright foci of Halo-Egg in the nucleus (Fig. 3.3D). In contrast, at this stage HP1a is uniformly distributed in the nucleus and not enriched to heterochromatic foci. Live imaging of Halo549-Egg together with GFP-HP1a over the next 4 cell cycles yielded several interesting observations (Fig. 3.3D). During each interphase Egg accumulated progressively to bright chromatin foci after a short (2 min.) delay following exit from the prior mitosis (Fig. 3.3D, Supplemental Movies 3.5 and 3.6). By tracking individual Egg foci over multiple frames of our records we documented a pattern (Fig. 3.3D, circled foci, and Supplemental Movie 3.5) where a small focus of Egg would appear and then be joined by a focus of HP1a within minutes. The two proteins then grew in intensity over the course of interphase. Upon entry into mitosis, HP1a dissociated from chromatin and Egg followed slightly later. Overall, the recruitment of Egg to specific foci preceded that of HP1a within the cell cycle and during development. The longer interphase durations in later cell cycles correlated with greater accumulation and longer retention of Egg at its chromatin targets. For instance, during the brief 7 min. interphase 11 Egg foci grew in number and intensity for 5.5 min., but then these foci rapidly disappeared as the nucleus prepared for mitosis (Fig. 3.3D). In contrast, during the prolonged interphase 14 Egg foci were brighter and remained on chromatin for the duration of our records. In conclusion, the recruitment of Egg to its chromatin substrates is a progressive process occurring in each cell cycle that begins early in embryogenesis (at least by cycle 10). These observations together with our real time records of H3K9me2 accumulation (Fig. 3.2A) indicate that changes in interphase duration may time the formation of the heterochromatin.

Our records also revealed some diversity in behaviors. The appearance and growth of Egg foci did not follow a single schedule, apparently different sequences recruit the protein at different times during interphase. By cycle 14, it was clear that HP1a was recruited to some foci

before Egg, a possible indication of the H3K9me2/3 carried over from prior cell cycles. Additionally, some foci of HP1a did not co-localize with Egg, which is consistent with our observation that a small amount of HP1a was still recruited after JabbaTrapping Egg (Fig. 3.2D).

Windei, an activator of Eggless, localizes to the heterochromatin in the early embryo

Studies on both Egg, and its mammalian counterpart SETDB1 suggest that it requires a cofactor for efficient methylation of H3K9. SETDB1 alone has very poor methyltransferase activity (Schultz et al. 2002), but it is greatly stimulated when in complex with the protein mAM/MCAF1 (Wang et al. 2003). The *Drosophila* ortholog of mAM known as *windei* (*wde*) was suggested to play a similar role in flies (Koch et al. 2009). The phenotypes of *wde* and *egg* mutants are similar, and *wde* is also required during oogenesis. The two proteins physically interact and were reported to co-localize at Chromosome 4 in polytene preparations, but both were absent from the chromocenter. Because we have documented a role for Egg at the constitutive heterochromatin in the early embryo we decided to examine Wde during this stage.

Immunostaining revealed that Wde localizes to the heterochromatin during its establishment at the MBT. Wde was enriched in the DAPI intense apical portion of the nucleus where the satellite sequences reside (Fig. 3.4A). Additionally, we observed broad colocalization between Wde and HP1a late in cycle 14 (Fig. 3.4B). Because we had shown that the association of H3K9me2/3-HP1a to the 359 bp repeat required Egg we wanted to know if Wde also bound to this satellite. TALE-light staining revealed that Wde does localize to 359 (Fig. 3.4C). By co-IP western blotting we documented that GFP-Egg interacts with endogenous Wde in the early embryo (Fig. 3.4D), in agreement with what was reported in S2 cells (Koch et al. 2009). We also noticed that Wde was found in the cytoplasm in embryos with JabbaTrapped Egg (Fig. 3.4E), indicating that the JabbaTrap may be useful to mislocalize entire protein

complexes. We conclude that in the early embryo Wde co-localizes with Egg during the formation of the constitutive heterochromatin.

Interphase duration controls Egg recruitment to and establishment of the heterochromatin.

To examine the relationship between heterochromatin establishment and the cell cycle more directly we injected Halo-Egg embryos with Cy5 labeled histone proteins, to visualize the chromatin, and imaged at high frame rate. As described previously, Egg accumulated to multiple nuclear foci during interphase with a slight delay following exit from the previous mitosis (Supplemental Movie 3.6). These foci abruptly disappeared upon chromosome condensation at prophase (Fig. 3.5A, Supplemental Movie 3.6). It appears that mitosis inhibits the chromatin association of Egg, which would prevent it from methylating H3K9.

Our observations over cycles 11-14 (Fig. 3.3D) when the cell cycle slows naturally suggested that interphase duration limits the recruitment of Eggless to the heterochromatin. To test this idea, we wanted to experimentally arrest the cell cycle in interphase and examine the consequences on Egg localization. Embryos injected with dsRNA against the 3 mitotic cyclins (A, B, and B3) during cycle 11 arrest during interphase 13 (McClelland and O'Farrell 2008). We then followed Halo549-Egg and GFP-HP1a by confocal microscopy during this prolonged interphase. In control embryos, Egg accumulated at nuclear foci over interphase, but by 13 min. into the cycle these foci began disappearing as chromosomes entered mitosis (Fig. 3.5B). In contrast, arresting nuclei in interphase permitted continued accumulation and chromatin association of Egg for the duration of our records (Fig. 3.5B, Supplemental Movie 3.7). Egg foci in arrested nuclei became brighter and larger than in the control and resembled Egg foci observed late in cycle 14 (Fig. 3.3D). This effect was paralleled by increased recruitment of HP1a to large heterochromatic foci (Supplemental Movie 3.7). We conclude that mitosis limits Egg accumulation and persistence on chromatin.

Our model would predict that reducing interphase duration would decrease the amount of heterochromatin established by Egg, so we shortened interphase using a *grapes (chk1)* mutant and counted the number of GFP-HP1a foci per nucleus as a readout. Embryos mutant for *grp* have faster cell cycles because the replication checkpoint is required for the progressive prolongation of interphase during cycles 11-13 (Sibon et al. 1997). Mutant *grp* embryos enter mitosis 13 before completing DNA replication and exhibit an 8 min. instead of 14 min. interphase. In heterozygous control embryos the number of HP1a foci increased over the initial 11-12 min. of interphase, reaching a maximum of over 14 foci per nucleus (Fig. 3.5 C and D), before declining rapidly as nuclei prepare for mitosis. In contrast, in *grp* embryos HP1a began to recruit to nuclear foci, but the increase in foci number ended abruptly at about 6 min. into interphase (Fig. 3.5 C and D). Interestingly the rate of increase was also reduced, although the cause of this change is unclear we note that cycles 11 and 12 are also shortened in *grp* embryos, which could result in a cumulative reduction in the amount of H3K9me_{2/3} carried over from prior cycles. Thus, shortening interphase reduces the amount of heterochromatin formed.

Injection of *twine* (Cdc25) mRNA during cycle 13 can shorten interphase 14 and lead to an additional mitosis by reintroducing CDK1 activity during a time when it is normally absent (Farrell et al. 2012). We found that the extra mitosis induced in this way interrupted the accumulation of GFP-HP1a (Fig. 3.5E). Thus, premature mitosis interferes with heterochromatin formation.

DISCUSSION

Histone modifications play a critical role in the epigenetic programs controlling development. The chromatin in the early *Drosophila* embryo lacks many of these modifications and their restoration begins in an unusual setting where cells divide remarkably quickly and in the absence of substantial transcription. The reappearance of stable chromatin states coincides with the slowing of the cell cycle and the onset of major transcription at the MBT. Here we have

focused on the initial events controlling the de novo formation of the heterochromatin. Using our new JabbaTrap method (Fig. 3.1), we showed that Eggless is the major H3K9 methyltransferase establishing heterochromatin domains in the embryo. Further using real time imaging, we documented the early steps of heterochromatin formation and uncovered a close relationship between the recruitment of Egg (Fig. 3.3E), the accumulation of H3K9me2/3-HP1a (Fig. 3.2A) and slowing of the cell cycle. Experiments manipulating interphase duration indicate that this relationship is regulatory (Fig. 3.5). We propose that the slowing of the cell cycle as the embryo approaches the MBT expands limited windows of opportunity for Egg action and thereby times heterochromatin formation.

JabbaTrapping – a new tool for inactivating maternal function

The early embryo poses unique challenges to functional studies. The vast maternal supply present for many gene products complicates traditional genetic analysis. Additionally, early embryonic events happen fast so that methods that depend on destruction of RNA and protein must quickly destroy a large pool of target to produce a phenotype. Our JabbaTrap approach can rapidly block maternal activities by mislocalizing target proteins to lipid droplets (Fig. 3.1). Additionally, by establishing a transgenic system we deployed the JabbaTrap to lipid droplets forming during oogenesis and mislocalized proteins during early embryogenesis. Interestingly, the JabbaTrap also mislocalizes proteins that interact with the target (Fig. 3.4E) suggesting that it may be a useful approach to inactivate entire nuclear protein complexes. In principle, the JabbaTrap could be applied to any protein with a cognate nanobody, and we observed that the method successfully interferes with many different nuclear functions. However, the function of cytoplasmic proteins might be less susceptible to inhibition by localization to lipid droplets. The combination of nanobody based inactivation approaches and CRISPR-Cas9 gene editing to endogenously epitope tag proteins will allow easy functional

studies in the future, and the JabbaTrap fills a special need for such techniques in the dissection of early development.

A new developmental model for the formation of heterochromatin

The restoration of a more standard cell cycle regulation and timing at the MBT coincides with the formation of mature heterochromatin. However, this is not a single change but a process involving a series of precisely controlled events with the satellite DNA progressively acquiring different defining characteristics of heterochromatin. Direct cytological examination demonstrated that satellite DNA is compacted as early as cycle 8 (Shermoen et al. 2010). Satellites begin exhibiting slight delays in replication time during cycles 10 through 13, and then show major delays during S phase 14. This onset of late replication, and the consequent prolongation of S phase 14 requires the action of the protein Rif1 (Seller and O'Farrell 2018). As the cell cycle slows during the nuclear divisions leading up to the MBT, Egg deposits H3K9me2/3, which recruits HP1a to the heterochromatin. By the end of cycle 14 the satellite sequences are stably marked by H3K9me2/3-HP1a, and they inherit or maintain this modified state throughout development.

Although no obligate coupling is apparent, the embryonic cell cycle program controls the actions of both Rif1 and Egg. Prior to the MBT high levels of cyclin-Cdk1 activity directly inhibit Rif1 by promoting its dissociation from the satellite DNA thus ensuring short S phases (Seller and O'Farrell 2018). The cell cycle itself controls the action of Eggless in two ways (Fig. 3.6). First, deposition of naïve histones during DNA replication halves the level of histone modification in daughter nuclei. Prior studies have shown that the post S phase recovery of the level of histone modification is slow (Alabert et al. 2015; Xu et al. 2012). Importantly, if a histone-modifying enzyme does not double the amount of its product during a cell cycle then the

level of modification will decrease over time. Second, rapid cell cycles limit the opportunity for Egg action. Egg accumulates gradually at chromatin foci during interphase, and accumulated Egg dissociates abruptly when chromosomes condense in preparation for mitosis (Fig. 3.5A). As interphase extends in the approach to the MBT, both the amount of recruited Egg and its residence time increase, leading to increased deposition of H3K9me2/3. For instance, during the 7-minute interphase 11 Egg does recruit to chromatin, but its accumulation is minimal due to the rush to mitosis (Fig. 3.3E). Only incremental increases in methyl marks occur prior to the much-elongated interphase 14. Indeed, the large 359 bp repeat only becomes stably associated with H3K9me2/3-HP1a during cycle 14 (Yuan and O'Farrell 2016), and this association requires Egg (Fig. 3.2). Importantly, experimentally arresting the cell cycle in interphase permitted continued accumulation of Egg and HP1a (Fig. 3.5B) while shortening interphase reduced the recruitment of HP1a (Fig. 5 C and D). We conclude that the speed of early cell cycle limits the activity of maternally provided Egg and that the schedule of cell cycle lengthening times the appearance of H3K9me2/3-HP1a to give the observed weak accumulations in the later pre-MBT cycles and more fully elaborated heterochromatin at the MBT (Fig 3.6).

Two recent studies reported that HP1 proteins display liquid like properties, and suggested that the formation of heterochromatin domains depends on the ability of HP1 to phase separate (Larson et al. 2017; Strom et al. 2017). In contrast, our previous observations (Shermoen et al. 2010; Yuan and O'Farrell 2016) suggest that specific interactions trigger the deposition of heterochromatin marks on pre-existing compacted foci of satellite sequences. Here we extend this view by uncovering a role for Egg in the early events of heterochromatin formation. Among methyltransferases, Egg is uniquely required for initiation (Fig. 3.2). Additionally, using live imaging we documented the first steps in the natural establishment of heterochromatin. Early Egg accumulation localized to small puncta within larger foci of satellite sequences, suggesting a nucleation process. Once recruited to chromatin, Egg deposits

H3K9me2/3, and this mark seeds a domain of HP1a, which then grows and spreads perhaps then utilizing HP1's liquid-like properties (Fig. 3.6). At least for some of the foci, the small Egg focus does not seem to expand in concert with methylation and HP1a recruitment (Fig. 3.3A), suggesting additional inputs.

We previously found that timely recruitment of ectopically introduced HP1a to the 359 satellite was blocked by a mutation in its chromoshadow domain that prevents binding to a PxVxL motif (Yuan and O'Farrell, 2106), a seemingly unexpected dependency. This same study found that HP1a bearing a mutation blocking K9me2/3 recognition (V26M mutant) still associated with this satellite, a finding that appears at odds with the present finding that recruitment of HP1 to 359 requires the methyltransferase Egg. The meaning of these observations is not clear. Perhaps dimerization or oligomerization allowed the ectopically introduced V26M mutant to localize with endogenous wild-type HP1a that was recruited to foci of H3K9me2/3. Alternatively, Egg might have methylation independent interactions that can recruit other proteins including HP1a in a heterochromatin complex. The findings suggest that complex interactions guide maturation of heterochromatin foci, and many details remain to be uncovered. Importantly, our present study identifies Egg as a key factor in the earliest steps of this process.

Given that we observed recruitment of Egg to specific chromatin foci as early as cycle 10 (Fig. 3.3D) the inputs specifying the future heterochromatic sequences must be present very early. However, we can currently only speculate about how Egg is targeted. One attractive hypothesis is that specificity comes from maternally deposited small RNAs that would recognize complementary nascent transcripts, much like the heterochromatin machinery of *S. pombe* (Allshire and Madhani 2018). In support of this notion the recruitment of HP1a to the 359 repeat requires the maternal presence of this satellite indicating that this process is maternally guided (Yuan and O'Farrell 2016). Additionally, Egg participates in the Piwi pathway and is directed to

transposons in the genome by complementary piRNAs, although the details of this mechanism are currently unclear (Sienski et al. 2015). A second possibility is that Egg binds to specific DNA binding proteins that act to specify its localization. A family of DNA binding proteins known as KRAB-ZFP repressors target SetDB1 in mammals (Schultz et al. 2002). While the KRAB family appears to be a tetrapod specific innovation, proteins recognizing specific satellite repeats have been identified in *Drosophila*, and it remains a possibility that they recruit Egg to chromatin (Aulner et al. 2002).

Developmental specificity of methyltransferase action

Development can employ the same protein for different purposes in different tissues and stages, and Egg is prime example of this. Our results demonstrate that Egg plays a major role in the initial deposition of heterochromatin in the embryo, but prior work had shown that loss of *egg* does not affect the association of H3K9me2/3-HP1a at the chromocenter in larval polytene chromosomes (Seum et al. 2007a; Tzeng et al. 2007). So Egg is critical for establishment, but not for the maintenance of heterochromatin. Interestingly, the reverse is true for the methyltransferase Su(var)3-9. It makes only minimal contribution during initiation (Fig. 3.2 B and C), but then plays a dominant role later in development. We suggest that one key difference between these two enzymes underlies this developmental specialization. Su(var)3-9, but not Egg, contains a chromodomain allowing it to bind its own product making it ideal for maintenance (Schotta et al. 2002). This capacity allows for positive feedback where prior methylation facilitates the modification of adjacent nucleosomes. In fission yeast the chromodomain of the K9 methyltransferase Clr4 is critical for the spread and maintenance of domains of H3K9me2/3 (Hall et al. 2002; Zhang et al. 2008; Al-Sady et al. 2013). Notably, a recent study in *C. elegans* embryos uncovered that the SETDB1 methyltransferase (MET-2) is critical in this species for the formation of heterochromatin, indicating that a special function for SETDB1 during initiation is conserved (Mutlu et al. 2018).

Do rapid embryonic cell cycles wipe the slate clean during development?

Although we have focused on the constitutive heterochromatin, our study could provide broader insight into the regulation of histone modifying enzymes during development. In fact many other histone modifications only appear at the MBT (Chen et al. 2013; Li et al. 2014), and direct examination of the enzymes installing these marks during embryogenesis would be informative. We have emphasized the limitations that cell cycle speed imposes on the restoration of the histone modifications, but we don't want to obscure what we think may be an important benefit of these rapid divisions. Embryos inherit their genomes from their parents, and these parental genomes come with parental chromatin modifications that are installed during gametogenesis (Loppin et al. 2005). The vast majority of animals develop externally from large eggs that begin with rapid cell divisions without growth or transcriptional input. We suggest these fast cell cycles provided an ancestral mechanism to reset the embryonic chromatin without the need for specific enzymes catalyzing the removal of histone modifications. Multiple rounds of short S phases would dilute parental modifications, and brief interphases would limit the action of maternally supplied chromatin modifying enzymes, which are present long before they are needed. Developmental programs could then re-introduce these so-called epigenetics marks as the embryo reaches the MBT, thereby coordinating the onset of zygotic transcription with the appearance of stable patterns of histone modification. Notably, the situation in mammalian embryos is different with repressive modifications appearing early during the cleavage stages (Fadloun et al. 2013). However, the evolution of placental development restructured mammalian embryogenesis and the post-fertilization divisions are much slower and transcription begins immediately. By controlling the speed of the embryonic cell cycle, development coordinates the deposition of epigenetic modifications with the onset of zygotic transcription.

ACKNOWLEDGEMENTS

We thank past and present members of the O'Farrell laboratory, especially Kai Yuan, Antony Shermoen, and Mark McClelland for guidance and reagents. We also thank Anna Holman for early work on this project. Hiroshi Kimura generously provided labeled Fab reagents for H3K9me2. Luke Lavis generously provided halotag ligands labeled with Janelia Fluorescent dyes. The Bloomington Stock Center and the *Drosophila* community provided important reagents and fly stocks throughout this work.

FIGURE 3.1

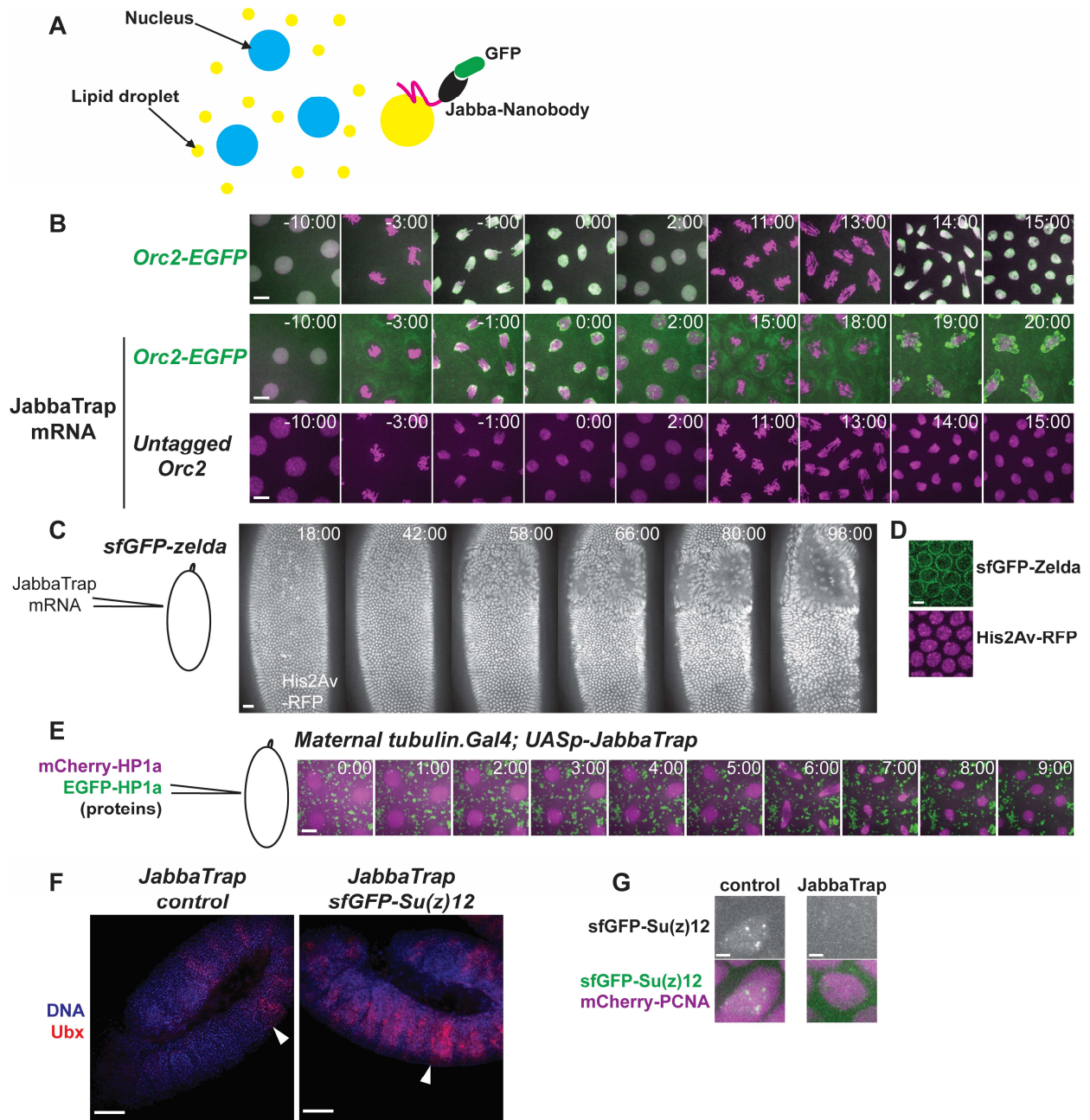


Fig. 3.1 JabbaTrap rapidly mis-localizes and blocks nuclear proteins in the embryo.

A) Schematic of the JabbaTrap technique. Lipid droplets (yellow circles), which serve as storage organelles, are distributed throughout the cytoplasm of the syncytial embryo. Ectopic expression of Jabba fused to an anti-GFP nanobody traps GFP tagged proteins on lipid droplets. **B)** The JabbaTrap mislocalizes Orc2 and blocks DNA replication. Stills from live imaging of embryos of the indicated genotype after injection of Cy5 labeled histone proteins alone or together with JabbaTrap mRNA. Top row, Orc2-GFP embryos injected with labeled histones (shown in magenta) only. Orc2 (shown in green) rapidly binds to the anaphase chromosomes (-1:00) and remains nuclear during the subsequent interphase. In Orc2-GFP embryos injected with both labeled histones and JabbaTrap message (middle row), Orc2 is prevented from binding to the chromosomes and mislocalized to both the reforming nuclear envelope and to puncta in the cytoplasm. Anaphase bridging occurs in the following mitosis (19:00). Bottom row, wildtype embryos injected with both Cy5-histones and JabbaTrap mRNA undergo normal mitotic cycles. Scale bar is 3 μ m. See Supplemental Movie 1. **C)** Stills from live imaging following His2Av-RFP in an sfGFP-Zelda embryo injected with JabbaTrap mRNA. Nuclei near the injection site failed to cellularize and collapsed out of the cortical layer. Scale bar is 10 μ m and the start of cycle 14 is set as 0:00. **D)** Single z plane showing the mislocalization of sfGFP-Zelda by expression of JabbaTrap mRNA. Scale bar is 2 μ m. **E)** Co-injection of mCherry-HP1a and GFP-HP1a into an embryo from mothers expressing transgenic JabbaTrap during oogenesis. Scale bar is 4 μ m. **F)** JabbaTrap expression blocks sfGFP-Su(z)12 leading to derepression of the homeotic protein Ubx. The white arrowhead indicates the wild-type anterior border of Ubx expression. Embryos stained with DAPI (blue) and anti-Ubx (red). Scale bar is 25 μ m. **G)** Control or JabbaTrap expressing sfGFP-Su(z)12 embryos injected with mCherry-PCNA to label the nucleus. The JabbaTrap mislocalizes Su(z)12 to the cytoplasm. Scale bar is 1 μ m.

FIGURE 3.2

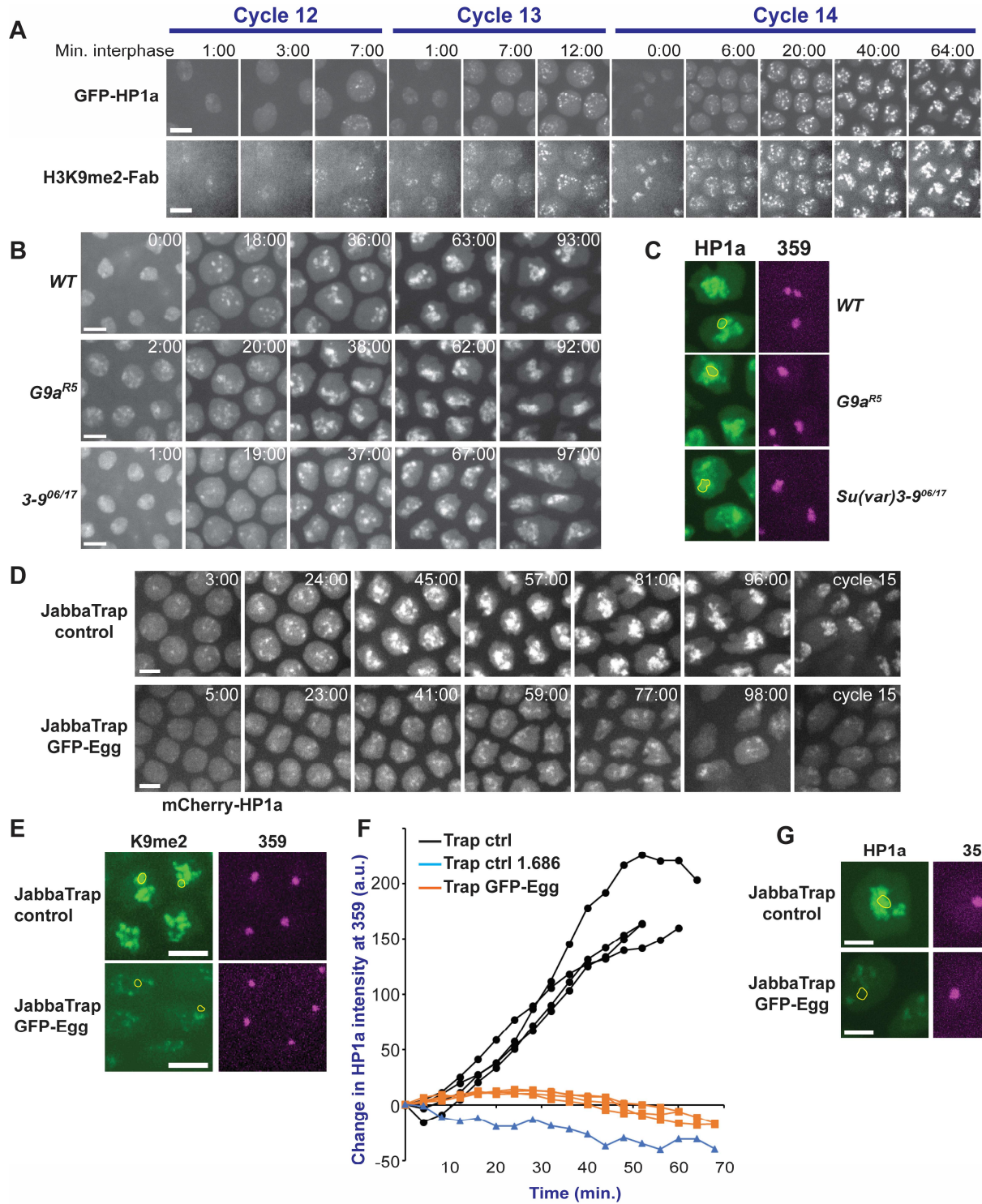


Fig. 3.2 Eggless is required for the embryonic establishment of heterochromatin.

A) Progressive accumulation of H3K9me2-HP1a in the early embryo. Selected stills from live imaging over 3 cell cycles of GFP-HP1a embryos injected with Cy5 labeled H3K9me2 Fab fragment. Scale bar is 3 μ m. See Supplemental Movie 2. **(B,C)** G9a and Su(var)3-9 are not required for the establishment of heterochromatin. **B)** Selected stills from live imaging of embryos of the indicated genotype injected with mCherry-HP1a protein. The beginning of interphase 14 was set as 0:00. The scale bar is 2 μ m. **C)** Stills of live embryos of the indicated genotype injected with GFP-HP1a and 359-TALE-mCherry. The location of 359 is outlined in yellow on the HP1a channel. Images were acquired approximately 1 hour into interphase 14. **(D-G)** JabbaTrapping Egg blocks the embryonic onset of H3K9me2-HP1. **D)** Live imaging of mCherry-HP1a injected into wildtype control or GFP-Egg embryos following maternal expression of the JabbaTrap. Mislocalization of Egg significantly reduced and delayed the accumulation of HP1a at the heterochromatin. The start of interphase 14 was set as 0:00. The scale bar is 3 μ m. Compare Supplemental Movies 3 and 4. **E)** Stills from live embryos of the indicated genotype injected with Cy5 labeled H3K9me2 Fab fragments and 359-TALE-mCherry. The position of 359 is outlined in yellow on the H3K9me2 channel. Images were acquired approximately 1 hour into interphase 14. Scale bar is 2 μ m. **F)** Plot of the change in mCherry-HP1a fluorescence at the 359 bp repeat over time during interphase 14. The 1.686 satellite, which does not recruit HP1a, serves as a negative control. Each line represents a different embryo, where fluorescence was measured in over 20 nuclei per embryo and the mean average for each time point was calculated. **G)** Stills from live embryos of the indicated genotype injected with mCherry-HP1a and 359-TALE-HaloJF646. The position of 359 is outlined in yellow on the HP1a channel. Embryos are approximately 80 minutes into interphase 14, during cephalic furrow formation. The scale bar is 1 μ m.

FIGURE 3.3

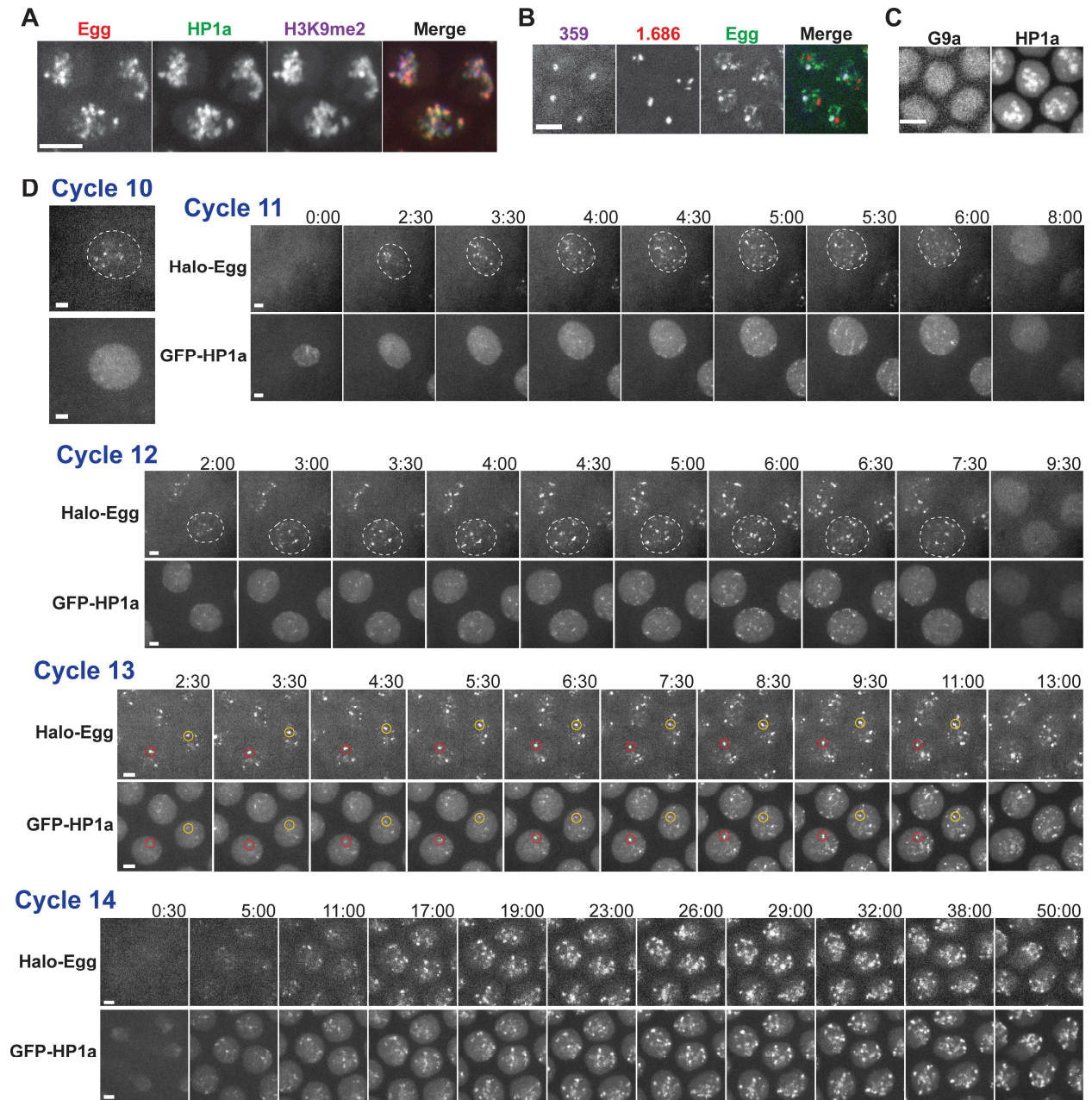


Fig. 3.3 localization and dynamics of Egg during the establishment of heterochromatin.

A) Confocal micrographs of a cycle 14 Halo(JF549)-Egg embryo injected with GFP-HP1a and Cy5 labeled H3K9me2 Fab. Scale bar 2 μm . **B)** Confocal micrograph of a cycle 14 GFP-Egg embryo injected with Halo(JF646)-359 and mCherry-1.686 TALE-Lights. Scale bar is 2 μm . **C)** Confocal micrographs of a live sfGFP-G9a embryo injected with mCherry-HP1a show that G9a does not localize to heterochromatin. Images were acquired approximately 50 min. into interphase 14. Scale bar 2 μm . **D)** Selected stills from live imaging of Halo(JF549)-Egg and GFP-HP1a during cycles 10-14 as interphase duration naturally extends. The recorded cycle is indicated above the micrographs. Egg accumulates at multiple bright foci in the interphase nucleus (denoted in dashed white line). Note that the recruitment of Egg precedes that of HP1a during development and during the cell cycle. Longer interphases permit increased accumulation of Egg on chromatin. Yellow and red circles in cycle 13 records track the fate of two foci of Egg and the corresponding locations in the HP1a channel. Each cell cycle was recorded from a different Halo-Egg embryo labeled with JF549 and the beginning of interphase was set as 0:00. Scale bars are 1 μm . See Supplemental Movie 5.

FIGURE 3.4

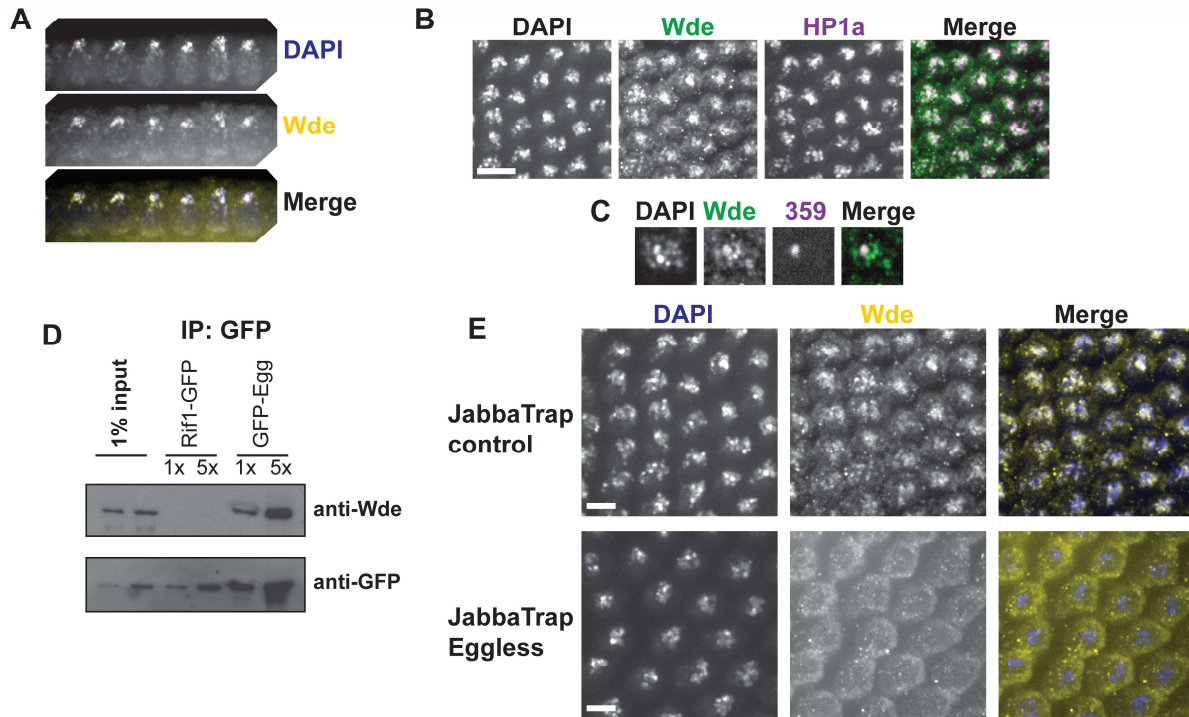


Fig. 3.4 Windei, a cofactor of Egg, localizes to the heterochromatin in the embryo and interacts with Egg.

(A-C) Wde is enriched at the constitutive heterochromatin in early embryos. **A)** Co-localization of Wde with the DAPI intense apical portion of the nucleus in fixed embryos. **B)** Cycle 14 embryos immunostained for HP1a and Wde. Scale bar is 5 μ m. **C)** Fixed cycle 14 embryo stained for Wde and with a TALE-light recognizing the 359 bp repeat. **D)** GFP-Egg was immunoprecipitated from 1 to 3 hour old embryos and analyzed by western blotting. Wde interacts with Egg in the early embryo. **E)** Fixed embryos expressing the JabbaTrap in either a control or GFP-Egg background were immunostained for Wde. Wde is mislocalized to the cytoplasm when GFP-Egg is JabbaTrapped. Scale bar is 3 μ m.

FIGURE 3.5

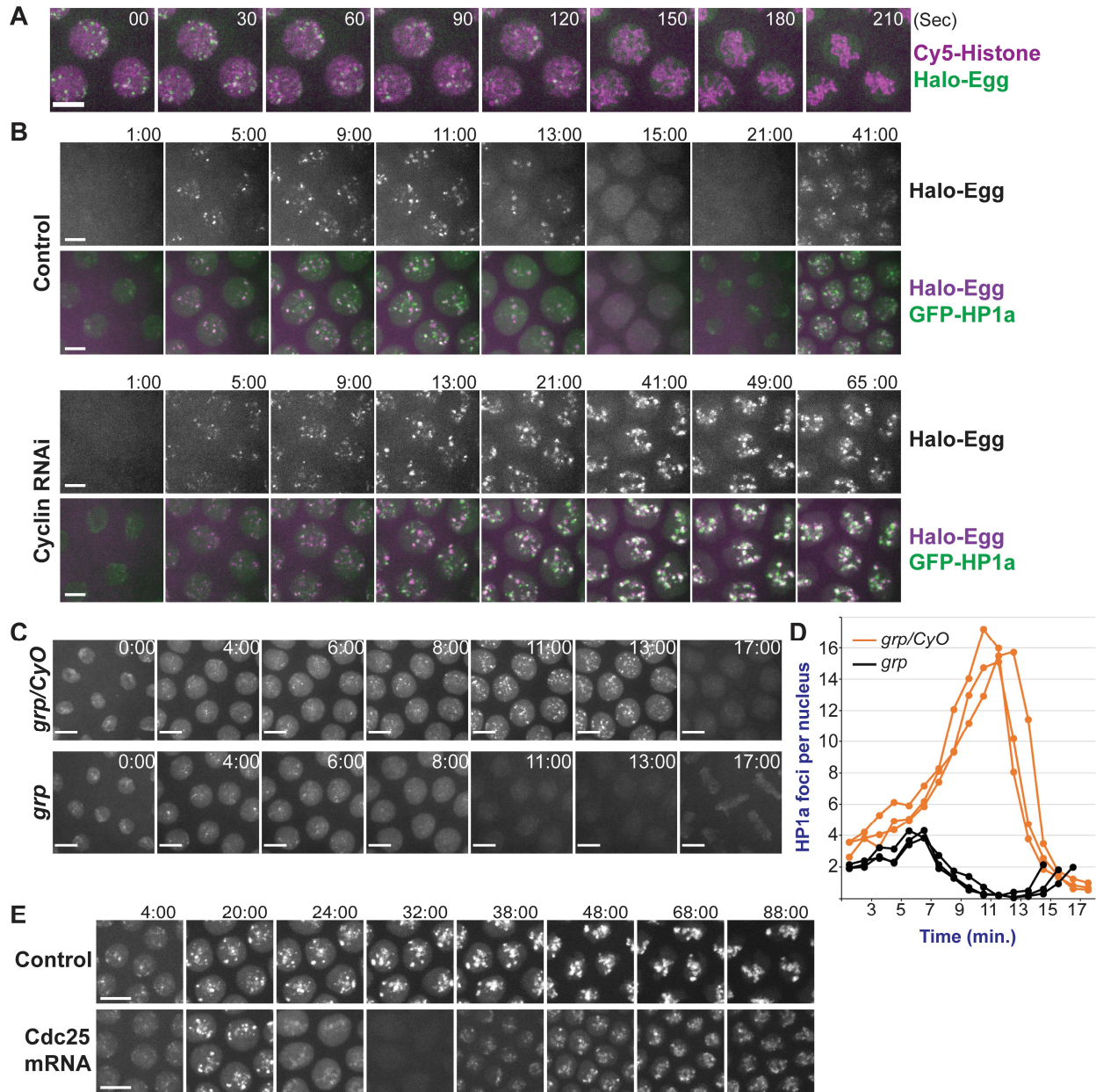


Fig. 3.5 Interphase duration limits the establishment of heterochromatin.

A) Selected stills from live imaging of Halo-Egg (shown in green) embryos injected with Cy5 labeled Histone proteins (shown in magenta). Egg dissociates from the chromatin upon mitotic chromosome condensation (150 sec.). Scale bar is 3 μm . See Supplemental Movie 6. **B)** Arresting the cell cycle in interphase 13 permits continued accumulation of Egg and HP1a at heterochromatin. Embryos were filmed by confocal microscopy after injection of buffer or dsRNA against cyclins A, B, and B3. Scale bar is 2 μm and the beginning of cycle 13 was set as 0:00. See Supplemental Movie 7. **(C-E)** Shortening interphase duration reduces HP1a accumulation. **C)** Stills from confocal microscopy tracking GFP-HP1a in embryos laid from mothers either heterozygous or homozygous for *grp*. Note that *grp* embryos enter mitosis 13 before completing S phase leading to anaphase bridges (17:00). Scale bar is 4 μm and the start of interphase 13 was set as 0:00. **D)** Plot of the average number of HP1a foci per nucleus over time in control embryos (orange) or *grp* embryos (black). Each line represents data from a different embryo, and foci of GFP-HP1a were counted in approximately 15 nuclei per embryo. **E)** Inducing an early mitosis 14 by expression of *twine* (*cdc25*) interrupts heterochromatin formation. Embryos expressing GFP-HP1a were filmed following injection of *twine* mRNA during cycle 13. Scale bar is 3 μm and the beginning of cycle 14 was set as 0:00.

FIGURE 3.6

Eggless

HP1a

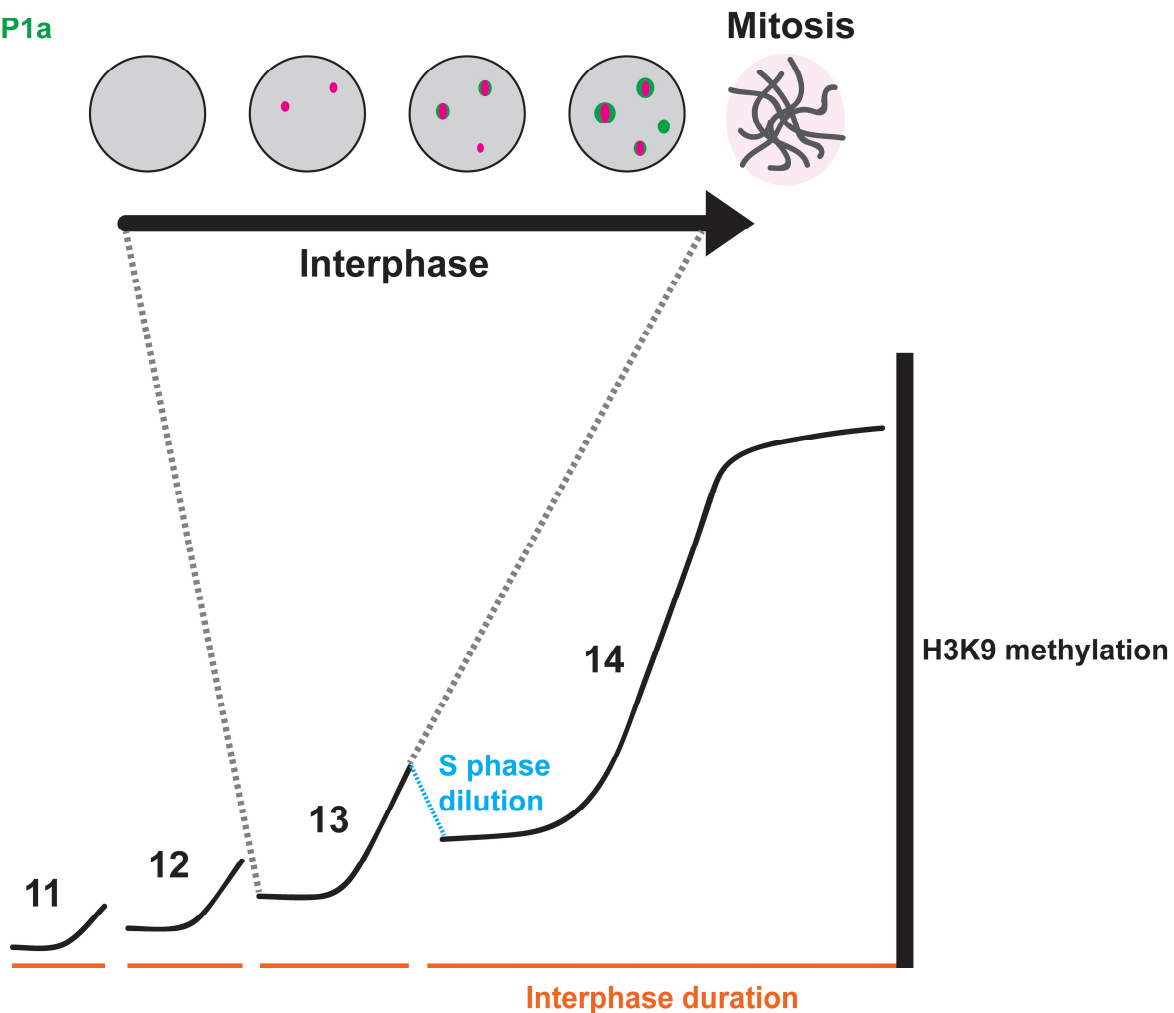
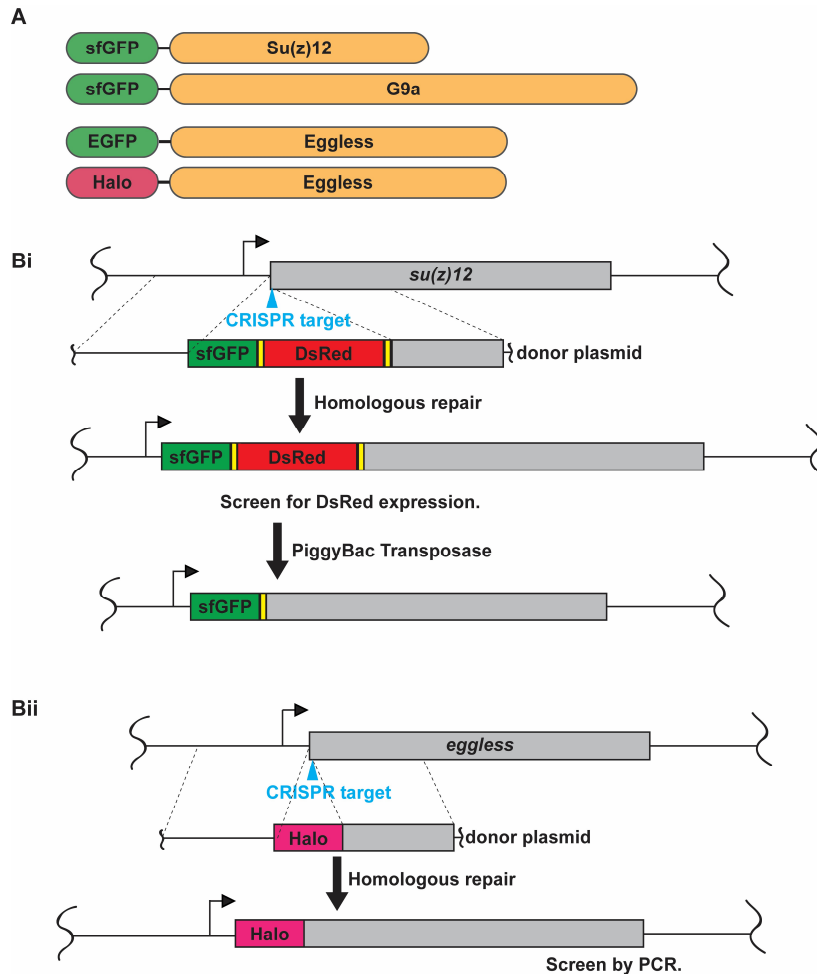


Figure 3.6. Model

Eggless initiates constitutive heterochromatin formation during early embryonic development. Egg is recruited to chromatin foci after a delay at the start of interphase. Egg foci grow in number and intensity as interphase proceeds. Later in interphase HP1a is recruited to sites occupied by Egg, although some HP1a recruitment is independent of Egg. The domain of HP1a grows and extends beyond the Egg signal. Finally, chromosome condensation in mitosis strips Egg from chromatin. Below a schematic showing that that the progressive accumulation of H3K9-methyl depends on the progressive lengthening of interphase during embryogenesis. Every S phase decreases the level of modification by half due to incorporation of newly synthesized histone proteins. Interphase duration limits the deposition of K9me2/3 by restricting the binding of Egg to its chromatin targets, therefore high levels of modification appear only later in embryogenesis when the cell cycle slows down.

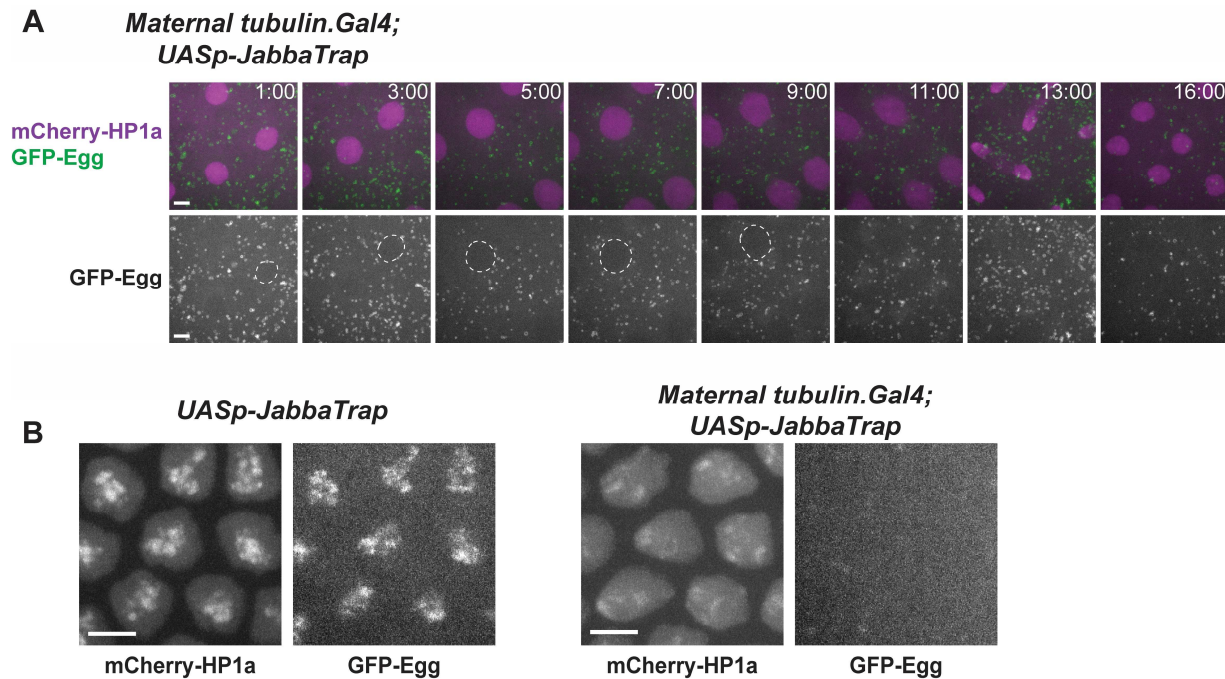
SUPPLEMENTAL FIGURE 3.1



Supplemental Figure 3.1

A) Diagram of the endogenously tagged *Drosophila melanogaster* stocks generated in this study. Fluorescent tags were fused to the N-terminus of the indicated proteins. Successful modification was confirmed by PCR followed by Sanger sequencing and by Western Blotting. Founding lines were backcrossed for at least five generation to our lab's wild-type stock (Canton-S). All lines were viable and fertile. **B)** Schematic showing the CRISPR-Cas9 strategies used to generate the tagged lines indicated in panel A. CRISPR gRNA targets near the N-terminus of the gene of interest were identified using the CRISPR Target Finder tool (Gratz et al. 2014). *Vasa-Cas9* embryos were co-injected with gRNA and Homology Donor plasmids by Rainbow Transgenic Flies Inc (Camarillo, CA). **(Bi)** Shows N-terminal tagging using the Scarless-DsRed method. The inserted fluorescent protein tag is accompanied by a DsRed marker under the control of the eye specific 3xP3 regulatory sequence. The 3xP3-DsRed cassette is flanked by recognition sequences for the PiggyBac Transposase (yellow boxes on schematic). Flies carrying successful integration of the donor DNA sequence were identified by DsRed expression in their eyes. DsRed positive flies were then crossed to a stock expressing the PiggyBac Transposase which catalyzes the excision of the 3xP3-DsRed cassette. **(Bii)** Tagging *eggless* with the Halotag sequence was performed without a screenable DsRed marker. Insertion of the *halotag* was assessed directly by single fly pcr.

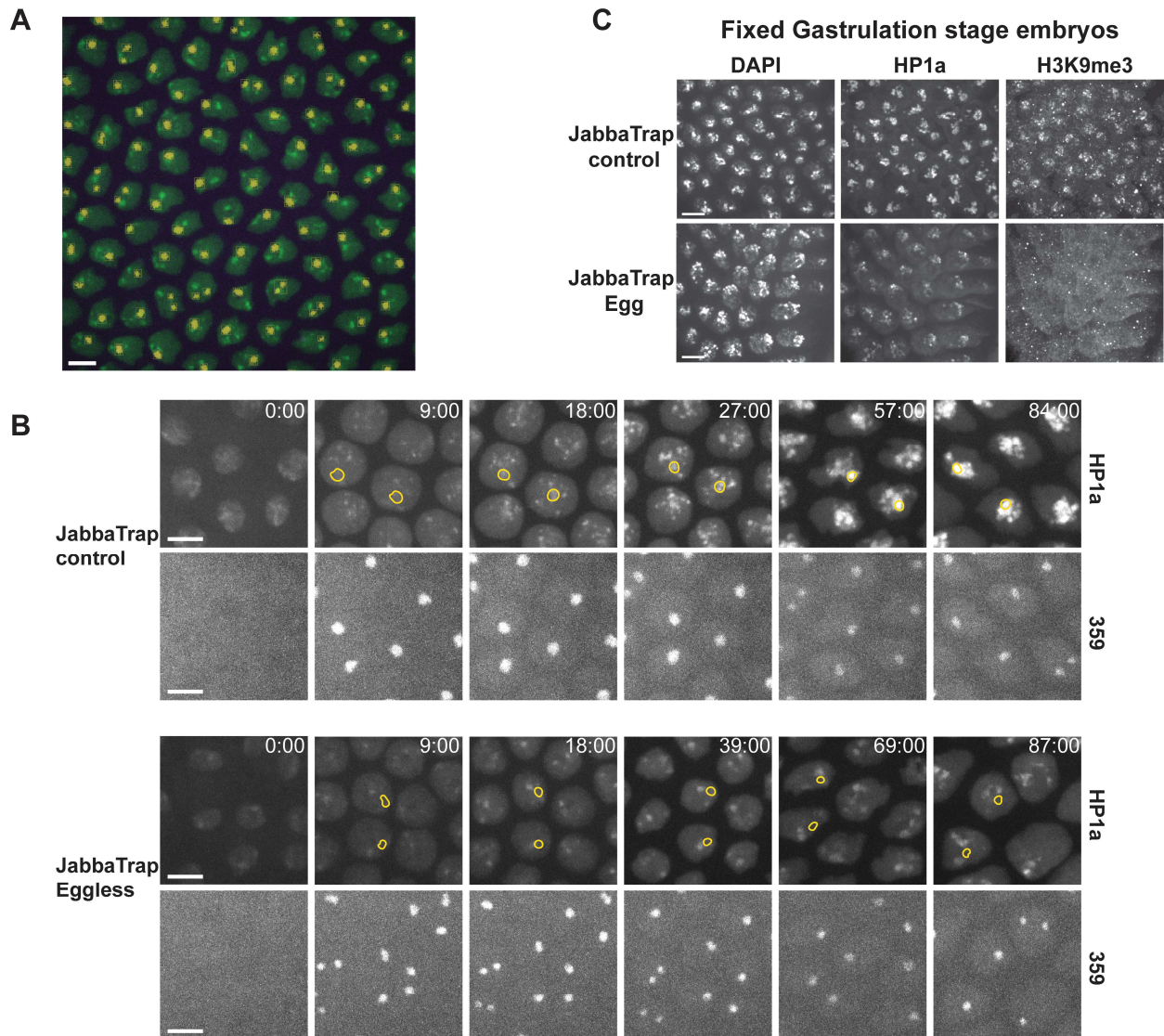
SUPPLEMENTAL FIGURE 3.2



Supplemental Figure 3.2

A) Selected live stills from live imaging during cycle 11 of a *GFP-egg* embryo after maternal expression of the JabbaTrap. Note that Egg localizes to small puncta in the cytoplasm, and not to foci in the nucleus as it does in embryos that do not express the JabbaTrap (compare to Figure 3). Scale bars are 2 μ m and the beginning of interphase 11 is set as 0:00. **B)** Maternally expressed JabbaTrap prevents the nuclear accumulation of GFP-Egg through the MBT. Selected live stills of late cycle 14 embryos from mothers of the indicated genotypes injected with mCherry-HP1a. In control embryos (no Gal4) GFP-Egg co-localizes with HP1a at heterochromatic foci. In contrast, GFP-Egg does not localize to the nucleus in embryos expressing the JabbaTrap.

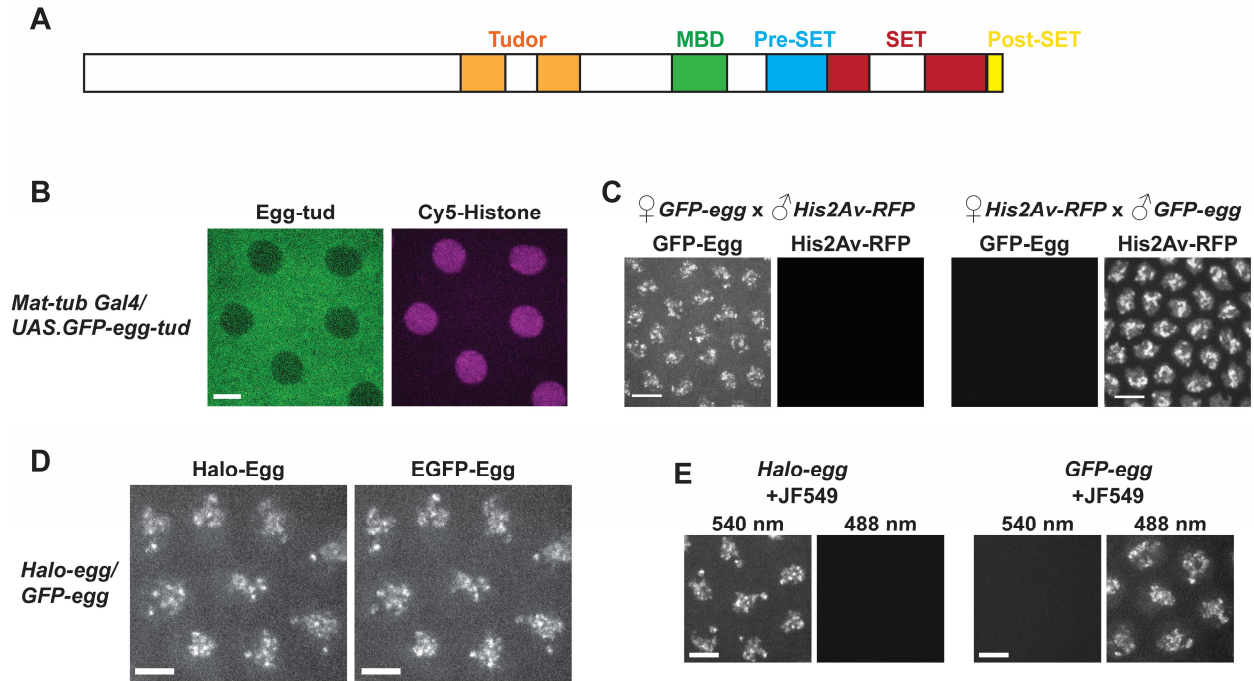
SUPPLEMENTAL FIGURE 3.3



Supplemental Figure 3.3

A) Confocal micrograph showing the representative output of the Volocity protocol used to identify the 359 bp repeat using signal from the 359-TALE-HaloJF646 protein. Briefly the software identified objects with an upper intensity threshold of 2 standard deviations and a size threshold of $0.21 \mu\text{m}^3$. The objects identified by the protocol are outlined in yellow, in green is the signal from mCherry-HP1a. Scale bar is $4 \mu\text{m}$. **B)** Representative stills from live imaging following mCherry-HP1a and 359-TALE-HaloJF646 during interphase 14 in either JabbaTrap control or JabbaTrap GFP-Egg embryos. Two representative 359-TALE signals are outlined in yellow on the mCherry-HP1a channel. Note that HP1a colocalizes with 359-TALE signal in the JabbaTrap control embryo (27:00 and on), but not in the JabbaTrap GFP-Egg embryo. Scale bars are $2 \mu\text{m}$, and the beginning of interphase 14 was set as 0:00. **C)** JabbaTrap mislocalization of Egg blocks establishment of H3K9me3-HP1a. Fixed gastrulation stage embryos of the indicated genotype immunostained for H3K9me3 and HP1a.

SUPPLEMENTAL FIGURE 3.4



Supplemental Figure 3.4

A) Domain structure of the Eggless protein (adapted from Clough et al. 2014). **B)** Selected live images of cycle 12 nuclei showing the localization of ectopically expressed GFP-Egg-tud and microinjected Cy5-Histones. A GFP tagged version of Egg lacking the tandem tudor domain was expressed maternally using Maternal-tubulin-Gal4. Images show a single confocal section and the scale bar is 3 μ m. **C)** The Egg protein present at the MBT is maternally provided. Embryos from the indicated crosses were collected and imaged by confocal microscopy. Scale bars are 5 μ m. **D)** Selected stills from a live cycle 14 embryo showing the coincidence of GFP-Egg and Halo549-Egg. The maternal genotype is indicated on the left. Scale bars are 3 μ m. **E)** Selected stills from live cycle 14 embryos showing the specificity of the *in vivo* Halo labeling. Embryos of the indicated genotypes were collected, permeabilized with Citrasolv, and labeled with the JF549 Halo ligand. Scale bars are 2 μ m.

Supplemental Movie legends.

Supplemental Movie 3.1

Transient expression of the JabbaTrap mislocalizes Orc2-GFP and blocks S phase. This movie accompanies Fig. 1B. Live imaging of Orc2-EGFP (in green) and His2Av-RFP (in magenta). An *orc2-EGFP* embryo was injected with *JabbaTrap* mRNA during cycle 11 and then live records were taken by confocal microscopy. The JabbaTrap mislocalizes Orc2 from the nucleus to cytoplasmic puncta and to membranous structures. Orc2 failed to bind to the anaphase chromosomes during the time when origin licensing normally occurs (00:09:00). Nuclei entered mitosis after a delay and underwent catastrophic anaphase bridging (00:29:00). Records were acquired every minute using a 100x oil objective.

Supplemental Movie 3.2

Imaging the progressive establishment of H3K9me2 in the early embryo. This movie accompanies Fig. 2A. Live imaging over cycles 12-14 of an embryo microinjected with Cy5 labeled H3K9me2-Fab fragments during cell cycle 10. The pool of injected K9me2 Fab is recruited to heterochromatic foci as the modification accumulates during embryogenesis. Note that the Fab fragment does not bind to chromatin during mitosis, but recruitment is fast once the nuclei exit from mitosis. The Fab signal at heterochromatin increases over the course of interphase, but also as the embryo develops through the MBT. Records were acquired every 2 minutes using a 100x oil objective.

Supplemental Movie 3.3

Recruitment of HP1a to heterochromatin in JabbaTrap control embryo during cycle 14. This movie accompanies Fig. 2D. Live imaging of the accumulation of mCherry-HP1a in a control embryo (No GFP tag) following maternal expression of the JabbaTrap. Movie begins at the start of cycle 14 and ends in interphase of cycle 15. HP1a is recruited to multiple bright foci that grow in number and size over the course of interphase 14. These foci ultimately coalesce into a bright chromocenter that is inherited into cycle 15 (01:54:00 and on). Compare with Movie 4. Records were acquired every 3 minutes using a 100x oil objective.

Supplemental Movie 3.4

JabbaTrapping GFP-Egg blocks the MBT recruitment of HP1a to heterochromatic foci. This movie accompanies Fig. 2D. Real time records following the accumulation of mCherry-HP1a in a *GFP-egg* embryo following maternal expression of the JabbaTrap. Movie begins in mitosis 13 and follows HP1a during cycle 14 and into cycle 15. Note that the recruitment of HP1a to heterochromatic foci is substantially reduced compared to control (Movie 3). The prominent HP1a rich chromocenter that normally forms at the end of cycle 14 is not evident, and the HP1a foci that do form remain separated into cycle 15. Records were acquired every 3 minutes using a 100x oil objective.

Supplemental Movie 3.5

Gradual recruitment of Egg to chromatin foci during interphase 12. This movie accompanies Fig. 3D. Live imaging of Halo-Egg (in magenta) and GFP-HP1a (in green), note that in this color scheme coincident signal will appear as white. This movie begins at the start of cycle 12 and ends in mitosis 12. After a brief delay at the start of the cycle, Egg begins to accumulate to bright foci on chromatin. The recruitment of Egg to foci precedes that of HP1a. Both Egg and HP1a dissociate from chromatin during mitosis. Records were acquired every 30 seconds using a 100x oil objective.

Supplemental Movie 3.6

Egg dissociates from chromatin when chromosomes condense in preparation for mitosis. This movie accompanies Fig. 5A. Live imaging of Halo-Egg (in green) and Cy5 labeled Histones (in purple). The movie begins in mitosis 11 and ends in mitosis 12. Records from a *Halo-egg* embryo labeled with JF549 and then injected with Cy5-labeled Histone proteins to mark the chromosomes. Egg is recruited to chromatin foci during interphase after a brief delay following the exit from mitosis. Accumulation of Egg to chromatin continues for most of interphase until mitotic chromatin condensation leads to its dissociation (00:12:00-00:14:00). Records were acquired every 30 seconds using a 100x oil objective.

Supplemental Movie 3.7

Arresting the embryonic cell cycle in interphase permits continued accumulation of Egg and HP1a at heterochromatin. This movie accompanies Fig. 5B. Live imaging of Halo-Egg (in magenta) and GFP-HP1a (in green). Note that coincident signal appears in white in this color scheme. This movie begins in Mitosis 12 and then continues through the arrested interphase 13. Arresting the cell cycle in interphase allows increased Egg recruitment to chromatin foci, which then persist for the duration of our record (over one hour). This leads to the accumulation of HP1a to large heterochromatic foci that coincide with Egg (00:26:00 – 01:08:00). Records were acquired every 2 minutes using a 100x oil objective.

METHODS

Fly stocks

Stocks of *Drosophila melanogaster* were cultured on standard cornmeal-yeast media. The following previously described stocks were used in this study: w^{1118} Canton-S (wild type), *His2Av-mRFP* (Bloomington stock number 23650), *EGFP-HP1a* (30561), *maternal tubulin-Gal4* (7063), *sfGFP-zelda* (M. Harrison), *ORC2-GFP; orc2^{1/y4}* (M. Gossen), *G9a^{RG5}* (P. Spierer), *grp⁰⁶⁰³⁴*, *Su(var)3-9⁰⁶*, *Su(var)3-9¹⁷*, and *RIF1-EGFP*.

Embryo injections for the transgenic lines described in this study were done by Rainbow Transgenic Flies in Camarillo, CA. PhiC31 mediated integration generated the JabbaTrap transgene *UASp-VhhGFP4-jabba-VhhGFP4^{attP-9A}*. The following stocks were created using CRISPR-Cas9 gene editing: *sfGFP-Su(z)12*, *sfGFP-G9a*, *EGFP-egg*, and *Halo-egg*. See Supplemental Fig. 1 for details of endogenous tagging. Following generation, modified flies were crossed to our lab's wild type stock (w^{1118} Canton-S) for at least 5 generations. Plasmid DNA and sequence files are available upon request.

Protein purification

Purified HP1a and TALE-light GFP/mCherry fusion proteins were described in previous studies (Shermoen et al. 2010; Yuan and O'Farrell 2016). Halo tagged 359 TALE-light protein was produced in BL21(DE3) *E. coli* cells. Protein expression was induced by treating cultures with 0.5 mM IPTG overnight at room temperature. Bacteria were lysed using B-PER supplemented with lysozyme, DNase I, and PMSF. TALE-light proteins were purified from cleared lysate using Ni-NTA agarose in gravity flow columns. After 2 washes, 10 μ M of the halo ligand JF646 in wash buffer was added to label the protein on column. Labeled proteins were eluted, dialyzed into 40 mM HEPES (pH 7.4) with 150 mM KCl, and then concentrated by spin column. The concentrated eluate was supplemented with glycerol to 10% and then snap frozen in liquid N₂.

In vivo Halotag labeling of Drosophila embryos

We adapted the embryo permeabilization method described in (Rand et al. 2010) to deliver the Halotag ligand into the embryo, and permeabilization and labeling were conducted in a single step. Embryos were collected in mesh baskets, dechorinated with 50% bleach, and then rinsed thoroughly with Embryo wash buffer and then water. Using a brush, embryos were transferred to microfuge tubes with a 1:10 solution of Citrasolv containing 1 μ M JF549. The tubes were incubated on a nutator in the dark for 8 to 9 minutes. Embryos were then poured into mesh baskets and cleaned thoroughly with wash buffer and water to remove excess detergent. Embryos were then prepared for imaging following our normal protocol. Permeabilization was not always successful, but embryos containing the dye could easily be identified microscopically.

Immunoprecipitation and Western blotting

Immunoprecipitation and western blotting were performed as described in (Seller and O'Farrell, 2018). The following primary antibodies were used at a dilution of 1:1000: rabbit anti-GFP (ab290, Abcam, Cambridge, United Kingdom) and rabbit anti-Wde (gift from A. Wodarz). A Goat anti-Rabbit HRP conjugated secondary antibody (Biorad) was used at a dilution of 1:10,000.

Embryo immunostaining

Embryos were collected on grape agar plates, washed into mesh baskets and dechorinated in 50% bleach for 2 minutes. Embryos were then devitellenized and fixed in a 1:1 mixture of methanol-heptane, before storing in methanol at -20°C. Embryos were gradually rehydrated in a series of increasing PTx:Methanol mixtures (1:3, 1:1, 3:1) before washing for 5 minutes in PTx (PBS with 0.1% Triton). Embryos were then blocked in PTx supplemented with 5% Normal Donkey Serum and 0.2% Azide for 1 hour at room temperature. Blocked embryos were then incubated with the primary antibody overnight at 4°C. The following primary antibodies were

used: rabbit anti-Wde at 1:500 (A. Wodarz), rabbit anti-H3K9me3 at 1:500, mouse anti-Ubx at 1:20 (DSHB FP3.38) and mouse anti-HP1a at 1:100 (DSHB CA19). Embryos were then washed with PTx for three times 15 minutes each, and then incubated with the appropriate fluorescently labeled secondary antibody (Molecular Probes) at 1:500 for 1 hour in the dark at room temperature. Embryos were then washed again with PTx for three times 15 minutes each. DAPI was added to the second wash. Finally, stained embryos were mounted on glass slides in Fluoromount.

Embryo microinjection and microscopy

Embryo microinjections were performed as described in (Farrell et al. 2012). JabbaTrap and Cdc25 (*twine*) mRNAs were synthesized using the CellScript T7 mRNA production system and injected at a concentration of 600 ng/ μ l. dsRNA against the cyclins A, B, and B3 was prepared as described in (McClelland and O'Farrell 2008). Imaging was performed using a spinning disk confocal microscope as described in (Seller and O'Farrell 2018). Image processing and analysis were done using Volocity (Perkin Elmer) and ImageJ. Unless otherwise noted, all images are presented as z-stack projections.

Chapter 4

Conclusion

Development transforms the embryo from simple and generalized to complex and differentiated. The differentiation of an initially naïve zygotic genome into specialized chromatin domains plays a critical role in this transformation. The division of the genome into euchromatin and heterochromatin is the most obvious instance of genomic differentiation. Megabase sized arrays of simple repeated sequences, known as satellite DNA, compose the bulk of the constitutive heterochromatin which displays conserved properties including compaction, replication late in S phase, and association with repressive chromatin modifications. However, in the embryos of many animals the satellite repeats do not exhibit these characteristics. Thus, embryogenesis involves the restoration of heterochromatin, and this restoration can serve as a paradigm for how epigenetic control arises during development. My thesis work has explored the initial formation of heterochromatin during embryogenesis in *Drosophila melanogaster*.

Cells divide rapidly in the early embryos of most animals. However, during a conserved period of development known as the mid-blastula transition (MBT), the cell cycle slows down dramatically. Down regulation of cyclin-CDK1 kinase activity initiates this slowing by delaying replication of the satellite sequences, thereby extending S phase. However, the factors responsible for mediating developmental onset of late replication were unknown. In recently published work (Seller and O'Farrell, PLoS Biol.) I used fly genetics and live imaging to show that the protein Rif1 is responsible for this change. At the MBT, Rif1 binds to and selectively delays the replication of satellite DNA. During the rapid pre-MBT cell cycles, the CDK1 kinase prevents Rif1 from slowing down S phase by driving its removal from chromatin. Developmental downregulation of CDK1 at the MBT releases constraints on Rif1 allowing it to bind to satellite DNA and introduce a late replication program. Additionally, I found that loss of Rif1 in mutant embryos shortened the MBT S phase and rescued cell cycle progression and development to embryos depleted of the essential S phase kinase Cdc7. This work provided new insights into

the temporal programming of S phase and into the embryonic origin of heterochromatic late replication.

In many organisms, constitutive heterochromatin is marked by di/tri methylation of histone H3K9 and the associated protein HP1a. These modifications enforce the unique epigenetic properties of heterochromatin. However, in the early embryo the heterochromatin lacks these modifications which only appear later when rapid embryonic cell cycles slow down at the MBT. In a second study currently in revision I focused on the initial steps restoring these heterochromatic modifications. The study of early embryonic events is complicated due to substantial maternal supply of many gene products, to overcome this I developed the JabbaTrap, a technique for inactivating proteins in embryos by selective mislocalization. Using the JabbaTrap I uncovered a major requirement for the methyltransferase Eggless/SetDB1 in the establishment of heterochromatin. Live-imaging revealed that endogenous Eggless gradually accumulates on chromatin in interphase, but then dissociates in mitosis and its accumulation must restart in the next cell cycle. Cell cycle slowing as the embryo approaches the MBT permits increasing accumulation and action of Eggless at its targets. Experimental manipulation of interphase duration showed that cell cycle speed regulates Eggless. This work supports a proposal that the developmental slowing of the cell cycle times embryonic heterochromatin formation.

By focusing on the initial events in the de novo formation of heterochromatin my work emphasizes how heterochromatin is integrated into the development of the embryo. Through regulation of the two proteins Rif1 and Egg, the embryonic cell cycle program times the appearance of late replication and repressive chromatin modifications, two widely conserved features of heterochromatin.

REFERENCES

- Aggarwal BD, Calvi BR. 2004. Chromatin regulates origin activity in *Drosophila* follicle cells. *Nature* **430**: 372–376.
- Alabert C, Barth TK, Reverón-Gómez N, Sidoli S, Schmidt A, Jensen ON, Imhof A, Groth A. 2015. Two distinct modes for propagation of histone PTMs across the cell cycle. *Genes Dev* **29**: 585–590.
- Allshire RC, Madhani HD. 2018. Ten principles of heterochromatin formation and function. *Nature Reviews Molecular Cell Biology* **19**: 229–244.
- Al-Sady B, Madhani HD, Narlikar GJ. 2013. Division of Labor between the Chromodomains of HP1 and Suv39 Methylase Enables Coordination of Heterochromatin Spread. *Molecular Cell* **51**: 80–91.
- Alver RC, Chadha GS, Gillespie PJ, Blow JJ. 2017. Reversal of DDK-Mediated MCM Phosphorylation by Rif1-PP1 Regulates Replication Initiation and Replisome Stability Independently of ATR/Chk1. *Cell Reports* **18**: 2508–2520.
- Aulner N, Monod C, Mandicourt G, Jullien D, Cuvier O, Sall A, Janssen S, Laemmli UK, Käs E. 2002. The AT-Hook Protein D1 Is Essential for *Drosophila melanogaster* Development and Is Implicated in Position-Effect Variegation. *Molecular and Cellular Biology* **22**: 1218–1232.
- Baldinger T, Gossen M. 2009. Binding of *Drosophila* Orc Proteins to Anaphase Chromosomes Requires Cessation of Mitotic Cyclin-Dependent Kinase Activity. *Molecular and Cellular Biology* **29**: 140–149.
- Birve A, Sengupta AK, Beuchle D, Larsson J, Kennison JA, Rasmuson-Lestander Å, Müller J. 2001. Su(z)12, a novel *Drosophila* Polycomb group gene that is conserved in vertebrates and plants. *Development* **128**: 3371–3379.
- Blumenthal AB, Kriegstein HJ, Hogness DS. 1974. The Units of DNA Replication in *Drosophila melanogaster* Chromosomes. *Cold Spring Harb Symp Quant Biol* **38**: 205–223.
- Blythe SA, Wieschaus EF. 2015. Zygotic Genome Activation Triggers the DNA Replication Checkpoint at the Midblastula Transition. *Cell* **160**: 1169–1181.
- Brower-Toland B, Riddle NC, Jiang H, Husinga KL, Elgin SCR. 2009. Multiple SET Methyltransferases Are Required to Maintain Normal Heterochromatin Domains in the Genome of *Drosophila melanogaster*. *Genetics* **181**: 1303–1319.
- Brown SW. 1966. Heterochromatin. *Science* **151**: 417–425.
- Chen K, Johnston J, Shao W, Meier S, Staber C, Zeitlinger J. 2013. A global change in RNA polymerase II pausing during the *Drosophila* midblastula transition. *eLife* **2**: e00861.
- Clough E, Moon W, Wang S, Smith K, Hazelrigg T. 2007. Histone methylation is required for oogenesis in *Drosophila*. *Development* **134**: 157–165.

- Clough E, Tedeschi T, Hazelrigg T. 2014. Epigenetic regulation of oogenesis and germ stem cell maintenance by the *Drosophila* histone methyltransferase Eggless/dSetDB1. *Developmental Biology* **388**: 181–191.
- Collart C, Allen GE, Bradshaw CR, Smith JC, Zegerman P. 2013. Titration of Four Replication Factors Is Essential for the *Xenopus laevis* Midblastula Transition. *Science* **341**: 893–896.
- Collart C, Smith JC, Zegerman P. 2017. Chk1 Inhibition of the Replication Factor Drf1 Guarantees Cell-Cycle Elongation at the *Xenopus laevis* Mid-blastula Transition. *Developmental Cell* **42**: 82–96.e3.
- Cornacchia D, Dileep V, Quivy J-P, Foti R, Tili F, Santarella-Mellwig R, Antony C, Almouzni G, Gilbert DM, Buonomo SBC. 2012. Mouse Rif1 is a key regulator of the replication-timing programme in mammalian cells. *The EMBO Journal* **31**: 3678–3690.
- Crest J, Oxnard N, Ji J-Y, Schubiger G. 2007. Onset of the DNA Replication Checkpoint in the Early *Drosophila* Embryo. *Genetics* **175**: 567–584.
- Davé A, Cooley C, Garg M, Bianchi A. 2014. Protein Phosphatase 1 Recruitment by Rif1 Regulates DNA Replication Origin Firing by Counteracting DDK Activity. *Cell Reports* **7**: 53–61.
- Deneke VE, Melbinger A, Vergassola M, Di Talia S. 2016. Waves of Cdk1 Activity in S Phase Synchronize the Cell Cycle in *Drosophila* Embryos. *Developmental Cell* **38**: 399–412.
- Dimitrova DS, Gilbert DM. 1999. The Spatial Position and Replication Timing of Chromosomal Domains Are Both Established in Early G1 Phase. *Molecular Cell* **4**: 983–993.
- Di Talia S, She R, Blythe SA, Lu X, Zhang QF, Wieschaus EF. 2013. Posttranslational Control of Cdc25 Degradation Terminates *Drosophila*'s Early Cell-Cycle Program. *Current Biology* **23**: 127–132.
- Edgar BA, Datar SA. 1996. Zygotic degradation of two maternal Cdc25 mRNAs terminates *Drosophila*'s early cell cycle program. *Genes Dev* **10**: 1966–1977.
- Edgar BA, O'Farrell PH. 1989. Genetic control of cell division patterns in the *Drosophila* embryo. *Cell* **57**: 177–187.
- Edgar BA, O'Farrell PH. 1990. The three postblastoderm cell cycles of *Drosophila* embryogenesis are regulated in G2 by string. *Cell* **62**: 469–480.
- Edgar BA, Sprenger F, Duronio RJ, Leopold P, O'Farrell PH. 1994. Distinct molecular mechanisms regulate cell cycle timing at successive stages of *Drosophila* embryogenesis. *Genes Dev* **8**: 440–452.
- Eissenberg JC, Elgin SCR. 2014. HP1a: a structural chromosomal protein regulating transcription. *Trends in Genetics* **30**: 103–110.
- Eissenberg JC, James TC, Foster-Hartnett DM, Hartnett T, Ngan V, Elgin SC. 1990. Mutation in a heterochromatin-specific chromosomal protein is associated with suppression of position-effect variegation in *Drosophila melanogaster*. *PNAS* **87**: 9923–9927.

- Elgin SCR, Reuter G. 2013. Position-Effect Variegation, Heterochromatin Formation, and Gene Silencing in *Drosophila*. *Cold Spring Harb Perspect Biol* **5**: a017780.
- Fadloun A, Eid A, Torres-Padilla M-E. 2013. Chapter One - Mechanisms and Dynamics of Heterochromatin Formation During Mammalian Development: Closed Paths and Open Questions. In *Current Topics in Developmental Biology* (ed. E. Heard), Vol. 104 of *Epigenetics and Development*, pp. 1–45.
- Farrell JA, O'Farrell PH. 2014. From Egg to Gastrula: How the Cell Cycle Is Remodeled During the *Drosophila* Mid-Blastula Transition. *Annual Review of Genetics* **48**: 269–294.
- Farrell JA, O'Farrell PH. 2013. Mechanism and Regulation of Cdc25/Twine Protein Destruction in Embryonic Cell-Cycle Remodeling. *Current Biology* **23**: 118–126.
- Farrell JA, Shermoen AW, Yuan K, O'Farrell PH. 2012. Embryonic onset of late replication requires Cdc25 down-regulation. *Genes Dev* **26**: 714–725.
- Foe VE. 1989. Mitotic domains reveal early commitment of cells in *Drosophila* embryos. *Development* **107**: 1–22.
- Fogarty P, Kalpin RF, Sullivan W. 1994. The *Drosophila* maternal-effect mutation grapes causes a metaphase arrest at nuclear cycle 13. *Development* **120**: 2131–2142.
- Gould KL, Nurse P. 1989. Tyrosine phosphorylation of the fission yeast cdc2+ protein kinase regulates entry into mitosis. *Nature* **342**: 39–45.
- Graham CF. 1966. The Regulation of DNA Synthesis and Mitosis in Multinucleate Frog Eggs. *Journal of Cell Science* **1**: 363–374.
- Grimm JB, English BP, Chen J, Slaughter JP, Zhang Z, Revyakin A, Patel R, Macklin JJ, Normanno D, Singer RH, et al. 2015. A general method to improve fluorophores for live-cell and single-molecule microscopy. *Nature Methods* **12**: 244–250.
- Hall IM, Shankaranarayana GD, Noma K, Ayoub N, Cohen A, Grewal SIS. 2002. Establishment and Maintenance of a Heterochromatin Domain. *Science* **297**: 2232–2237.
- Harrison MM, Eisen MB. 2015. Chapter Three - Transcriptional Activation of the Zygotic Genome in *Drosophila*. In *Current Topics in Developmental Biology* (ed. H.D. Lipshitz), Vol. 113 of *The Maternal-to-Zygotic Transition*, pp. 85–112.
- Haruki H, Nishikawa J, Laemmli UK. 2008. The Anchor-Away Technique: Rapid, Conditional Establishment of Yeast Mutant Phenotypes. *Molecular Cell* **31**: 925–932.
- Hayano M, Kanoh Y, Matsumoto S, Renard-Guillet C, Shirahige K, Masai H. 2012. Rif1 is a global regulator of timing of replication origin firing in fission yeast. *Genes Dev* **26**: 137–150.
- Hayashi-Takanaka Y, Yamagata K, Wakayama T, Stasevich TJ, Kainuma T, Tsurimoto T, Tachibana M, Shinkai Y, Kurumizaka H, Nozaki N, et al. 2011. Tracking epigenetic histone modifications in

- single cells using Fab-based live endogenous modification labeling. *Nucleic Acids Res* **39**: 6475–6488.
- Hiraga S, Alvino GM, Chang F, Lian H, Sridhar A, Kubota T, Brewer BJ, Weinreich M, Raghuraman MK, Donaldson AD. 2014. Rif1 controls DNA replication by directing Protein Phosphatase 1 to reverse Cdc7-mediated phosphorylation of the MCM complex. *Genes Dev* **28**: 372–383.
- Hiratani I, Ryba T, Itoh M, Yokochi T, Schwaiger M, Chang C-W, Lyou Y, Townes TM, Schübeler D, Gilbert DM. 2008. Global Reorganization of Replication Domains During Embryonic Stem Cell Differentiation. *PLOS Biology* **6**: e245.
- Holt LJ, Tuch BB, Villén J, Johnson AD, Gygi SP, Morgan DO. 2009. Global Analysis of Cdk1 Substrate Phosphorylation Sites Provides Insights into Evolution. *Science* **325**: 1682–1686.
- Jackson DA, Pombo A. 1998. Replicon Clusters Are Stable Units of Chromosome Structure: Evidence That Nuclear Organization Contributes to the Efficient Activation and Propagation of S Phase in Human Cells. *The Journal of Cell Biology* **140**: 1285–1295.
- Janssen A, Colmenares SU, Karpen GH. 2018. Heterochromatin: Guardian of the Genome. *Annual Review of Cell and Developmental Biology* **34**: 265–288.
- Kellum R, Raff JW, Alberts BM. 1995. Heterochromatin protein 1 distribution during development and during the cell cycle in *Drosophila* embryos. *Journal of Cell Science* **108**: 1407–1418.
- Knott SRV, Peace JM, Ostrow AZ, Gan Y, Rex AE, Viggiani CJ, Tavaré S, Aparicio OM. 2012. Forkhead Transcription Factors Establish Origin Timing and Long-Range Clustering in *S. cerevisiae*. *Cell* **148**: 99–111.
- Koch CM, Honemann-Capito M, Egger-Adam D, Wodarz A. 2009. Windei, the *Drosophila* Homolog of mAM/MCAF1, Is an Essential Cofactor of the H3K9 Methyl Transferase dSETDB1/Eggless in Germ Line Development. *PLOS Genetics* **5**: e1000644.
- Kumar S, Yoo HY, Kumagai A, Shevchenko A, Shevchenko A, Dunphy WG. 2012. Role for Rif1 in the checkpoint response to damaged DNA in *Xenopus* egg extracts. *Cell Cycle* **11**: 1183–1194.
- Labib K. 2010. How do Cdc7 and cyclin-dependent kinases trigger the initiation of chromosome replication in eukaryotic cells? *Genes Dev* **24**: 1208–1219.
- Larson AG, Elnatan D, Keenen MM, Trnka MJ, Johnston JB, Burlingame AL, Agard DA, Redding S, Narlikar GJ. 2017. Liquid droplet formation by HP1 α suggests a role for phase separation in heterochromatin. *Nature* **547**: 236–240.
- Li X-Y, Harrison MM, Villalta JE, Kaplan T, Eisen MB. 2014. Establishment of regions of genomic activity during the *Drosophila* maternal to zygotic transition. *eLife* **3**: e03737
- Li Z, Thiel K, Thul PJ, Beller M, Kühnlein RP, Welte MA. 2012. Lipid Droplets Control the Maternal Histone Supply of *Drosophila* Embryos. *Current Biology* **22**: 2104–2113.

- Liang H-L, Nien C-Y, Liu H-Y, Metzstein MM, Kirov N, Rushlow C. 2008. The zinc-finger protein Zelda is a key activator of the early zygotic genome in *Drosophila*. *Nature* **456**: 400–403.
- Lima-de-Faria A. 1959. Differential Uptake of Tritiated Thymidine into Hetero- and Euchromatin in *Melanoplus* and *Secale*. *The Journal of Cell Biology* **6**: 457–466.
- Lima-de-Faria A, Jaworska H. 1968. Late DNA synthesis in heterochromatin. *Nature* **217**: 138–142.
- Lohe AR, Hilliker AJ, Roberts PA. 1993. Mapping simple repeated DNA sequences in heterochromatin of *Drosophila melanogaster*. *Genetics* **134**: 1149–1174.
- Loppin B, Bonnefoy E, Anselme C, Laurençon A, Karr TL, Couble P. 2005. The histone H3.3 chaperone HIRA is essential for chromatin assembly in the male pronucleus. *Nature* **437**: 1386–1390.
- Lott SE, Villalta JE, Schroth GP, Luo S, Tonkin LA, Eisen MB. 2011. Noncanonical Compensation of Zygotic X Transcription in Early *Drosophila melanogaster* Development Revealed through Single-Embryo RNA-Seq. *PLOS Biology* **9**: e1000590.
- Lu X, Li JM, Elemento O, Tavazoie S, Wieschaus EF. 2009. Coupling of zygotic transcription to mitotic control at the *Drosophila* mid-blastula transition. *Development* **136**: 2101–2110.
- Makunin IV, Volkova EI, Belyaeva ES, Nabirochkina EN, Pirrotta V, Zhimulev IF. 2002. The *Drosophila* Suppressor of Underreplication Protein Binds to Late-Replicating Regions of Polytene Chromosomes. *Genetics* **160**: 1023–1034.
- Mantiero D, Mackenzie A, Donaldson A, Zegerman P. 2011. Limiting replication initiation factors execute the temporal programme of origin firing in budding yeast. *The EMBO Journal* **30**: 4805–4814.
- Mattarocci S, Hafner L, Lezaja A, Shyian M, Shore D. 2016. Rif1: A Conserved Regulator of DNA Replication and Repair Hijacked by Telomeres in Yeasts. *Front Genet* **7**.
- Mattarocci S, Shyian M, Lemmens L, Damay P, Altintas DM, Shi T, Bartholomew CR, Thomä NH, Hardy CFJ, Shore D. 2014. Rif1 Controls DNA Replication Timing in Yeast through the PP1 Phosphatase Glc7. *Cell Reports* **7**: 62–69.
- McClelland ML, O'Farrell PH. 2008. RNAi of Mitotic Cyclins in *Drosophila* Uncouples the Nuclear and Centrosome Cycle. *Current Biology* **18**: 245–254.
- McClelland ML, Shermoen AW, O'Farrell PH. 2009. DNA replication times the cell cycle and contributes to the mid-blastula transition in *Drosophila* embryos. *The Journal of Cell Biology* **187**: 7–14.
- McKnight SL, Miller OL. 1977. Electron microscopic analysis of chromatin replication in the cellular blastoderm *drosophila melanogaster* embryo. *Cell* **12**: 795–804.
- Milán M, Campuzano S, García-Bellido A. 1996. Cell cycling and patterned cell proliferation in the *Drosophila* wing during metamorphosis. *PNAS* **93**: 11687–11692.
- Mis J, Ner SS, Grigliatti TA. 2006. Identification of three histone methyltransferases in *Drosophila*: dG9a is a suppressor of PEV and is required for gene silencing. *Mol Genet Genomics* **275**: 513–526.

- Muller HJ. 1930. Types of visible variations induced by X-rays in *Drosophila*. *J Genet* **22**: 299–334.
- Mutlu B, Chen H-M, Moresco JJ, Orelo BD, Yang B, Gaspar JM, Keppler-Ross S, Yates JR, Hall DH, Maine EM, et al. 2018. Regulated nuclear accumulation of a histone methyltransferase times the onset of heterochromatin formation in *C. elegans* embryos. *Science Advances* **4**: eaat6224.
- Neufeld TP, de la Cruz AFA, Johnston LA, Edgar BA. 1998. Coordination of Growth and Cell Division in the *Drosophila* Wing. *Cell* **93**: 1183–1193.
- O’Farrell PH. 2015. Growing an Embryo from a Single Cell: A Hurdle in Animal Life. *Cold Spring Harb Perspect Biol* **7**: a019042.
- O’Farrell PH. 2004. *How Metazoans Reach Their Full Size: The Natural History of Bigness*. Cell Growth: Control of Cell Size. Cold Spring Harbor Press, NY.
- O’Farrell PH. 2001. Triggering the all-or-nothing switch into mitosis. *Trends in Cell Biology* **11**: 512–519.
- Penke TJR, McKay DJ, Strahl BD, Matera AG, Duronio RJ. 2016. Direct interrogation of the role of H3K9 in metazoan heterochromatin function. *Genes Dev* **30**: 1866–1880.
- Penke TJR, McKay DJ, Strahl BD, Matera AG, Duronio RJ. 2018. Functional Redundancy of Variant and Canonical Histone H3 Lysine 9 Modification in *Drosophila*. *Genetics* **208**: 229–244.
- Price D, Rabinovitch S, O’Farrell PH, Campbell SD. 2000. *Drosophila wee1* Has an Essential Role in the Nuclear Divisions of Early Embryogenesis. *Genetics* **155**: 159–166.
- Prioleau M-N, MacAlpine DM. 2016. DNA replication origins—where do we begin? *Genes Dev* **30**: 1683–1697.
- Raff JW, Glover DM. 1988. Nuclear and cytoplasmic mitotic cycles continue in *Drosophila* embryos in which DNA synthesis is inhibited with aphidicolin. *The Journal of Cell Biology* **107**: 2009–2019.
- Raghuraman MK, Brewer BJ, Fangman WL. 1997. Cell Cycle-Dependent Establishment of a Late Replication Program. *Science* **276**: 806–809.
- Rand MD, Kearney AL, Dao J, Clason T. 2010. Permeabilization of *Drosophila* embryos for introduction of small molecules. *Insect Biochemistry and Molecular Biology* **40**: 792–804.
- Rangan P, Malone CD, Navarro C, Newbold SP, Hayes PS, Sachidanandam R, Hannon GJ, Lehmann R. 2011. piRNA Production Requires Heterochromatin Formation in *Drosophila*. *Current Biology* **21**: 1373–1379.
- Renzis SD, Elemento O, Tavazoie S, Wieschaus EF. 2007. Unmasking Activation of the Zygotic Genome Using Chromosomal Deletions in the *Drosophila* Embryo. *PLOS Biology* **5**: e117.
- Rhind N, Gilbert DM. 2013. DNA Replication Timing. *Cold Spring Harb Perspect Biol* **5**: a010132.
- Riddle NC, Jung YL, Gu T, Alekseyenko AA, Asker D, Gui H, Kharchenko PV, Minoda A, Plachetka A, Schwartz YB, et al. 2012. Enrichment of HP1a on *Drosophila* Chromosome 4 Genes Creates an

- Alternate Chromatin Structure Critical for Regulation in this Heterochromatic Domain. *PLOS Genetics* **8**: e1002954.
- Rothbauer U, Zolghadr K, Muyldermans S, Schepers A, Cardoso MC, Leonhardt H. 2008. A Versatile Nanotrap for Biochemical and Functional Studies with Fluorescent Fusion Proteins. *Molecular & Cellular Proteomics* **7**: 282–289.
- Schotta G, Ebert A, Krauss V, Fischer A, Hoffmann J, Rea S, Jenuwein T, Dorn R, Reuter G. 2002. Central role of *Drosophila* SU(VAR)3–9 in histone H3-K9 methylation and heterochromatic gene silencing. *The EMBO Journal* **21**: 1121–1131.
- Schultz DC, Ayyanathan K, Negorev D, Maul GG, Rauscher FJ. 2002. SETDB1: a novel KAP-1-associated histone H3, lysine 9-specific methyltransferase that contributes to HP1-mediated silencing of euchromatic genes by KRAB zinc-finger proteins. *Genes Dev* **16**: 919–932.
- Seller CA, O'Farrell PH. 2018. Rif1 prolongs the embryonic S phase at the *Drosophila* mid-blastula transition. *PLOS Biology* **16**: e2005687.
- Seum C, Bontron S, Reo E, Delattre M, Spierer P. 2007a. *Drosophila* G9a Is a Nonessential Gene. *Genetics* **177**: 1955–1957.
- Seum C, Reo E, Peng H, Iii FJR, Spierer P, Bontron S. 2007b. *Drosophila* SETDB1 Is Required for Chromosome 4 Silencing. *PLOS Genetics* **3**: e76.
- Shermoen AW, McClelland ML, O'Farrell PH. 2010. Developmental Control of Late Replication and S Phase Length. *Current Biology* **20**: 2067–2077.
- Shermoen AW, O'Farrell PH. 1991. Progression of the cell cycle through mitosis leads to abortion of nascent transcripts. *Cell* **67**: 303–310.
- Sheu Y-J, Stillman B. 2010. The Dbf4–Cdc7 kinase promotes S phase by alleviating an inhibitory activity in Mcm4. *Nature* **463**: 113–117.
- Sibon OCM, Laurençon A, Hawley RS, Theurkauf WE. 1999. The *Drosophila* ATM homologue Mei-41 has an essential checkpoint function at the midblastula transition. *Current Biology* **9**: 302–312.
- Sibon OCM, Stevenson VA, Theurkauf WE. 1997. DNA-replication checkpoint control at the *Drosophila* midblastula transition. *Nature* **388**: 93–97.
- Siddiqui K, On KF, Diffley JFX. 2013. Regulating DNA Replication in Eukarya. *Cold Spring Harb Perspect Biol* **5**: a012930.
- Sienski G, Batki J, Senti K-A, Dönertas D, Tirian L, Meixner K, Brennecke J. 2015. Silencio/CG9754 connects the Piwi–piRNA complex to the cellular heterochromatin machinery. *Genes Dev* **29**: 2258–2271.
- Snow MHL. 2008. Embryo Growth During the Immediate Postimplantation Period. In *Ciba Foundation Symposium 40 - Embryogenesis in Mammals*, pp. 53–70, John Wiley & Sons, Ltd.

- Sreesankar E, Bharathi V, Mishra RK, Mishra K. 2015. *Drosophila* Rif1 is an essential gene and controls late developmental events by direct interaction with PP1-87B. *Scientific Reports* **5**: 10679.
- Sreesankar E, Senthilkumar R, Bharathi V, Mishra RK, Mishra K. 2012. Functional diversification of yeast telomere associated protein, Rif1, in higher eukaryotes. *BMC Genomics* **13**: 255.
- Stephenson R, Hosler MR, Gavande NS, Ghosh AK, Weake VM. 2015. Characterization of a *Drosophila* Ortholog of the Cdc7 Kinase A ROLE FOR Cdc7 IN ENDOREPLICATION INDEPENDENT OF CHIFFON. *J Biol Chem* **290**: 1332–1347.
- Stepińska U, Olszańska B. 1983. Cell multiplication and blastoderm development in relation to egg envelope formation during uterine development of quail (*Coturnix coturnix japonica*) embryo. *Journal of Experimental Zoology* **228**: 505–510.
- Strom AR, Emelyanov AV, Mir M, Fyodorov DV, Darzacq X, Karpen GH. 2017. Phase separation drives heterochromatin domain formation. *Nature* **547**: 241–245.
- Strong I, Yuan K, O'Farrell PH. 2017. Interphase-Arrested *Drosophila* Embryos Initiate Mid-Blastula Transition At A Low Nuclear-Cytoplasmic Ratio. *bioRxiv* 143719.
- Stumpff J, Duncan T, Homola E, Campbell SD, Su TT. 2004. *Drosophila* Wee1 Kinase Regulates Cdk1 and Mitotic Entry during Embryogenesis. *Current Biology* **14**: 2143–2148.
- Su TT, O'Farrell PH. 1997. Chromosome Association of Minichromosome Maintenance Proteins in *Drosophila* Mitotic Cycles. *The Journal of Cell Biology* **139**: 13–21.
- Sukackaite R, Cornacchia D, Jensen MR, Mas PJ, Blackledge M, Envervald E, Duan G, Auchynnikava T, Köhn M, Hart DJ, et al. 2017. Mouse Rif1 is a regulatory subunit of protein phosphatase 1 (PP1). *Scientific Reports* **7**: 2119.
- Tadros W, Goldman AL, Babak T, Menzies F, Vardy L, Orr-Weaver T, Hughes TR, Westwood JT, Smibert CA, Lipshitz HD. 2007. SMAUG Is a Major Regulator of Maternal mRNA Destabilization in *Drosophila* and Its Translation Is Activated by the PAN GU Kinase. *Developmental Cell* **12**: 143–155.
- Tanaka S, Araki H. 2013. Helicase Activation and Establishment of Replication Forks at Chromosomal Origins of Replication. *Cold Spring Harb Perspect Biol* **5**: a010371.
- Tanaka S, Nakato R, Katou Y, Shirahige K, Araki H. 2011. Origin Association of Sld3, Sld7, and Cdc45 Proteins Is a Key Step for Determination of Origin-Firing Timing. *Current Biology* **21**: 2055–2063.
- Tanaka S, Umemori T, Hirai K, Muramatsu S, Kamimura Y, Araki H. 2007. CDK-dependent phosphorylation of Sld2 and Sld3 initiates DNA replication in budding yeast. *Nature* **445**: 328–332.
- Taylor JH. 1960. Nucleic Acid Synthesis in Relation to the Cell Division Cycle*. *Annals of the New York Academy of Sciences* **90**: 409–421.

- Tschiersch B, Hofmann A, Krauss V, Dorn R, Korge G, Reuter G. 1994. The protein encoded by the *Drosophila* position-effect variegation suppressor gene *Su(var)3-9* combines domains of antagonistic regulators of homeotic gene complexes. *EMBO J* **13**: 3822–3831.
- Tzeng T-Y, Lee C-H, Chan L-W, Shen C-KJ. 2007. Epigenetic regulation of the *Drosophila* chromosome 4 by the histone H3K9 methyltransferase dSETDB1. *PNAS* **104**: 12691–12696.
- Vogelauer M, Rubbi L, Lucas I, Brewer BJ, Grunstein M. 2002. Histone Acetylation Regulates the Time of Replication Origin Firing. *Molecular Cell* **10**: 1223–1233.
- Walter J, Newport JW. 1997. Regulation of replicon size in *Xenopus* egg extracts. *Science* **275**: 993–995.
- Wang H, An W, Cao R, Xia L, Erdjument-Bromage H, Chatton B, Tempst P, Roeder RG, Zhang Y. 2003. mAM Facilitates Conversion by ESET of Dimethyl to Trimethyl Lysine 9 of Histone H3 to Cause Transcriptional Repression. *Molecular Cell* **12**: 475–487.
- Wang X, Pan L, Wang S, Zhou J, McDowell W, Park J, Haug J, Staehling K, Tang H, Xie T. 2011. Histone H3K9 Trimethylase Eggless Controls Germline Stem Cell Maintenance and Differentiation. *PLOS Genetics* **7**: e1002426.
- Welte MA. 2015. As the fat flies: The dynamic lipid droplets of *Drosophila* embryos. *Biochimica et Biophysica Acta (BBA) - Molecular and Cell Biology of Lipids* **1851**: 1156–1185.
- Xu L, Blackburn EH. 2004. Human Rif1 protein binds aberrant telomeres and aligns along anaphase midzone microtubules. *J Cell Biol* **167**: 819–830.
- Xu M, Wang W, Chen S, Zhu B. 2012. A model for mitotic inheritance of histone lysine methylation. *EMBO reports* **13**: 60–67.
- Yadav T, Quivy J-P, Almouzni G. 2018. Chromatin plasticity: A versatile landscape that underlies cell fate and identity. *Science* **361**: 1332–1336.
- Yamazaki S, Hayano M, Masai H. 2013. Replication timing regulation of eukaryotic replicons: Rif1 as a global regulator of replication timing. *Trends in Genetics* **29**: 449–460.
- Yamazaki S, Ishii A, Kanoh Y, Oda M, Nishito Y, Masai H. 2012. Rif1 regulates the replication timing domains on the human genome. *The EMBO Journal* **31**: 3667–3677.
- Yeeles JTP, Deegan TD, Janska A, Early A, Diffley JFX. 2015. Regulated eukaryotic DNA replication origin firing with purified proteins. *Nature* **519**: 431–435.
- Yu Y, Gu J, Jin Y, Luo Y, Preall JB, Ma J, Czech B, Hannon GJ. 2015. Panoramix enforces piRNA-dependent cotranscriptional silencing. *Science* **350**: 339–342.
- Yuan K, O'Farrell PH. 2016. TALE-light imaging reveals maternally guided, H3K9me2/3-independent emergence of functional heterochromatin in *Drosophila* embryos. *Genes Dev* **30**: 579–593.
- Yuan K, Seller CA, Shermoen AW, O'Farrell PH. 2016. Timing the *Drosophila* Mid-Blastula Transition: A Cell Cycle-Centered View. *Trends in Genetics* **32**: 496–507.

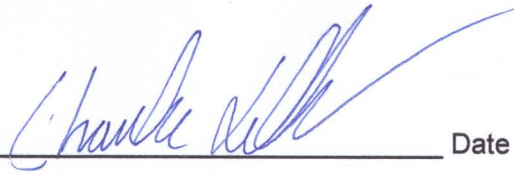
- Yuan K, Shermoen AW, O'Farrell PH. 2014. Illuminating DNA replication during *Drosophila* development using TALE-lights. *Current Biology* **24**: R144–R145.
- Zegerman P, Diffley JFX. 2007. Phosphorylation of Sld2 and Sld3 by cyclin-dependent kinases promotes DNA replication in budding yeast. *Nature* **445**: 281–285.
- Zhang K, Mosch K, Fischle W, Grewal SIS. 2008. Roles of the Clr4 methyltransferase complex in nucleation, spreading and maintenance of heterochromatin. *Nature Structural & Molecular Biology* **15**: 381–388.
- Zhimulev IF, Belyaeva ES, Fomina OV, Protopopov MO, Bolshakov VN. 1986. Cytogenetic and molecular aspects of position effect variegation in *Drosophila melanogaster*. *Chromosoma* **94**: 492–504.
- Zofall M, Smith DR, Mizuguchi T, Dhakshnamoorthy J, Grewal SIS. 2016. Taz1-Shelterin Promotes Facultative Heterochromatin Assembly at Chromosome-Internal Sites Containing Late Replication Origins. *Molecular Cell* **62**: 862–874.

Publishing Agreement

It is the policy of the University to encourage the distribution of all theses, dissertations, and manuscripts. Copies of all UCSF theses, dissertations, and manuscripts will be routed to the library via the Graduate Division. The library will make all theses, dissertations, and manuscripts accessible to the public and will preserve these to the best of their abilities, in perpetuity.

I hereby grant permission to the Graduate Division of the University of California, San Francisco to release copies of my thesis, dissertation, or manuscript to the Campus Library to provide access and preservation, in whole or in part, in perpetuity.

Author Signature



Date

12-18-18.